UNIVERSITY OF CALGARY

The Phase Behavior of Heavy Oil and Propane Mixtures

by

Adel Alberto Mancilla Polanco

A THESIS

SUBMITTED TO THE FACULTY OF GRADUATE STUDIES

IN PARTIAL FULFILMENT OF THE REQUIREMENTS FOR THE

DEGREE OF MASTER OF SCIENCE

GRADUATE PROGRAM IN CHEMICAL AND PETROLEUM ENGINEERING

CALGARY, ALBERTA

NOVEMBER, 2017

Abstract

The phase behavior of propane diluted bitumen was mapped from temperatures between 20 and 180°C and pressures up to 10 MPa. Both vapor-liquid (VL) and liquid-liquid (LL) regions were observed. High pressure micrographs demonstrated that the heavy phase (a pitch phase) transitioned from a glass to a liquid state with increased temperature and feed propane content. Pressure-temperature and pressure-composition phase diagrams were constructed from saturation pressure and pitch phase onset data. The amount and composition of the heavy phase was also measured. Solvent-free pitch yields as high as 70 wt% of the bitumen were observed. Pseudo-ternary diagrams were also constructed to observe the partitioning of the species between the phases. Finally, the ability of a cubic equation-of-state with two forms of mixing rules were explored to model the data. The results can be used in the design of *in situ* and surface processes involving the addition of propane to bitumen.

Keywords: Heavy oil, propane, pitch, onset, yield, cubic equation of state.

Acknowledgements

During this journey, I have known valuable people who have somehow demonstrated me all their support, guidance, and assistance. I owe all my gratitude to them and therefore I have saved a special space for them. First and foremost, I would like to thank God who is the one that gave us the life and provides every tool for the formation of our integrity. I would like to make a special mention to Dr. Yarranton for his true commitment with this work, support, and guidance. His manner of leading this extraordinary research group has positively marked my life. It has been an honor to be his student and I express my profound admiration to him.

I also want to make a special call to Florian, the best immediate boss that a person could ever have. His continuous support and teaching methodology have encouraged me to produce the best. I am really grateful for his advices, which have boosted me to be both a better person and professional. I also want to have an attention to Dr. Adrianne, my co-supervisor, for her helpful discussions and funny stories. Thanks also to Elaine for helping me with all the tedious paperwork.

I want to extend this gratitude to the current and past members of the HOPP research group, mainly to Sandra, Andres, Franklin, Nicolay, Jhon, Yulman, Jair, Francisco, Jairo, Michaela, Will, Yoshi, Yechun and Hosiberto. Two people that also deserved a place in this acknowledgement are Daniel and Anderson. Each one somehow collaborates with a grain of sand to make this dream real. Thanks to the NSERC Industrial Research Chair in Heavy Oil Properties and Processing, Shell Canada, Schlumberger, Suncor, Petrobras, Nexen, and VMG for the funding of this project. Obviously, thanks also to the Department of Chemical and Petroleum Engineering.

Finally, I reserved the most important spot to render thanks to my family. I am who I am because of them. Thanks for all the effort you have made for me to be where I am. Thanks to my gorgeous girlfriend as well for her support and assistance at the end of this trip. I could not imagine this triumph without her. Thanks everyone again, God bless you all!

Dedication

To my father, Adel Mancilla, who is my true inspiration

To my mother, Genny Polanco, who is my true love

To my sister, Zuly Mancilla, who is my vault of secrets

To my brother, Jose Mancilla, who is my soulmate

To my girlfriend, Micheline Ramos, who is my true company

To Nitro who is my gorgeous nephew

Table of Contents

List of Tables

List of Figures and Illustrations

List of Symbols, Abbreviations and Nomenclature

a	Attractive parameter in EoS; Adjustable constant in the compositional k_{ij} correlation, Eq. 4.11
a_A, b_A	Adjustable constant to capture LL boundary, Eq. 4.9
A	Helmholtz energy; Adjustable constant in modified Henry's law model, Eqs. 5.2, 5.3; Adjustable parameter in yield uncertainty correlation, Eq. A1
A^{chain}	Helmholtz energy contribution from covalent bonds in SAFT, Eq. 2.9
A^{res}	Residual Helmholtz energy, Eq. 2.9
A^{assoc}	Helmholtz energy contribution from association, Eq. 2.9
A^{seg}	Helmholtz energy contribution from segment in SAFT, Eq. 2.9
A_0^{hs}	Helmholtz energy contribution from hard spheres in SAFT, Eq. 2.9
A_0^{disp}	Helmholtz energy contribution from dispersion forces in SAFT, Eq. 2.9
b	Volume parameter in CEoS; Adjustable constant in the compositional k_{ij} correlation, Eq. 4.11
B	Adjustable constant in modified Henry's law model, Eqs. 5.2, 5.3; Adjustable parameter in yield uncertainty correlation, Eq. A1
b_{ij}	Adjustable constant to capture temperature dependence, Eq. 2.7
c	Volume translation term, Eq. 4.4
C	Adjustable constant in the modified Henry's law model, Eq. 5.2
$g(v)^{ref}$	Radial distribution function for the reference fluid in SAFT EoS,
H	Henry's constant, Eqs. 5.1, 5.2
H/F	Heavy phase split ratio
k_{ij}	Adjustable interaction parameter
k_{ij}^0, k_{ij}^1, *and* k_{ij}^2	Interaction parameters in temperature dependence estimation of k_{ij}, Eq. 4.8
K	Equilibrium constant, Eq. 2.1
m	Mass, Eq. 5.4
n	Adjustable parameter in the Gao correlation, Eq. 4.7
P	Pressure
P_c	Critical pressure, Eqs. 4.2, 4.3
P_{sat}	Saturation pressure, Eq. 5.1
P_v	Vapor pressure, Eq. 5.1
R	Universal gas constant, 8.314 J/mol*K
T	Temperature
T_R	Reduced temperature
T_c	Critical temperature
v	Molar volume
w	Mass fraction, Eqs. 4.11, A1
x	Mole Fraction

Superscripts

F	Feed component
H	Heavy phase
L	Light phase

Subscripts

asph	Asphaltene component
bit	Bitumen component
c3	Propane component
C5	*n*-Pentane component
i	Component i
j	Component j
m	Mixture
solv	Solvent component

Greek symbols

α	Alpha function in CEoS,
$\beta^{A_iB_j}$	Association volume parameter in CPA EoS,
δ	Solubility parameter
$\varepsilon^{A_iB_j}$	Association energy parameter in CPA EoS,
$\Delta^{A_iB_i}$	Association strength between two sites from two different molecules
ω	Acentric factor
χ_{A_i}, χ_{B_j}	Mole fraction of molecule i or j not bonded at A or B-sites with other active sites
γ	Activity coefficient

Abbreviations

APR	Advanced Peng Robinson EoS
AET	Atmospheric Equivalent Temperature
AVR	Athabasca Vacuum Residue
BPR	Back Pressure Regulator
CDvdW	Compositionally Dependent van der Waals mixing rules
CEoS	Cubic Equation of State
CPA	Cubic Plus Association EoS
DSC	Differential Scanning Calorimetry
EoS	Equation of State
ES-SAGD	Expanding Solvent SAGD
GC	Gas Chromatograph
HPM	High Pressure Microscope
LLE	Liquid-Liquid Equilibrium
MRS	Modified Regular Solution
NBP	Normal Boiling Point
PC-SAFT	Perturbed Chain Statistical Associating Fluid Theory
PNA	Paraffins-Napthenes-Aromatics
PR	Peng Robinson EoS

P-X	Pressure-Composition
SAFT	Statistical Association Fluid Theory
SAGD	Steam Assisted Gravity Drainage
SANS	Small Angle Neutron Scattering
SAR	Saturates-Aromatic-Resins
SARA	Saturates-Aromatics-Resins-Asphaltenes
SAXS	Small Angle X-Ray Scattering
SimDist	Simulated Distillation
SRK	Soave-Redlich-Kwong EoS
SvdW	Symmetric van der Waals mixing rules
TBP	True Boiling Point
VAPEX	Vapor Extraction
VLE	Vapor-Liquid Equilibrium
VPO	Vapor Pressure Osmometry
WA	With Association
WOA	Without Association

Chapter 1: Introduction

Heavy oil and oil sands are unconventional resources expected to play an essential role in the world oil supply, particularly in North America. The heavy oil resources of the world are about 10 trillion barrels; nearly three times the conventional oil in place (Ali, 2015). Alberta has proven oil reserves of 170 billion barrels, of which 168 billions are bitumen and heavy oil resources (Ali, 2015). Shallow deposits (oil sands) are mined while deeper deposits (*in situ* heavy oil and bitumen) must be produced from oil wells.

By definition, heavy oils have a density between 10 and 20 API and bitumens a density below 10 API (Gray, 1994). Their viscosities range from 1000 to over 1,000,000 mPa.s at reservoir conditions. One reason for their high viscosity is their relatively low content of light components and high content of asphaltenes. Asphaltenes are the densest, highest molecular weight, most aromatic, and most polar fraction of a crude oil. They are defined as the fraction of crude oil insoluble in an excess volume of a paraffinic solvent (usually *n*-pentane or *n*-heptane) but soluble in aromatic fluids, such as toluene (Speight, 2007). Under certain conditions, asphaltenes can separate from the oil and form deposits that plug flowlines and foul equipment (Mullins, 2008; Sheu, 2002).

For convenience, in general in this thesis, *in situ* heavy oil or bitumen will be referred to as heavy oil. Heavy oils are challenging to produce because they are so viscous. Most commercially successful *in situ* recovery processes for heavy oil are based on steam-based injection methods. Steam is used to reduce the oil viscosity so that the oil can flow and be produced (Farouq Ali, 2013). However, thermal methods are energy and water intensive and; therefore, are relatively expensive and have a high greenhouse gas fingerprint.

One approach to reduce the intensity of thermal processes is to co-inject a low molar mass *n*-alkane with the steam. In this case, the heavy oil viscosity is decreased from both heat conduction and the diffusion of the solvent into the oil (Memarzadeh and Rahnema, 2015). Solvent assisted steam processes, such as the expanding solvent-SAGD (ES-SAGD) process, have been successfully field-tested resulting in improved oil rates, improved oil to steam ratios, as well as the reduction

of the water and energy requirements compared to SAGD (Nasr *et al*., 2003). However, it is challenging to predict the performance of solvent-added recovery methods, particular solvent losses in the reservoir, partly because the phase behavior of mixtures of heavy oil and solvents is not well known. The introduction of a low molar mass solvent can lead to complex phase behavior such as the formation of vapor-liquid (VL), liquid-liquid (LL), VLL, and possibly VLLL (where the liquids are solvent-rich, bitumen-rich, asphaltene-rich phases) regions depending on the solvent type, content, temperature, and pressure (Mehrotra and Svrcek, 1988; Zou *et al.*, 2007; Badamchi-Zahed *et al.*, 2009a; Dini *et al.*, 2016). The phase behavior of heavy oil and solvent mixtures is also a key factor for surface processes, such as deasphalting, and for flow assurance issues, such as asphaltene precipitation and further deposition.

To design and optimize processes involving mixtures of heavy oil and *n*-alkanes, an accurate prediction of the phase behavior is required over the entire range of process conditions including the number and type of phases, the amount of each phase, the phase composition, and the properties of the phases. Such data have been reported for mixtures of various *n*-alkanes with bitumen. In mixtures of methane and bitumen, only liquid and vapour (VL) regions have been reported (Mehrotra and Svrcek, 1985). However, both VL and VLL regions have been observed (Mehrotra and Svrcek, 1985) for ethane-bitumen systems where the two liquid phases are a solvent/maltene-rich and a bitumen-rich phase. It is well known that mixtures of *n*-pentane (or higher carbon number *n*-alkanes) and bitumen can form two liquid phases, a solvent/maltene-rich phase and an asphaltene-rich phase (Akbarzadeh *et al.*, 2005). Johnston *et al*., (2007) observed the formation of VL and confirmed the existence of LL regions for *n*-pentane diluted bitumen. Up to approximately 20 wt% of the bitumen reported to the asphaltene-rich phase (typical composition of approximately 50 wt% asphaltenes and 25 wt% *n*-pentane), depending on temperature and pressure. Three liquid phases (VLLL) were observed in mixtures of *n*-pentane and an Athabasca vacuum residue (AVR) (Zou *et al.*, 2007).

The asphaltene-rich phase exhibits a glass transition that depends on the temperature and the composition of the asphaltene-rich phase. Below its glass transition temperature, it appears as glassy particles (Rastegari *et al*., 2004) due to the kinetic inability of the droplets to coalesce

(Sirota, 2005). Above its glass transition temperature, it appears as spherical droplets which coalesce forming a separate liquid phase (Agrawal *et al*., 2012; Johnston *et al*., 2017a). Hence, the amount, composition, and properties of asphaltene-rich phase can vary considerably with conditions.

Other than saturation pressure measurements, there are relatively few public sources of data for mixtures of propane or butane and bitumen and it is not yet fully established what phases form in these mixtures at different conditions. Badamchi-Zadeh *et al.* (2009a) and Jossy *et al.* (2009) observed VL and LL boundaries for propane diluted bitumen but did not measure phase compositions. Dini *et al.* (2016) also observed VL and LL regions and predicted a VLL boundary. However, they also did not directly measure the composition of the liquid phases or their morphology.

The phase behavior of mixtures of bitumen and solvent, particularly asphaltene yields, is challenging to predict. Regular solution based models (Yarranton and Masliyah, 1996; Alboudwarej *et al*., 2003; Akbarzadeh *et al*., 2005; Tharanivasan *et al*., 2011; Powers *et al*., 2016) are capable of fitting asphaltene data and predicting the effect of hydrocarbon solvents on asphaltene precipitation. However, they are limited to the liquid-liquid phase region and, as currently implement, do not allow solvent to partition to the heavy phase.

Cubic equations of state (CEoS) are widely used in most commercial software for modeling the phase behavior of crude oils. These models are capable of predicting the full range of phase behavior but, until recently, have had limited success in predicting the amount of heavy phase in the LL region, as will be discussed in more detail later. Chapman and coworkers (Chapman *et al*., 1989; Ting *et al*., 2003; Gonzalez *et al*., 2005, 2007; Panuganti *et al*., 2012, Alhammadi *et al*., 2015) have modeled a range of petroleum phase behavior, including VL and LL boundaries, using the Perturbed Chain form of Statistical Association Fluid Theory (PC-SAFT). Kontogeorgis, Firoozabadi and coworkers (Kontogeorgis and Folas, 2009; Li and Firoozabadi, 2010a, 2010b; Arya *et al*., 2015, 2016a, 2016b) have shown similarly promising results using the Cubic Plus Association equation of state (CPA EoS). Both models require a more complex flash than a

conventional cubic equation of state, are more challenging to tune, and have not been tested on phase composition data for the LL region with petroleum fluids.

To use an equation of state, a complete fluid characterization is required including the molecular weight, density, and critical properties of each component or pseudo-component of the crude oil. However, a complete compositional analysis for heavy oils is not available. Instead, characterizations are usually constructed from distillation or gas chromatographic assays. For example, a distillation curve is divided into a number of pseudo-components each representing a boiling cut. Correlations are used to set the properties of each pseudo-component. Once the characterization is set, the equation of state is tuned to match measured phase behavior data by adjusting binary interaction parameters for pairs of components.

This thesis is built on a previously developed equation of state framework work (Castellanos *et al.*, 2011). They developed a distillation assay based methodology to characterize Athabasca bitumen and model the phase behavior of *n*-pentane and bitumen mixtures using the Advanced Peng Robinson Equation-of-State implemented in VMGsim software. Agrawal *et al*., (2012) introduced temperature-dependent binary interaction parameters to this model to predict the VL equilibria data at high temperatures. The interaction parameters between *n*-pentane and the bitumen pseudo-component were tuned to successfully model the saturation pressures and the VLL boundary region for these mixtures. However, the model under-predicted the heavy phase yields at high dilution. The model does not correctly determine the activity coefficients in each liquid phase at all compositions and therefore could not match both the LL boundary and the heavy phase yields. This deficiency could not be overcome with the binary interaction parameters used in this study.

Johnston *et al*., (2017b) evaluated this CEoS approach with several sets of asymmetric mixing rules to model *n*-pentane diluted bitumen systems. The match to the asphaltene yield data was significantly improved; however, the yields at high dilution were under-predicted. They then introduced compositionally dependent solvent-asphaltene binary interaction parameters to

accurately fit asphaltene yield data over the entire composition range. To date, this approach has only been tested on mixtures of *n*-pentane/bitumen and live heavy oil diluted with condensate.

1.1 Objectives

The phase behavior of mixtures of *n*-pentane and bitumen was recently mapped over conditions relevant to heavy oil processes (Johnston *et al*., 2017a). A modeling approach using the APR EoS with compositionally dependent mixing rules was also developed to model these data (Johnston, 2017). Similar data have yet to be collected and modeled for other solvents such as propane. Propane is of interest because it has a low dew point pressure and therefore is suitable for solvent-added and solvent based recovery processes, particularly for the VAPEX process (Nourozieh *et al*., 2015).

The overall objectives of this thesis are to:

1. Map the phase behavior of mixtures of propane and bitumen, including phase boundary diagrams, heavy pitch phase (solvent-free basis) yield curves, the heavy pitch phase morphology, and the composition of both the light solvent-rich phase (L_1) and the heavy pitch phase (L_2)
2. Test the ability of the APR EoS with symmetric and composition dependent mixing rules to predict the phase behavior data.

Specific objectives for this project are:

1. Determine the VL boundary for propane diluted bitumen systems from saturation pressures measured in blind cells.
2. Identify the LL boundary for mixtures of propane and a Western Canadian bitumen from onset data (solvent content at which heavy pitch phase appeared) measured in a high pressure microscope (HPM) apparatus.
3. Study the morphology of the heavy pitch phases through micrograph images taken from a digital camera.
4. Develop a procedure to measure pitch-rich and propane-rich phase composition data and construct pseudo-ternary diagrams from samples obtained using PVT cell in the LL region.

5. Construct *n*-pentane-insoluble asphaltene (C5-asphaltene) and solvent-free pitch (pitch*) yield curves for propane diluted bitumen systems from light solvent-rich phase composition measure in blind cells and a material balance.
6. Test the ability of a cubic equation of state to predict the phase behavior of heavy oil and propane mixtures including the modeling of the saturation pressures, heavy pitch phase onset, phase composition, and C5-asphaltene and pitch* yields measured data.

The investigation was performed on a Western Canadian bitumen at temperatures from 20 to 180°C and pressures up to 10 MPa. The APR (Advanced Peng Robinson) EoS (VMG 2017) with the temperature dependent binary interaction parameters and compositionally dependent binary interaction parameters was selected to model the data. The Peng Robinson cubic EoS is commonly used in oil industry applications and the APR version has successfully modeled phase boundaries for mixtures of heavy oil and solvents in previous studies (Castellanos *et al*., 2011; Agrawal *et al*., 2012; Johnston *et al*., 2017).

1.2 Thesis Structure

This project is organized in six chapters as follows:

Chapter Two provides some background on the phase behavior of mixtures involving heavy oil and solvents. It includes a brief review of the chemistry and characterization of crude oils, a discussion of the observed phase behavior of heavy oil/solvent systems, and a description of the more successful thermodynamic models for the phase behavior of solvent diluted heavy oil.

Chapter Three outlines the experimental methods used in this thesis starting with the materials (bitumen samples and solvents) used. The distillation assays and property measurements for the bitumen samples are presented. The experimental procedures are provided including saturation pressure, heavy pitch phase onset, heavy phase yields, and phase composition measurements.

Chapter Four provides the oil characterization and modeling approaches employed in this thesis. The oil characterization includes the extrapolation of the true boiling point curve from deep vacuum distillation assay data; the definition of the pseudo-components, and; the correlations used for the estimation of their critical properties and acentric factors. The APR EoS is presented including the application of symmetric and compositionally dependent binary interaction parameters.

Chapter Five presents the experimental and modeling results. The data collected to map the phase behavior of propane diluted bitumen systems is discussed, including saturation pressure, heavy pitch phase onset, C5-asphaltene and pitch* yields, and phase composition data. The performance of the APR EoS with symmetric and compositionally dependent mixing rules is assessed.

Chapter Six highlights the major outcomes of the project and provides guidance for future studies.

Chapter 2: Literature Review

This chapter provides a review of the known phase behavior of mixtures of heavy oil or bitumen and solvents. First, the chemistry and characterization of crude oils are reviewed, particularly the characterization techniques required as input to phase behavior models. Previous studies on the phase behavior of bitumen and *n*-alkanes solvent mixtures are summarized, including the identification of multiphase regions, phase boundaries, asphaltene yields, and the phase morphology of the asphaltene-rich heavy phase. Finally, the current and the most successful thermodynamic models used to represent the phase behavior of heavy oil/solvent systems are presented.

2.1 Chemistry of Crude Oil

Petroleum is defined as naturally occurring hydrocarbon mixture, usually encountered in sedimentary rocks in the form of a gas (natural gas), liquid (crude oil), semi-solid (bitumen), or solid (asphaltite). Petroleum may also contain sulfur, nitrogen, oxygen, metals, and other elements (Speight, 2007; Riazi, 2005). Crude oil composition varies from field to field and, in some cases, from well to well or with depth. Crude oils are typically classified based on their API gravity (density) and viscosity, Table 2.1 (Gray, 1994).

Table 2.1 UNITAR classification of petroleum by its physical properties at standard temperature of 15.6°C adapted from Gray (1994).

Classification	Viscosity MPa*s	Density kg/m^3	API Gravity
Conventional Oil	$<10^2$	<934	>20°
Heavy Oil	10^2-10^5	934-1000	20°-10°
Bitumen	$>10^5$	>1000	<10°

The chemical species present in petroleum cover a wide range of molecular weights and boiling points. The complexity of the molecules increases with molecular weight and boiling point as shown in Figure 2.1. These hydrocarbon and non-hydrocarbon compounds can be classified into the following chemical families (Altgert and Boduszynsky, 1994):

- Paraffins: saturated hydrocarbons that consist of either straight chains (normal paraffins) or branched chains (isoparaffins).
- Naphthenes (cycloparaffins): saturated hydrocarbons that include ring structures. The majority of naphthenes in crude oils have one or more paraffinic side-chains, as well as more than one ring in the molecule.
- Aromatics: cyclic but unsaturated hydrocarbons compounds containing at least one aromatic group such as a benzene ring. Aromatics in crude oil can include paraffinic side chains and/or naphthenic rings.

Many of these species are heterocompounds; that is, hydrocarbon molecules in which one or more heteroatoms (S, O, N, and other metallic constituents) are attached to them. The presence of heteroatoms complicates even further the complete characterization of crude oil due to its higher molecular complexity. Although heteroatoms show up within the entire range of boiling range of crude oil, they are commonly concentrated in the heavier fractions.

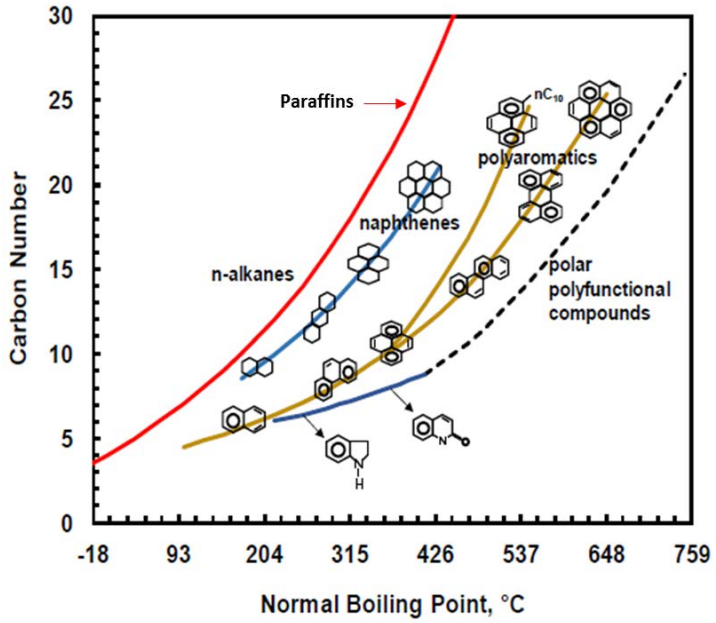

Figure 2.1 Relationship between carbon number, boiling point, and structure of chemical compounds in crude oil. Adapted from Altgelt and Boduszynsky, (1994).

The aromatics can be considered as a continuum of species of increasing molecular weight, density, heretoatom content, aromaticity, and polarity. They can be further subdivided based on a SARA assay which separates a crude oil into three adsorption classes, saturates (S), aromatics (A), and resins (R), and one solubility class, asphaltenes (A). First, the asphaltenes are precipitated with the addition of an excess of an *n*-alkane, commonly *n*-pentane or *n*-heptane. Saturates, aromatics, and resins (SAR) are then separated through liquid chromatography as shown in Figure 2.2.

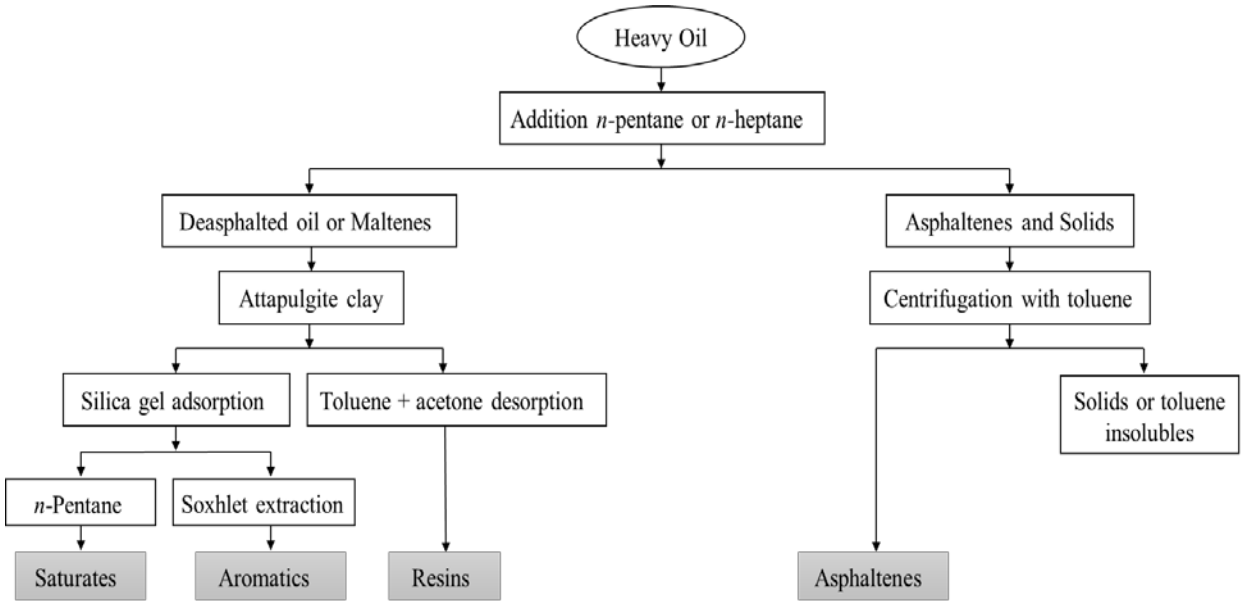

Figure 2.2 Scheme of the SARA fractionation procedure (Powers, 2014).

The SARA fractions are chemically distinct as described below:

- Saturates consist primarily of heavy paraffins and cycloparaffins (Speight, 2007) with molecular weights between 300 and 600 g/mol and densities between 0.869 and 0.880 g/cm³ (Powers, 2014). They are the least polar fraction of the crude oil.
- Aromatics contain one or more aromatic ring with alkyl-chains. Naphthenic rings can also be linked to aromatic rings (Speight, 2007). Their molecular weights range from 300 and 800 g/mol and their densities from 0.990 and 0.999 g/cm³ (Powers, 2014).
- Resins are similar to aromatics but have higher polarity and lower H/C ratios (Speight, 2007). They have larger aromatic cores with naphthenic rings, alkyl side chains, and some

heteroatomic species. Their molecular weights range from 700 and 1300 g/mol and their densities from 1.044 and 1.049 g/cm³ (Powers, 2014).

- Asphaltenes are similar to resins but are the densest, highest molecular weight, and most polar compounds of the crude oil. This fraction includes a wide variety of structures containing aromatic rings with paraffinic chains, naphthenic rings, and heteroatoms (Speight, 2007). Asphaltenes, or some of the asphaltenes, self-associate into nano-aggregates (Yarranton *et al*. 2013; Mullins, 2008). The molecular weight and density of asphaltene monomers is considered to be between 500 and 2000 g/mol (Yarranton *et al*. 2007; Mullins, 2007), and 1078 and 1146 kg/m^3 (Barrera *et al*. 2013), respectively. Since asphaltenes are larger and more polar molecules and they self-associate, they can separate from the oil as a second heavy phase under certain conditions, as will be discussed later.

SARA assays from a number of heavy oils and bitumens are provided in Figure 2.3. SARA assays are used by refiners as one input for reaction modeling. The SARA assay is also used as a starting point for modeling asphaltene phase behavior with the regular solution approach to be discussed later. Since asphaltenes are an important factor in heavy oil and bitumen phase behavior, their chemistry is discussed in more detail below.

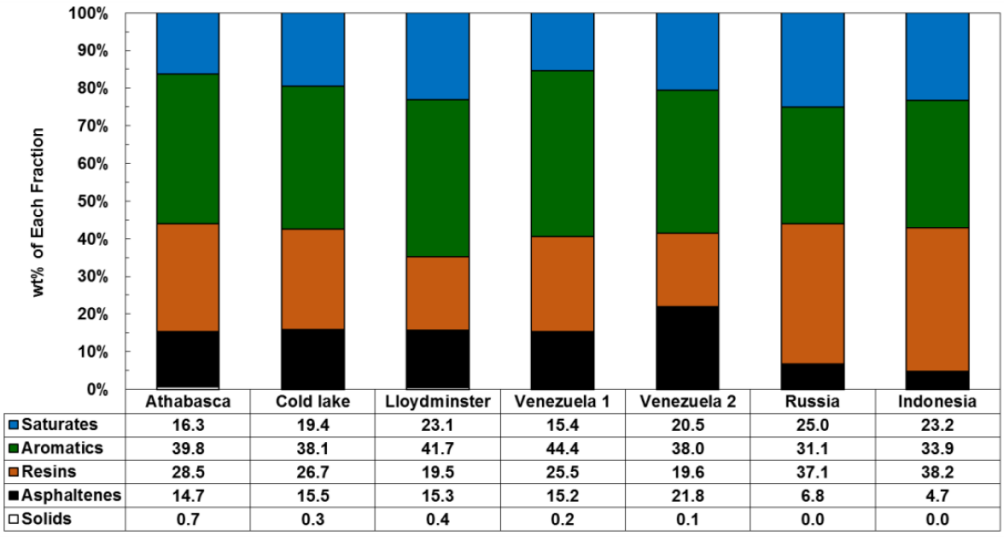

	Athabasca	Cold lake	Lloydminster	Venezuela 1	Venezuela 2	Russia	Indonesia
Saturates	16.3	19.4	23.1	15.4	20.5	25.0	23.2
Aromatics	39.8	38.1	41.7	44.4	38.0	31.1	33.9
Resins	28.5	26.7	19.5	25.5	19.6	37.1	38.2
Asphaltenes	14.7	15.5	15.3	15.2	21.8	6.8	4.7
Solids	0.7	0.3	0.4	0.2	0.1	0.0	0.0

Figure 2.3 SARA composition results of conventional and heavy oils from different sources (Powers, 2014).

There are two asphaltene molecular structure models that have been widely used to represent asphaltene molecules: the condensed (island/continental) and the dispersed (archipelago) structures, Figure 2.4. The "condensed" structure as its name reflects it consists of a highly condensed aromatic core with alkyl chains on the periphery (Dickie and Yen, 1967). The dispersed structure, otherwise, consists of smaller aromatic clusters linked with aliphatic bridges (Straunz *et al*., 1992).

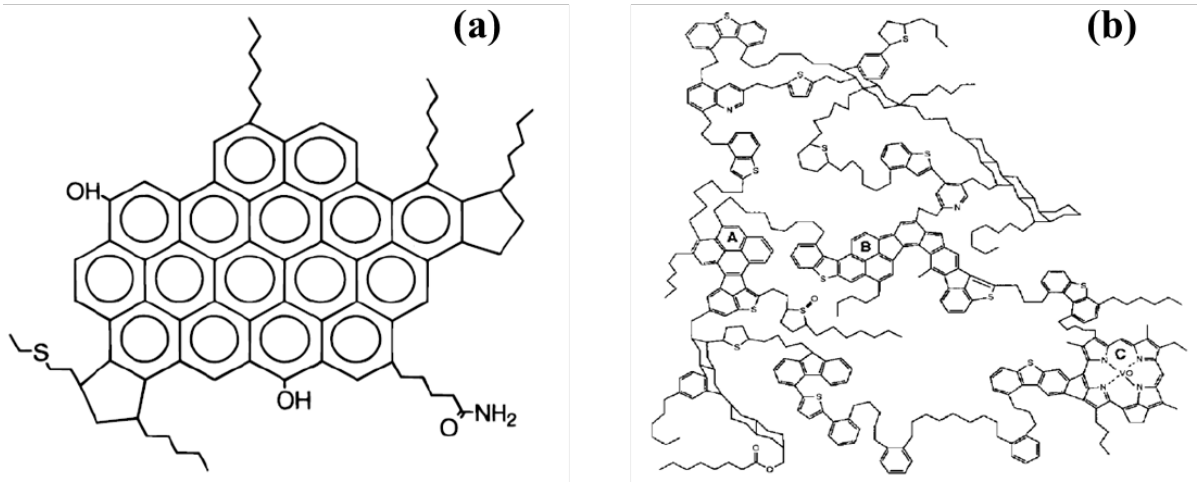

Figure 2.4 Hypothetical asphaltene molecular structures: (a) condensed asphaltene molecular structure, (b) dispersed asphaltene molecular structure (Tharanivasan thesis, 2012).

These two molecular structures lead to different asphaltene self-association models, the colloidal and the oligomer model. The colloidal model is based on the continental structure and considers asphaltenes to be colloids formed from stacks of molecules held together with π-π bonds (Dickie and Yen, 1967). The colloids are believed to be dispersed in the oil by resins adsorbed on the surface of the colloid or concentrated around it. The oligomer model is based more on the archipelago structure and assumes that asphaltene nano-aggregates are formed from monomers linked together in a manner analogous to polymerization but via π-π, acid-base, and/or hydrogen bonds rather than covalent bonds (Agrawala and Yarranton, 2001). The nano-aggregates are believed to be in solution with the oil rather than dispersed within it.

2.2 Crude Oil Characterization for Phase Behavior Modeling

To design and optimize processes involving mixtures of bitumen and solvent, accurate prediction of the phase behavior and physical properties of these systems are required over the entire range of upstream and downstream process conditions. The first step to carry out the modeling of the phase behavior is to represent the property distribution within the crude oil. Crude oil encompasses a great variety of hydrocarbons with a wide range of organic functionality, size, and molecular weight. Therefore, a complete compound-by compound description of the constituents of the crude oil is currently impossible and, in any case, would be impractical (Speight, 2007). Instead, crude oils are typically characterized as a series of pseudo-components representing boiling point cuts (Katz and Firoozabadi, 1978; Castellanos-Diaz *et al*., 2011) or molecular weight cuts (Whitson and Brule, 2000).

In refinery applications, conventional crude oils are commonly characterized based on distillation assays along with the average density and molecular weight of the crude oil. In downhole applications, a gas chromatography assay is often used instead of a distillation assay. The characterization of bitumen and heavy oil is more challenging due to its high content of large and complex molecular species. Only 20 to 30 wt% of a bitumen basis can be vacuum distilled or separated into GC cuts and therefore the bulk of the bitumen must be characterized based on extrapolated properties (Castellanos-Diaz *et al*., 2011). Each type of assay is described below.

2.2.1 Distillation

Distillation separates chemical compounds based on the difference in their vapor pressures; in other words, by the difference in their volatility (Speight, 2007). For a multi-component fluid like a heavy crude oil, a distillation curve is obtained as shown in Figure 2.5. The complexity of compounds increases with molecular weight and thus boiling point; paraffinic derivatives tend to be distilled first followed by aromatic derivatives and heteroatom derivatives compounds. Advantages of distillation are that the boiling points are measured directly and the physical properties of the distillation cuts can be measured directly. The main disadvantage is that distillation is relatively slow and costly.

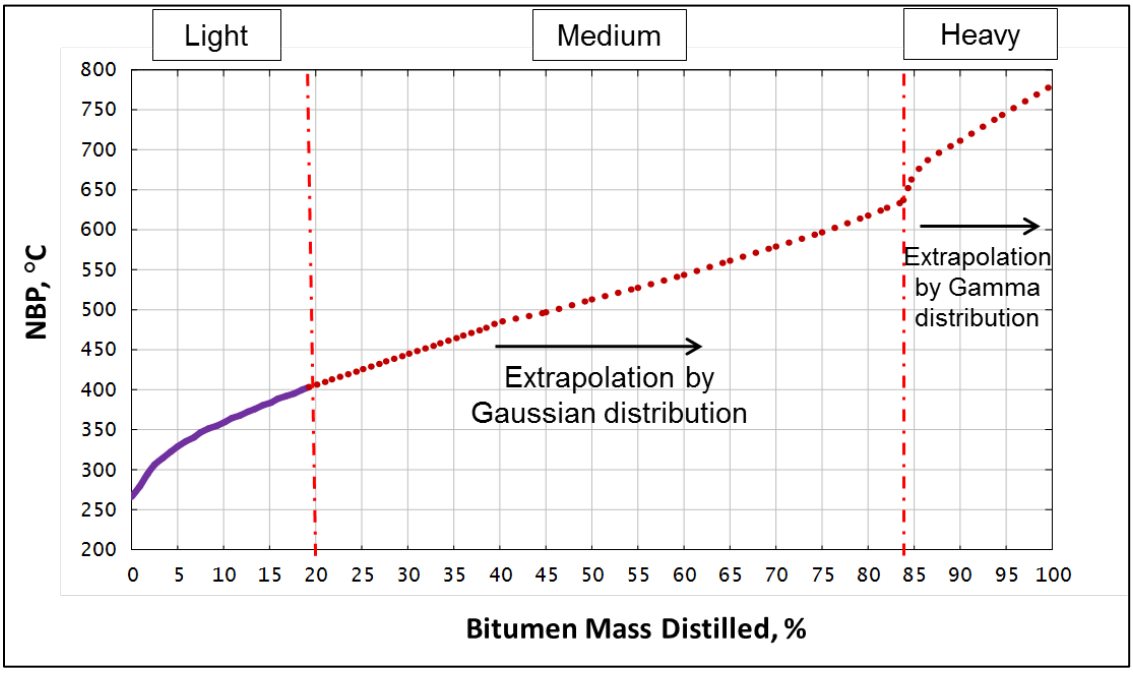

Figure 2.5 NBP curve for a heavy oil: solid line is a spinning band vacuum distillation; dotted line until 40% bitumen distilled is a deep vacuum fractionation; dotted line after 40% is an extrapolation using a Gaussian distribution for the maltenes and a Gamma distribution function for the asphaltenes.

Several distillation techniques have been developed for crude oils, such as ASTM D2892 (TBP), ASTM D5236, ASTM D86, ASTM D1160, and SBD adapted from ASTM 2892 (Sanchez, 2015; Powers, 2012). True boiling point (ASTM Standard D2892 2009) distillation is the most accurate method to estimate boiling point ranges for a petroleum stream. However, TBP is not practical in most applications because it is time consuming and costly. Not all methods are suitable for heavy oil and bitumen, especially those which are performed at atmospheric conditions where little of the oil is distillable. Reduced pressure distillation techniques have been developed to extend the range of distillable materials and provide a better characterization, principally for heavy oil and bitumen. Reduced pressure distillation allows more material to be distilled at temperatures below the cracking temperature (approximately 300°C) because the boiling points of each component is reduced at lower pressure (Speight, 2007). In general, atmospheric distillation techniques can distill up to approximately 5 wt% of the bitumen, whereas at reduced pressures can reach up to

approximately 30 wt% without thermal cracking. The measured boiling points obtained in vacuum distillation must be converted to atmospheric equivalent temperature.

Castellanos-Diaz *et al*., (2014) designed an apparatus and a methodology capable of distilling up to 50 wt% of the bitumen without generating cracked samples. Operation pressures as low as 10^{-6} Pa. The equipment also allows the collection of 6 distilled fractions which are subjected to further measurements such as determination of their physical properties. The low pressure boiling point were interconverted to atmospheric equivalent temperature following the methodology established by Sanchez-Lemus *et al*., (2014).

2.2.2 Gas Chromatography

Gas chromatography (GC) is a separation method based on retention times of the components of the crude oil on a packed column. The retention time is correlated to the component carbon number in conventional GC assays and to boiling point in simulated distillation (SimDist) assays. The advantage of GC is that is a simple, fast, reproducible, and more economical method compared to laboratory-scale physical distillation. However, it is an indirect measurement of the boiling points. The accuracy of the method depends on the calibration of the equipment and the validity of the correlation used for the boiling points.

Several standard test methods for determination of boiling range distribution of crude oil by gas chromatography have been developed. The four most commonly used methods are ASTM D2887, D5307, D6352, and D7169. ASTM D7169 extends the applicability of SimDist to the heavier fraction of the crude oil. It encompasses wide range of boiling point temperature, about 720°C, representing the elution of *n*-C_{100} (Vickers, 2002). However, the extrapolation over non-distillable part of the oil is not supported by experimental data and deviates from recent data collected for heavy cuts (Sanchez-Lemus, 2015). The correlations used in SimDist may deviate with the high content of aromatic compounds.

2.2.3 Oil Characterization Based on Distillation Assays

In this thesis, distillation assays will be used for characterization heavy oil and bitumen. Sanchez-Lemus *et al*., (2014) developed a methodology and correlations capable of characterizing heavy oils based on conventional distillation data. They demonstrated that using a Gaussian extrapolation approach was sufficient to extrapolate the maltene (everything that is not asphaltenes) boiling points from spinning band distillation data, Figure 2.5. The remaining part of the NBP curve, the C5-asphaltenes (pentane insoluble asphaltenes), was characterized using a Gamma distribution function. This function has been demonstrated that represent the molecular weight distribution of asphaltene nano-aggregates for phase behavior modeling (Huang *et al*., 1991; Alboudwarej *et al*., 2003, Castellanos-Diaz *et al*., 2011, Agrawal *et al*., 2012, and Johnston *et al*., 2017a).

To generate the set of representative pseudo-component constituents of the crude oil, the boiling point distribution is divided into mass fractions, each of which represents a boiling range. Based on the information required to perform the phase behavior modeling, properties are assigned to each pseudo-components using empirical correlations such as the Riazi-Daubert (Riazi and Daubert, 1987), Lee-Kesler (Lee and Kesler, 1975) or Twu correlations (1984). The correlations are constrained or tuned to match experimental data such as the average molecular weight and density of the oil. The oil characterization methodology used in this thesis is described in more detail in Chapter 4.

2.3 Bitumen/*n*-Alkane Phase Behavior

2.3.1 Bitumen/n-Alkane Phase Regions

Most proposed solvent based *in situ* processes for heavy oil and bitumen involve *n*-alkane solvents. The reported phase behavior of mixtures of bitumen and an *n*-alkane includes vapor-liquid (VL), liquid-liquid (LL), VLL, and possibly VLLL regions, depending on the solvent type, content, temperature, and pressure conditions (Mehrotra and Svrcek, 1988; Zou *et al*., 2007; Badamchi-Zahed *et al*., 2009a; Dini *et al*., 2016). The range of phase behavior encountered at typical process conditions depends strongly on the carbon number of the *n*-alkane. For mixtures of methane and bitumen, only vapor and liquid (VL) regions have been reported (Mehrotra and Svrcek, 1985), as

shown in Figure 2.6a. The solubility of the methane in the bitumen is too low to generate a second liquid phase. For ethane-bitumen systems, both VL and VLL regions have been observed (Mehrotra and Svrcek, 1985), Figure 2.6b. The two liquid phases formed were a solvent/maltene-rich and a bitumen-rich phase.

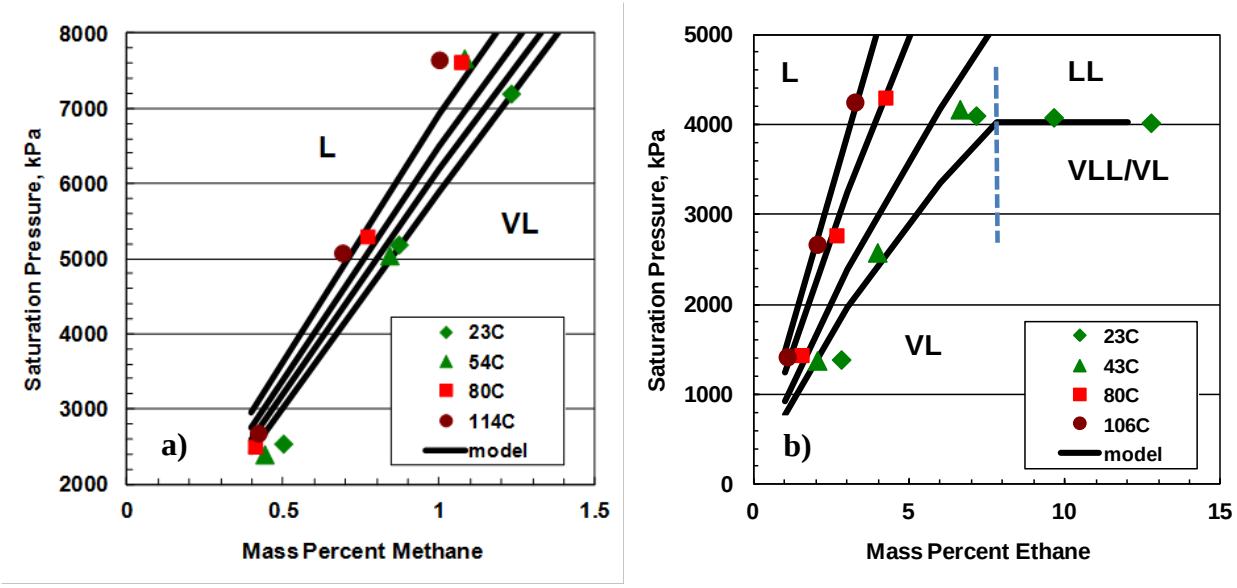

Figure 2.6 Pressure-composition phase boundary diagrams for mixtures of: a) methane and Peace River and b) ethane and Peace River bitumen (Mehrotra and Svrcek, 1985).

Both VL and LL regions were observed for mixtures of bitumen and propane (Badamchi-Zadeh *et al.*, 2009a; Jossy *et al.*, (2009); Nourozieh *et al.*, 2015). Dini *et al.*, (2016) also observed VL and LL regions and predicted a VLL boundary. They identified the two liquid phases as a solvent/maltene-rich and a bitumen-rich phase. Similarly, both VL and LL regions were observed for mixtures of Frog Lake heavy oil and butane (Yazdani and Maini, 2010) observed. The nature of the two liquid phases were not reported. Phase compositions were not reported for any of these mixtures.

Both VL and LL phase boundaries were also observed for *n*-pentane and bitumen systems (Johnston *et al.*, 2017a). The two liquid phases were a solvent/maltene-rich phase (L_1) and an asphaltene-rich phase (L_2). The asphaltene-rich phase appeared as glassy particles at temperatures below 90°C and as a liquid phase above 140°C, Figure 2.7. In this case, the *n*-pentane had a high

solubility in the bitumen but was incompatible with the asphaltenes, rejecting an asphaltene-rich phase. Approximately 20 wt% of the bitumen reported to the asphaltene-rich phase and the *n*-pentane content of this phase was approximately 25 wt%, depending on temperature and pressure (Johnston, 2017).

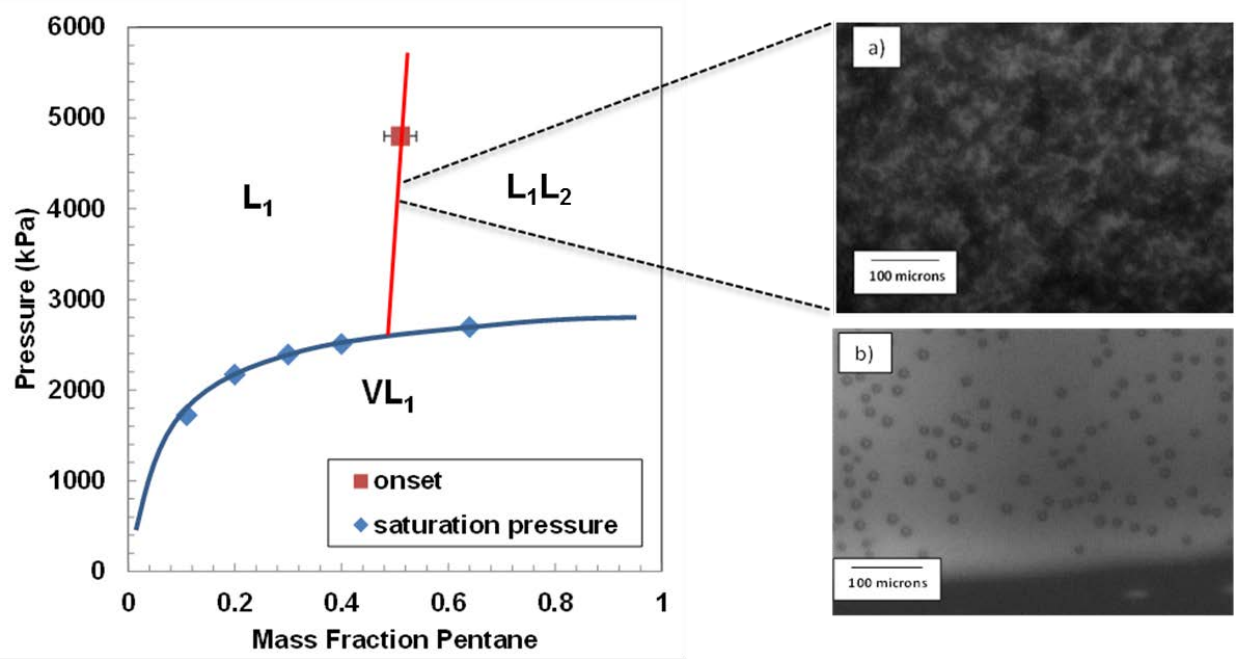

Figure 2.7 Pressure-composition diagram for *n*-pentane diluted bitumen at 180°C. Micrograph images on the asphaltene phase morphology at: 23°C (glass-like particles) and b) 165°C (liquid droplets) (Johnston *et al*., 2017a).

Zou *et al*., (2007) observed the formation of an unexpected four-phase zone (LLLV) in *n*-pentane and Athabasca vacuum residue (AVR) mixtures in an x-ray transmission tomography PVT apparatus. The three liquid phases were identified as a bitumen-rich phase (L_1), a solvent-rich phase (L_2), and an asphaltene-rich phase (L_3). The four phase equilibria region was observed over a narrow range of composition between the two three phase equilibria regions (L_1L_2V, L_2L_3V), Figure 2.8.

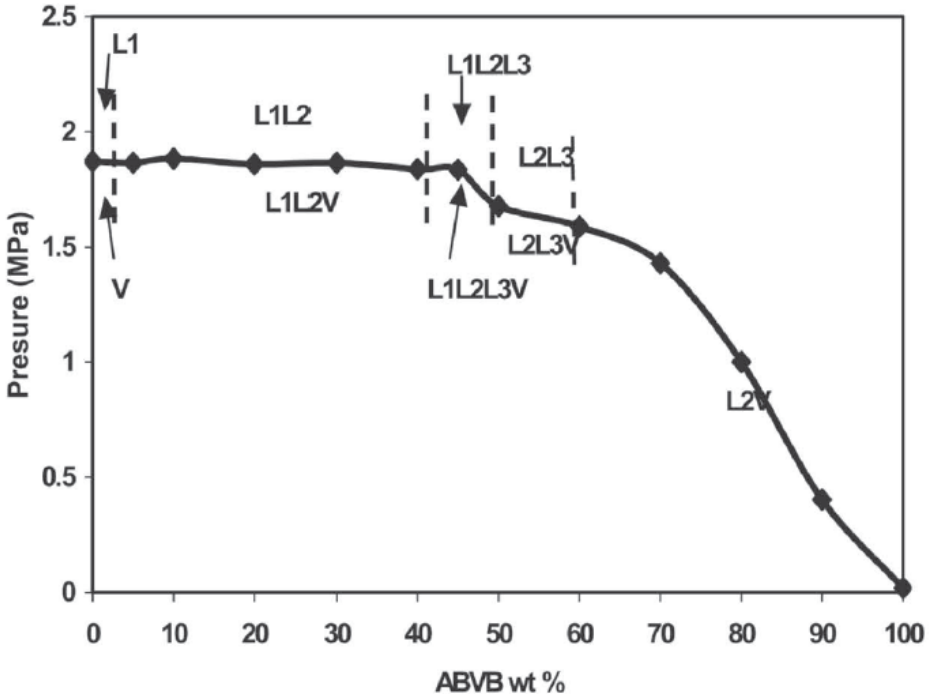

Figure 2.8 Pressure-composition diagram for vacuum bottom (ABVB) + pentane mixtures at 160°C (Zou *et al*., 2007). Note, the x-axis is the ABVB content in contrast with the other P-x diagrams in this thesis which are plotted versus the solvent content.

Most research on bitumen phase behavior has focused on asphaltene "precipitation"; that is the formation of an asphaltene-rich phase. Asphaltenes precipitate from crude oils upon a change in pressure, temperature, and/or composition. The onset of precipitation (the conditions at which the asphaltene-rich phase appears) is relevant for flow assurance. The amount of precipitation is relevant for deasphalting processes. This type of data is often presented as a yield curve as shown in Figure 2.9 for *n*-pentane diluted bitumen (Johnston *et al*., 2017a).

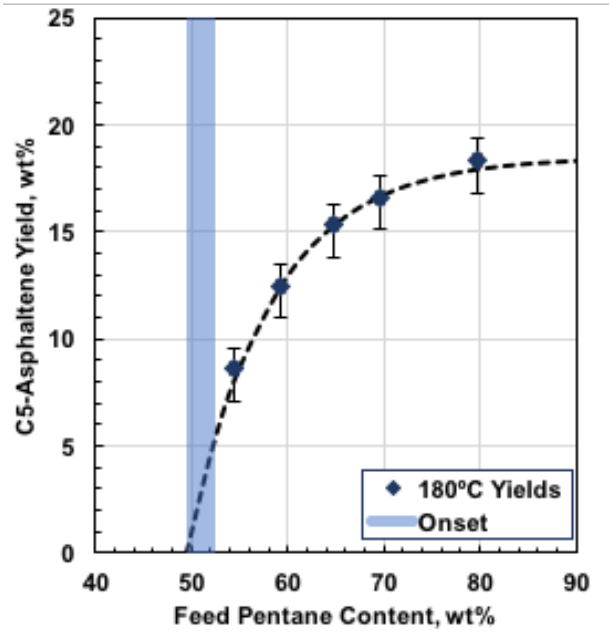

Figure 2.9 C5-asphaltene yield curve at 180°C for *n*-pentane diluted bitumen (Johnston *et al*., 2017a). Symbols are the experimental data and the shaded area is the onset (LL boundary).

For *n*-alkane diluted bitumen, asphaltene solubility increases (amount of heavy phase decreases) as the carbon number of the *n*-alkane solvent increases from 3 to 7 and increases slightly at carbon number above 10 (Hu and Guo, 2001; Andersen and Birdi, 1991; Mannistu *et al*., 1997; Ali and Al-Ghannam, 1981; Wiehe *et al*., 2005).

Asphaltenes in *n*-alkane diluted bitumen also become slightly less soluble at lower pressures (Akbarzadeh *et al*., 2005; Johnston *et al*., 2017a). The pressure effect on asphaltene phase separation is more pronounced for light oils far above their bubble point (Ting *et al*., 2003). Asphaltenes are barely soluble in these oils because the oils have a relatively high saturate content and saturates are a poor solvent for asphaltenes. Hence, asphaltenes tend to precipitate when the oil is depressurized and its density decreases (Joshi *et al*., 2001; Tharanivasan *et al*., 2011; Ting *et al*., 2003; Pedersen and Christensen, 2007). The maximum amount of asphaltene precipitated at a given temperature is encountered at its bubble point (Panuganti *et al*., 2012). Below the bubble point, the solubility of the asphaltenes increases and they redissolve as the light ends (methane, ethane, nitrogen, etc) evolve from the crude oil.

The temperature effect on the asphaltene solubility does not follow a definite trend. Asphaltene solubility appears to increase as the temperature increases up to 100°C (Akbarzadeh *et al*., 2005; Ali and Al-Ghannam, 1981; Hu and Guo, 2001). Andersen and co-workers (Andersen, 1994; Andersen *et al*., 1998) found that asphaltenes may become less soluble at temperature above 100°C but for a very limited dataset. Johnston *et al*., (2017a) found that asphaltene solubility in *n*-pentane diluted bitumen increased slightly to 100°C and decreased slightly above 130°C. The effect of temperature is best explained in terms of the activity coefficient of the asphaltenes which has been shown to depend on the ratio of molar volume of the asphaltenes to the molar volume of the solution and to the difference between the solubility parameter of the asphaltenes and the surrounding medium (Akbarzadeh *et al*., 2005; Tharanivasan *et al*., 2011; Powers *et al*., 2016). It has been proposed that an increase in temperature has opposing two effects: 1) it decreases the oil density relative to the asphaltene density; 2) it decreases the solubility parameter of the oil relative to the asphaltenes (Sirota, 2005). For example, the solubility parameter of the lower molecular weight and more aliphatic molecules decreases more with temperature than those of the asphaltenes. The first effect increases the relative molar volume of the asphaltenes which increases their solubility. The second effect increases the difference between the asphaltene and oil solubility parameters which decreases the asphaltene solubility. It appears that the molar volume changes dominates at temperatures below 100°C but the solubility parameter changes tend to dominate at higher temperatures.

2.3.2 Asphaltene-Rich Phase Morphology and Glass Transition

Asphaltenes precipitated from crude oils may present different phase morphology depending on the conditions such as solvent type, solvent content, and temperature (Sirota, 2005). The asphaltene-rich phase at temperatures below its glass transition temperature (T_g) appears as glassy particles (Rastegari *et al*., 2004) but at higher temperatures appears as a continuous liquid phase (Agrawal *et al*., 2012).

Kriz *et al*., (2011) examined the glass transition in asphalt binders and stated that the transition from liquid to glassy state is accompanied by sudden change in the thermodynamic properties of the fluid. As the viscosity of the fluid increased near the glass transition, the fluid became glossy

in appearance, brittle, and rigid. The glass transition of the asphalts depends on their molecular weight, functional groups, molecular interactions, and the solvent used for dilution. For example, the glass transition temperature (T_g) increases with the increase of molecular weight because large molecules are less mobile than small molecules (Fox *et al*., 1955; Kriz *et al*., 2011). Saturated molecules have a much lower glass transition temperature than unsaturated molecules because the attractive forces between saturated molecules are weaker (dispersion forces). Glass transition temperatures are also a function of pressure and have been shown to increase with pressure in polymers (Bianchi, 1965). The glass transition temperature in asphalt binders increased when pressure was applied on pavement by traffic (Kriz *et al*., 2011).

Zhang *et al*., (2004) used a differential scanning calorimetry (DSC) to study the thermal behavior of four asphaltenes obtained from different vacuum residue sources: Iranian Light (IL), Khafji (KF), Kuwait (KW, and Maya (MY) crude oils. They determined the glass transition temperature of all four asphaltenes to be between 120 and 130°C. The asphaltenes attained completely liquid behavior at temperatures between 220 and 240°C. Gray *et al*., (2004) evaluated the melting behavior of five different heptane-insoluble asphaltenes: Athabasca asphaltenes from Canada, Arabian Heavy and Light from Saudi Arabia, Gudao from China, and Maya from Mexico. They provided evidence for formation of liquid melt at temperature between 214 and 311°C and reported melting point ranging between 224 and 245°C except for the Maya which was significantly higher (294°C).

Johnston *et al*., (2017a) examined the phase behavior of heavy oil and *n*-pentane mixtures. They observed a glass transition temperature between 90 and 140°C. Below 90°C asphaltene rich phases appears as glassy particles, whereas above 140°C it appears as liquid droplets that coalescence into a continuous liquid phase. Between 90 and 140°C, the glass-like particles tend to form irregular but smoother shapes. Nielsen *et al*., (1994) found similar glass transition temperature ranging from 75-150°C for "*n*-pentane asphaltenes" precipitated from a Cold Lake bitumen. Mehrotra *et al*., (1989), otherwise, reported a softening temperature, similar to glass transition temperature, of approximately 100°C for the heaviest fraction of a Cold Lake bitumen.

2.4 Models for Bitumen/Solvent Phase Behavior

The phase behavior models applied to mixtures of bitumen and solvent include models specifically for asphaltene precipitation and equation of state based models for the full range of phase behavior. Each type of model is reviewed below.

2.4.1 Asphaltene Phase Behavior Models

There are two main types of asphaltene precipitation model: the colloidal model and the solution model. The colloidal model is based on the colloidal view of asphaltene association. In this model, asphaltene precipitation occurs when an external driving force strips the resins from the colloidal asphaltenes, allowing their aggregation and physical separation. In general, the colloidal models predict that the precipitation is an irreversible process. The solution model considers asphaltenes to be macromolecules that are in solution with the other crude oil components. Asphaltene precipitation is considered to be a phase transition and modeled as liquid-liquid equilibrium. Solution theory predicts that asphaltene precipitation is a reversible process.

Although the colloidal models were beneficial as benchmark to understand the phase behavior of asphaltenes (Pfeiffer and Saal, 1940; Dickie and Yen, 1967), there are some indications that colloidal models do not accurately represent the phase behavior of asphaltenes in crude oils. For example, Sirota (2005) studied the physical structure of asphaltenes through SAXS and SANS and concluded that the scattering of asphaltene in solution is consistent with the solution theory of molecular mixtures and cannot be explained using the colloidal theory. Furthermore, asphaltene precipitation has been demonstrated to be reversible (Hirshberg, 1984; Permanu *et al*., 2001) and it has been shown that resins may not provide a steric shell for asphaltenes (Sedghi and Goual, 2010).

Vapor pressure osmometry measurements demonstrate that asphaltenes are in solution with aromatic solvents such as toluene (Yarranton *et al*., 2000). The technique is based on boiling point elevation and this elevation only occurs if the solute (asphaltenes) is in solution with the solvent. If asphaltenes are in solution with the oil, their precipitation can be described with an activity

model and the most common approach is to use regular solution theory. Regular solution theory includes the enthalpy and entropy of mixing of regular solutions. It was first applied by Hirschberg *et al*., (1984) to model asphaltene precipitation, assuming asphaltene fraction as single component. They predicted the asphalt precipitation as a liquid-liquid phase separation (asphalt-rich phase and a solvent-rich phase) using the modified Flory Huggins (Prausnitz, 1969) theory, which introduced the entropy of mixing of monodisperse polymer-like molecules.

Yarranton and coworkers (Yarranton and Masliyah, 1996; Alboudwarej *et al*., 2003; Akbarzadeh *et al*., 2005; Tharanivasan *et al*., 2011; Powers *et al*., 2016) extended this approach to predict the asphaltene precipitation from heavy oils and bitumens diluted with *n*-alkanes over a range of temperatures and pressures. Yarranton and Masliyah (1996) modeled asphaltene precipitation solvents by treating the asphaltene as a mixture of components of different density and molar mass. Alboudwarej *et al*., (2003) successfully predicted the onset and amount of asphaltene precipitation of Western Canadian bitumens/*n*-alkane mixtures at atmospheric conditions, treating the asphaltene as a mixtures of different associated molar mass based on Schultz-Zimm distribution function. Akbarzadeh *et al*., (2005) extended the model to predict the asphaltene yields from mixtures of heavy oils and bitumen around the globe with *n*-alkanes over at temperatures ranging from 0 to 100°C and pressures up to 7 MPa. The effect of the temperature and pressure was accounted for with the estimation of solubility parameter and densities. The asphaltene fraction was divided into pseudo-component based on a molar mass Gamma distribution function. Tharanivasan *et al*., (2011) used the regular solution approach to successfully model the asphaltene precipitation from a depressurized live oil. Powers *et al*., (2016) employed the modified regular solution model to successfully represent the asphaltene precipitation from mixtures of heptol (heptane to toluene ratio) with asphaltene precipitated from native and reacted oil.

The version of the regular solution model developed by Yarranton and co-workers assumes a liquid-liquid equilibrium between the heavy phase (asphaltene-rich phase including asphaltenes and resins) and the light liquid phase (oil-rich phase including all components). The equilibrium constant required for the flash calculation is determined from regular solution theory with a Flory Huggins entropic contribution and is given by:

$$K_i^{HL} = \frac{x_i^H}{x_i^L} = exp[\frac{v_i^H}{v_m^H} - \frac{v_i^L}{v_m^L} + ln\left(\frac{v_i^L}{v_m^L}\right) - ln\left(\frac{v_i^H}{v_m^H}\right) + \frac{v_i^L}{RT}\left(\delta_i^L - \delta_m^L\right)^2 - \frac{v_i^H}{RT}\left(\delta_i^H - \delta_m^H\right)^2 \qquad \textbf{2.1}$$

where K_i^{HL} is the equilibrium constant, x is the mole fraction, v is the molar volume, and δ is the solubility parameter. The subscript i and m denotes the component or pseudo-component and mixtures, respectively. The superscripts L and H refer to the light and heavy phase, respectively. R is the universal gas constant, and T is temperature. The assumption that the heavy phase consists of only asphaltene and resins is supported by experimental data at atmospheric conditions (Yarranton *et al*., 2007) but may not be valid at higher temperatures. Allowing all components to partition significantly increases the time for the model to converge and does not significantly alter the yield calculation in cases where experimental yields are less than or equal to the pentane insoluble asphaltene content of the oil (Akbarzadeh *et al*., 2005). The heavy phase activity coefficient are assumed to be approximately unity.

To use this model, the mole fraction, molar volume, and solubility parameter of each component in the mixture must be specified. The crude oil is divided into three pseudo-components corresponding to saturates, aromatics, and resins plus a set of pseudo-components representing the property distribution of the pentane insoluble asphaltenes. The mole fraction and molar volume are determined from the SARA (saturate, aromatic, resin, asphaltene) composition and the measured density and molecular weight of each fraction. The solubility parameters were obtained by fitting the model to asphaltene solubility data for mixtures of asphaltenes and solvents (Akbarzadeh *et al*., 2005). The regular solution approach is successful at predicting precipitation from different solvents at temperatures below 100°C. However, it does not predict the solvent content of the asphaltene-rich phase, is not well suited for the full range of phase behavior, and is not commonly used in simulators.

2.4.2 Equation of State Phase Behavior Models

The equation of states applied to bitumen/solvent behavior include cubic equations of state (CEoS), cubic plus association (CPA), and the perturbed chain form of the statistical associating fluid theory (PC-SAFT). A brief description of each model is provided below.

Cubic Equations of State (CEoS)

CEoS models are commonly used in most commercial software for predicting the phase behavior of hydrocarbons. There are several different CEoS and the one most commonly used for petroleum systems is the Peng Robinson EoS (Peng and Robinson, 1976) given by:

$$P = \frac{RT}{v-b} - \frac{a\alpha(T_r,\omega)}{v(v+b)+b(v-b)} \quad \textbf{2.2}$$

where P is pressure, R is the universal gas constant, T is temperature, v is the molar volume, a is an attractive parameter, b is the co-volume, and the term $\alpha(T_r,\omega)$ is defined as:

$$a\alpha(T_r,\omega) = (1+m(1-\sqrt{T_r})^2 \quad \textbf{2.3}$$

and T_r is the reduced temperature and m is a function of the acentric factor (ω) given by:

$$m = 0.37464 + 1.54226\omega - 0.26992\omega^2, \text{ for } \omega < 0.49 \quad \textbf{2.4}$$

The a and b parameters for pure components are calculated from their critical properties and acentric factor. The parameters for mixtures are calculated from the pure component parameters using mixing rules. The equilibrium constants required for the phase equilibrium calculations are calculated from the component fugacities which in turn are calculated from the relevant thermodynamic derivatives of the equation of state equation.

CEoS models and their associated correlations were first applied to the phase behavior of light hydrocarbons. A number of studies have been performed to develop a characterization methodology and associated correlations to apply CEoS to the phase behavior of heavy hydrocarbons. Mehrotra and Svrcek (1988) successfully predicted the gas-solubility data for mixtures of Cold Lake bitumen and nitrogen, methane, carbon dioxide, and ethane using the PR EoS. Jamaluddin *et al*., (1991) predicted the solubility and saturated liquid density of mixtures involving heavy oil and bitumen with carbon dioxide using a modified-three parameter Martin

EoS (CEoS). Castellanos-Diaz *et al*., (2011) and Agrawal *et al*., (2012) proposed and tested an oil characterization methodology with temperature-dependent binary interaction parameters to predict saturation pressures and asphaltene onsets from mixtures of bitumen with propane, carbon dioxide, and pentane using the APR EoS. However, the model with the commonly used symmetric mixing rules were unable to predict the asphaltenes yields.

Castellanos-Diaz *et al*., (2011) proposed the use of asymmetric mixing rules as an alternative to overcome this failure. Johnston (2017b) used several asymmetric mixing rules to predict asphaltene phase behavior using the APR EoS. She considered the asymmetric van der Waals (AVDW), Stryjek-Vera (S-V), Huron-Vidal (H-V) with Non-Random, Two Liquid (NRTL) theory, and compositionally dependent mixing rules. The compositionally dependent mixing rules fit saturation pressure, asphaltene onset, and yield data but the model still failed to predict accurate phase compositions.

Cubic Plus Association Equation of State (CPA EoS) Model

The cubic plus association (CPA) EoS was initially developed to extend the capabilities of CEoS to complex multicomponent systems that contains hydrogen bonding compounds, mainly when both vapor-liquid and liquid-liquid equilibria are of interest over wide temperature and pressure conditions (Kontogeorgis *et al*., 2006). It reduces to the CEoS when no hydrogen bonding compounds are involved. The CPA EoS has been widely accepted in the oil and gas industry because of its versatility.

The model combines the classical simple Soave-Redlich-Kwong (SRK) with an advanced association term derived from the Wertheim's theory (Kontogeorgis and Folas, 2009). The physical interactions and the polar/association effects are described by the CEoS and perturbation theory, respectively. The CPA EoS can be expressed for mixtures in terms of pressure as a sum of the SRK EoS and contribution of the association term (Kontogeorgis *et al*., 2006), as follows:

$$P = \frac{RT}{v-b} - \frac{\alpha(T)}{v(v+b)} - \frac{1}{2}\left(\frac{RT}{v}\right)\left(1 + \frac{1}{v}\frac{\partial lng}{\partial\left({}^{1}/_{v}\right)}\right)\sum_{i} x_i \sum_{A_i}\left(1 - \chi_{A_i}\right) \qquad \textbf{2.5}$$

where V_m is the molar volume, x_i is the mole fraction of component i, and χ_{A_i} is the mole fraction of molecule i that is not bonded at A-sites with other active sites. The letters i and j are used to classify the molecule, while *A* and *B* indicate the bonding sites for a given molecule. χ_{A_i} is the key element of the association term and is further related to the association strength, $\Delta^{A_iB_j}$, between two sites from two different molecules:

$$\chi_{A_i} = \left(1 + (1/v)\sum_j x_j \sum_{B_j} \chi_{B_j} \Delta^{A_iB_j}\right)^{-1} \quad \textbf{2.6}$$

where,

$$\Delta^{A_iB_j} = g(v)^{ref}\left[exp\left(\frac{\varepsilon^{A_iB_j}}{RT} - 1\right)\right] b_{ij}\beta^{A_iB_j} \quad \textbf{2.7}$$

$$g(v)^{ref} = \frac{1}{1-1.9\eta}\ ,\ \eta = \left(\frac{1}{4v}\right)b \quad \textbf{2.8}$$

where B_j refers to the summation over all sites. In the expression of the association strength ($\Delta^{A_iB_j}$), the parameters $\varepsilon^{A_iB_j}$ and $\beta^{A_iB_j}$ are defined as the association energy and the association volume, respectively, and $g(V_m)^{ref}$ is the radial distribution function for the reference fluid. The energy parameter $\alpha(T)$ in the SRK term and the combining rules for association energy and volume parameters between different associating molecules are detailed in Kontogeorgis *et al*. (2006).

Within the CPA framework, the interaction between the molecules can be represented based on different association schemes. For example, the one-site scheme is used for acids, two-site and three-site are used for alcohols and amines, and four-site are used for highly hydrogen bonding substances as glycols and water (Kontogeorgis *et al*., 2006). The CPA requires five pure-compounds parameters, three for the SRK term (a_0, b, a_1) and two for associating components ($\varepsilon^{A_iB_j}$, $\beta^{A_iB_j}$). The parameters are determined by fitting vapor pressure and saturated liquid density data. The CPA EoS has been proven to be successful on modeling phase equilibria of systems that contains alcohols, glycols, water and alkanes (Kontogeorgis *et al*., 2006).

Arya *et al*., 2015 used the CPA EoS to successfully fit the asphaltene precipitation onset conditions for nine different reservoir fluids. They lumped the saturates, aromatics and resins fractions into

one single fraction called the heavy component with one cross-association site. Asphaltenes were considered as monomeric molecules with four association sites.

Li and Firoozabadi (2010a) also used the CPA to successfully describe the overall trend of asphaltene precipitation literature data from mixtures of various *n*-alkanes with "model solutions" and seven heavy oils over a wide range of temperatures, pressures, and compositions. They proposed several assumptions to reduce the number of tuning parameters and only one adjustable parameter (the cross-association energy between asphaltene and aromatics/resins molecules). Li and Firoozabadi (2010b) also fitted the effect of pressure and temperature on vapor-liquid equilibria data and asphaltene precipitation amount from different live oils.

Finally, Arya *et al*. (2016b) compared the asphaltene precipitation results obtained from the CPA, PC-SAFT without association (WOA) and PC-SAFT with association (WA). They demonstrated that the CPA and the PC-SAFT WA could predict the asphaltene upper onset pressure, lower onset pressure and bubble point data for all six fluids used. Unlike, the PC-SAFT WOA which was unable to predict the upper onset boundary of two fluids.

Perturbed Chain form of Statistical Association Fluid Theory (PC-SAFT)

The SAFT EoS model was originally developed for predicting the phase equilibria of associating fluids (Chapman *et al*., 1989). In this approach, molecules are modeled as chains of bonded spherical segments. The equation of state is defined in terms of the residual Helmholtz energy made up from three different intermolecular force contribution terms. The first term, A^{seg} accounts for the contribution of the dispersion forces between segments. The second term, A^{chain}, accounts for the contribution of the covalent chain-forming bonds between segments. The third term, A^{assoc}, accounts for the association between molecules. The model was capable of reproducing experimental phase equilibria data for pure compounds.

Gross and Sadowsky (2001) developed the perturbed chain form of the SAFT EoS by extending the perturbation theory of Barker and Henderson (Barker and Henderson, 1967) to account for the effect of chain length on segment dispersion energy. PC-SAFT used a hard sphere reference fluid

described by the Mansoori-Carnahan-Starling-Leland (Mansoori *et al*., 1971). This form of SAFT predicts the phase behavior of mixtures involving high molecular weight fluids (polymer solutions) similar to asphaltene molecules. The residual Helmholtz free energy, A^{res}, for PC-SAFT is given by (Gonzalez *et al*., 2005):

$$\frac{A^{res}}{RT} = \frac{A^{seg}}{RT} + \frac{A^{chain}}{RT} + \frac{A^{assoc}}{RT} = m\left(\frac{A_0^{hs}}{RT} + \frac{A_0^{disp}}{RT}\right) + \frac{A^{chain}}{RT} \qquad \textbf{2.9}$$

where, A^{seg}, A^{chain}, A^{assoc}, A_0^{hs}, and A_0^{disp} are respectively the segment, chain, association, hard sphere, and dispersion contributions to the model. The specific form for each term can be found in Gonzalez *et al*., 2005.

Ting *et al*., (2003) applied the PC-SAFT to asphaltene phase behavior. They treated asphaltenes as nano-aggregates and assumed that the interactions between nano-aggregates can be qualitatively described through London dispersion interactions. The polar-polar interactions between asphaltenes were considered to be negligible, and hence, the contribution of the association part of the model was not used. Three parameters were required for each non-associating component or pseudo-component: the diameter of each molecular segment (σ), the number of segment per molecule (m), and the segment dispersion energy (ε/k). Correlations to estimate these parameters can be found in Gross and Sadowski (2001) and Ting *et al*., (2003).

Gonzalez *et al*., (2005) used PC-SAFT to model the onset of asphaltene precipitation and vapor-liquid equilibria from a live oil model (mixture of asphaltene, toluene, and precipitant gas) and a recombined oil (reservoir oil with a mixture of CH_4, N_2, CO_2, and light *n*-alkanes). They simulated reservoir pressure depletion and gas injection (CO_2, N_2, CH_4, and C_2H_6) processes. Gonzalez *et al*., (2007) also demonstrated that PC-SAFT is capable of predicting not only the onset of asphaltene precipitation and the bubble point but also the amount and the composition of the asphaltene-rich phase from live oils.

Panuganti *et al*., (2012) presented a new characterization methodology for use with PC-SAFT that improved the match to experimental asphaltene onset precipitation and bubble point pressure data. This approach has shown promise for modeling the phase behavior of the behavior of heavy oil

and solvent mixtures. However, further efforts must be focused on extending the equation of state (including critical regions), improving the oil characterization methodology, and modeling polydisperse asphaltenes (Vargas *et al*., 2009).

Chapter 3: Experimental Methods

This chapter provides the experimental techniques employed to collect phase behavior data for propane diluted bitumen systems. The experimental approach is outline in Figure 3.1. The vapor-liquid (VL) boundary was determined from saturation pressures measured in blind cells using the constant composition expansion method. The liquid-liquid (LL) boundary was determined from onset data (solvent content at which heavy pitch phase appeared) measured in a high pressure microscope (HPM) apparatus using a propane titration method. The morphology of the heavy pitch phases was also examined in the HPM. Phase compositions were measured from samples obtained from a PVT cell in the LL region. The *n*-pentane-insoluble asphaltene (C5-asphaltene) and solvent-free pitch (pitch*) yields were determined from light solvent-rich phase compositions measured in blind cells and a material balance. Each method is described below. Distillation assays data and property measurements of the bitumen samples are also presented.

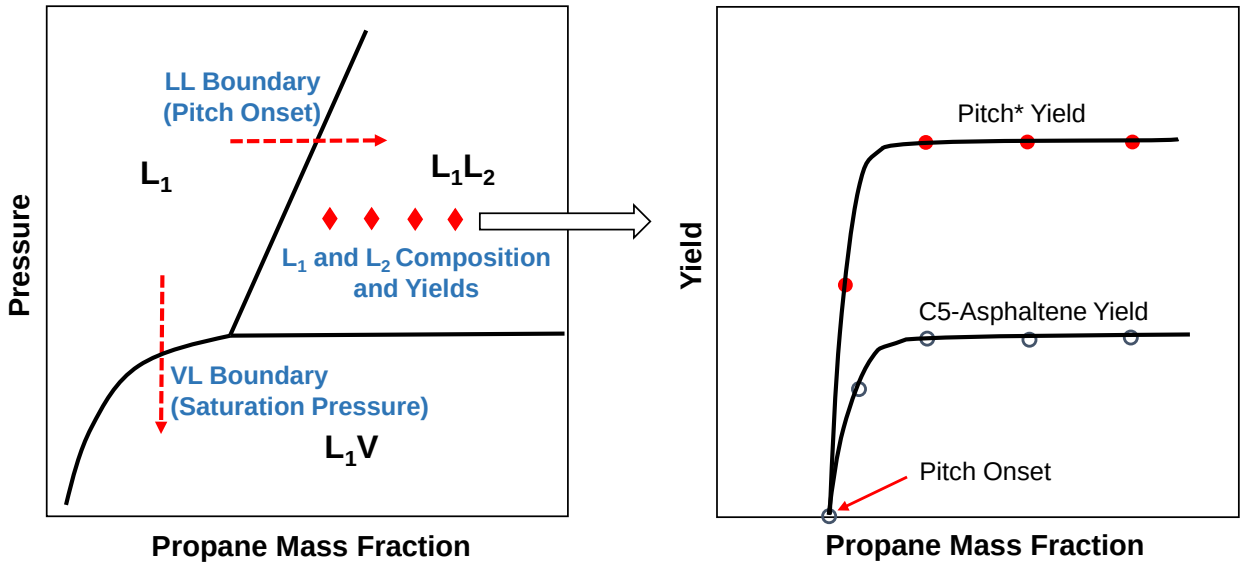

Figure 3.1 Schematic of type of data and experimental methods used to map the phase boundary diagrams, yield curves, and LL phase compositions for mixtures of propane and bitumen.

3.1 Chemical and Materials

The bitumen samples used in this project, WC-B-B3 and WC-B-B4, are well-head samples from a SAGD process operated by Shell. The samples contained emulsified water and free water. Prior to any measurements, the water was removed by sonication at ambient conditions for 24 hours and later placed in a separatory funnel at 60°C. After two weeks, the emulsion had broken and the water was drained from the funnel. The final content was less than 1 wt%. Selected properties of the water-free bitumen and a spinning band distillation assay are provided in Table 3.1 and Table 3.2, respectively. The distillation assay was performed on a very similar sample, WC-B-B2, from the same source reservoir (Johnston *et al*., 2017a). The WC-B-B2 and WC-B-B3 samples had similar properties as shown in Table 3.1. The WC-B-B4 sample had a higher asphaltene content, density, and viscosity. This sample was only used for small number of measurements. Technical grade (99+% pure) propane, *n*-pentane, toluene were purchased from Praxair, VWR International, LLC.

Table 3.1 Selected properties of WC-B-B3.

Property	**WC-B-B2**	**WC-B-B3**	**WC-B-B4**
Specific Gravity	1.015	1.020	1.023
Viscosity at 50°C, 1 atm, cP	2,900	3,100	8,100
Saturates, wt%	17	-	-
Aromatics, wt%	46.9	-	-
Resins, wt%	16.7	-	-
C5-asphaltenes, wt%	19.4	19.2	22.3

Table 3.2 Spinning band distillation assay of WC-B-B2 (Johnston *et al*., 2017).

Volume Distilled vol%	Normal Boiling Point, °C
1.6	218.0
3.2	237.4
4.9	252.4
6.5	267.9
8.1	278.6
9.7	289.4
11.4	301.7
13.0	313.5
14.6	324.0
17.9	339.8
19.5	349.6
21.1	358.0
22.7	367.3
24.3	375.2
26.0	380.0
27.6	382.5
29.2	384.0
30.8	385.0

3.2 Vapor-Liquid Boundary: Saturation Pressure Measurements

The saturation pressures were measured by another student (Richardson, 2017) in the same lab working on a related project. The apparatus and methodology used for the determination of the bubble point are summarized to illustrate the nature and estimation of the experimental errors. The vapor-liquid boundary data were collected for propane diluted WC-B-B3 bitumen at propane contents up to 11 wt% and temperatures ranging from 50 to 180°C. The method is summarized below.

3.2.1 Apparatus

The saturation pressures were measured using a blind cell apparatus, as shown in Figure 3.2. The apparatus consists of five 100 cm^3 blind cells (PVT cells without a sight glass) with floating pistons but no mixers. The maximum pressure rating for each blind cell is 100 MPa. The blind cells are housed in an air bath which controls the temperature within ±0.1°C and can operate at temperature from 20 to 300°C. The volume of each blind cell, and hence the pressure of the sample fluid under investigation, is controlled by a variable volume computer-controlled positive displacement pump which allows the injection and the removal of hydraulic oil.

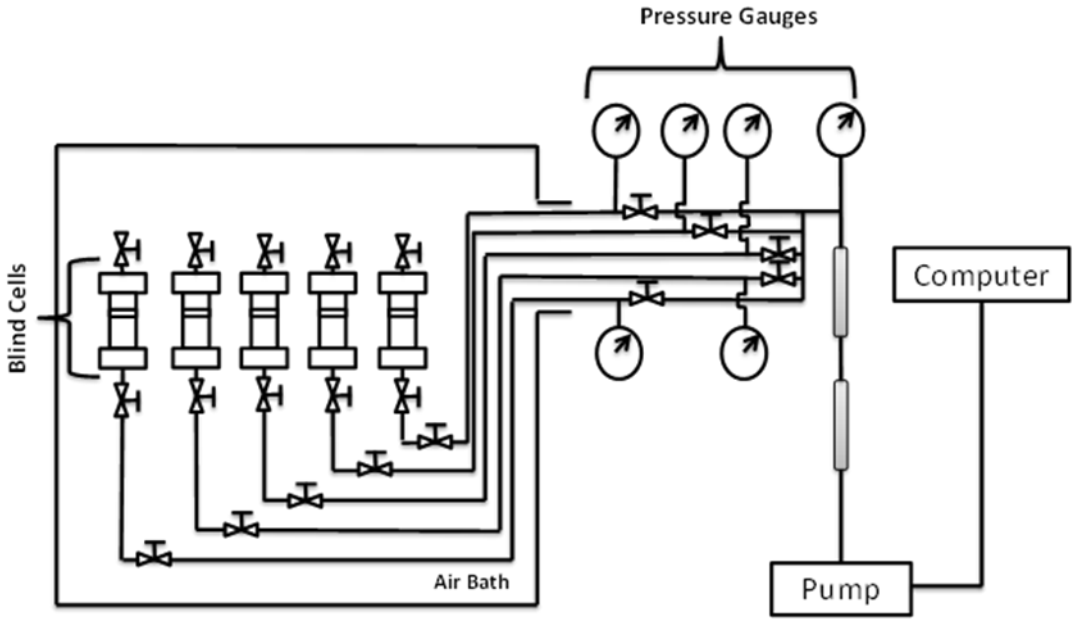

Figure 3.2 Schematic of the blind cell apparatus used to measure saturation pressures and yields.

3.2.2 Procedure

To perform the experiment, bitumen was placed into each blind cell at atmospheric conditions and then the blind cells were placed under vacuum to remove any air present. Propane was injected at sufficient pressure to maintain a liquid phase. The mass of each fluid was determined gravimetrically with a precision of ±0.01 g. The blind cells were pressurized to well over the bubble point and placed on the roller mixer for three days. After mixing, the saturation pressure

was determined by step-wise isothermal expansion method based on the methodology described by Agrawal *et al*. (2012). The sample fluid was first compressed to a pressure well above its expected bubble point and the air bath was then set at experimental temperature. The pressure was decreased with a stepwise volume expansion. At each pressure step, the mixture was considered to have reached equilibrium when the pressure, temperature, and the volume were all constant for a minimum of two hours. Equilibration time ranged from 12 to 24 hours. The volume was measured by the computer-controlled pump with a precision of ±0.2 cm^3. The saturation pressure was determined from the change in slope of the pressure-volume isotherm, as described in Figure 3.3. The blind cell methodology was tested on pure *n*-pentane at 180°C and the measured vapor pressure was 2.58 MPa compared with 2.60 MPa from Linstrom and Mallard (2015).

There are three main sources of uncertainty in the measurement of the saturation pressures: 1) the error in the solvent content of the mixture; 2) the air content of the hydraulic oil; 3) and the pressure difference required to move the piston between the hydraulic oil and the sample. The log of the saturation pressure is approximately proportional to the solvent content and therefore an error in the solvent content translate exponentially to an error in the saturation pressure. Any small amount of air trapped in the hydraulic oil when filling the apparatus dissolves in the oil when the apparatus pressure is raised. This air will evolve when the pressure is reduced to the saturation pressure of the air in the hydraulic oil. If this saturation pressure is greater than the saturation pressure of the propane/bitumen mixture, only the saturation pressure of the air (a false saturation pressure) will be detected. This error will only occur at low saturation pressures (low propane contents). The pressure required to move the piston and the associated error is difficult to quantify because the piston can stick and jump during a pressure release step. Since it was difficult to quantify each source of error, the uncertainty in the saturation pressure was determined from the deviations from a modified Henry Law model (Badamchi-Zadeh *et al*., 2009b) fit to the data (see Chapter 5). The uncertainty in the saturation pressure measurements was ±0.3 MPa based on a 90% confidence interval.

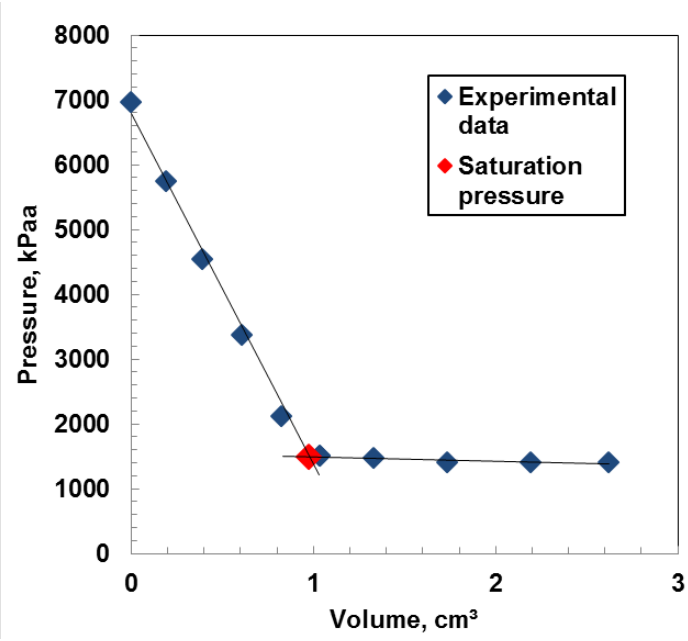

Figure 3.3 Pressure-volume isotherm of 6 wt% propane in bitumen at 90°C (Richardson, 2017).

3.3 Liquid-Liquid Boundary: Onset Measurements

The heavy pitch phase onset is defined as the propane content at which two liquids first appear forming a propane/maltene-rich light phase (L_1) and a heavy pitch phase (L_2). The heavy pitch phase onsets were collected for mixtures of propane and WC-B-B3 bitumen at temperatures ranging from 20 to 130°C and pressures up 10 MPa. All onsets were measured for this thesis except for 20°C (2 MPa and 10 MPa), 50°C (6.9 MPa and 10 MPa), and 90°C, 10 MPa (Johnston, 2017).

3.3.1 Apparatus

The heavy pitch phase onset was measured visually using a high pressure microscope (HPM) coupled with a PVT cell, Figure 3.4. The HPM system consists of a cell with two sapphire windows, a light source, and a high focal length camera connected to a computer in order to capture digital images and video. The gap between the windows is adjustable (100-400 μm) and was set to 100 μm. The HPM system is placed in-line between two high pressure cylinders with floating pistons and magnetic stirrers, both of which are connected to a computer-controlled pump and a back pressure regulator. The pump and regulator are used to push fluid back and forth from one

mixing cylinder, through the gap between windows in the HPM, to the second cylinder for mixing purposes. The HPM is rated for temperatures up to 200°C and pressures up to 138 MPa.

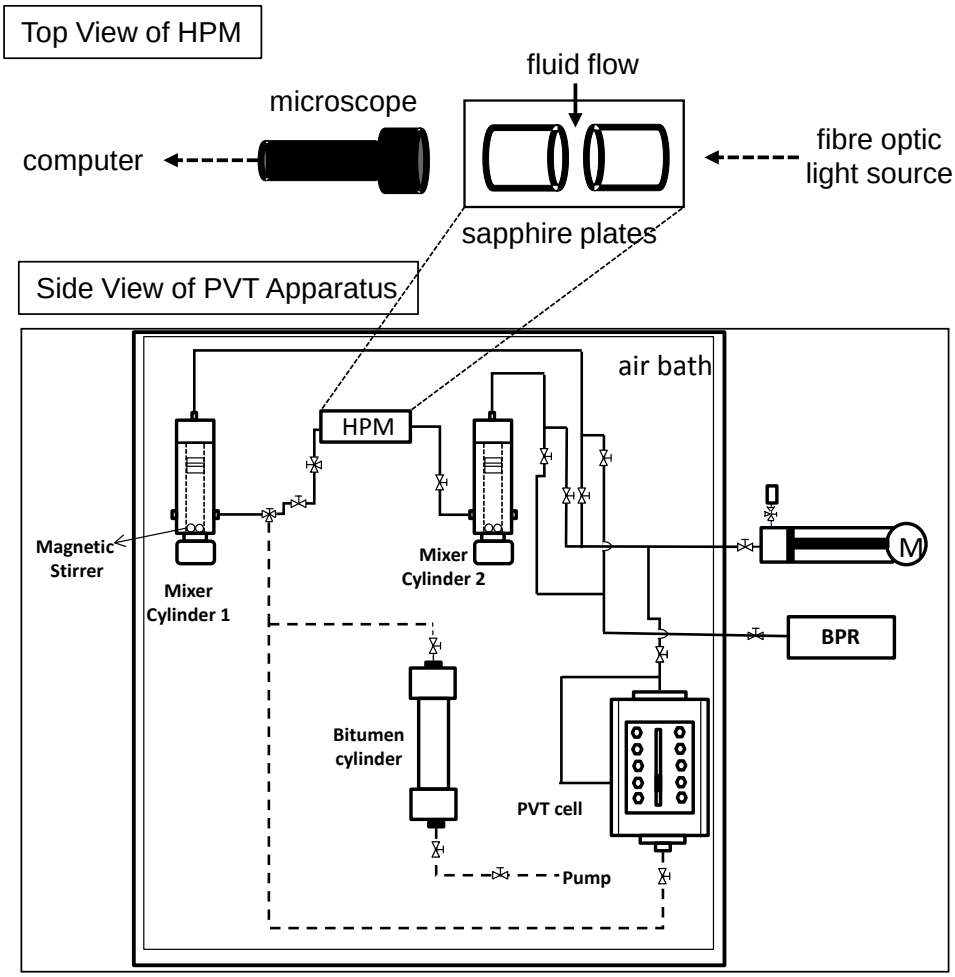

Figure 3.4 Schematic of the HPM apparatus used to measure pitch onsets (Agrawal *et al.*, 2012).

The dead volume of the apparatus is required to accurately determine the injected fluid volumes that enter the mixing cylinders. Here, the dead volume is the volume of the transfer lines that connect the HPM cell to both mixing cylinders and it was measured by Agrawal (2012). To measure the dead volume, the floating pistons of both mixer cylinder were displaced to the bottom of the cylinders. A constant pressure was applied on the hydraulic oil side of the piston using a back pressure regulator (BPR). Toluene was injected on the sample side using a computer-controlled pump at a pressure lower than that recorded by the BPR. The volume of injection was

determined from the pump displacement once the pressure stabilized and was determined to be 7.7 ±0.2 cm^3.

3.3.2 Procedure

The asphaltene onset point was measured by titrating the bitumen with diluent (in this case propane), using the methodology described by Agrawal *et al*. (2012). Prior to any measurement, the HPM assembly was cleaned with toluene and vacuumed out. The floating pistons of both mixing cylinders were displaced to the bottom of each cylinder. The specified pressure was applied on the hydraulic oil side of the piston using a back pressure regulator (BPR). The initial pump reading, the mass of the hydraulic oil container, the temperature, and the pressure were recorded.

A specified amount of dewatered bitumen was injected into the sample side of the HPM mixing cylinders while maintaining a constant pressure. The pump reading, mass of the hydraulic oil container, temperature, and pressure were again recorded. The volume of the bitumen injected was determined in two ways: 1) from the difference between the initial and the final pump readings; 2) from the volume of displaced hydraulic oil after subtracting the dead volume. The pump displacement was taken as the accurate measurement and the hydraulic oil displacement was used only for validation. The hydraulic oil displacement was within 3% in average of the volume from the pump readings. The mass of the bitumen injected was calculated from its density at operating pressure and temperature.

The solvent, in this case propane, was first placed at pressure (propane in liquid state) in a cleaned and vacuumed PVT cell. The propane was then injected in a step-wise fashion process at a flow rate of 10 cm^3/h from the PVT cell to the mixing cylinder containing the bitumen. This relatively low flow rate was selected to avoid high local solvent concentrations which would cause premature asphaltene precipitation. The magnetic stirrer in the mixer cylinders was turned on for injections. After each injection, the volume of injected propane was determined from the cathetometer readings and verified with pump displacements. After injection of the propane, the contents of the mixing cylinder were displaced slowly to the other mixing cylinder in order to displace the propane remaining in the transfer line. Then, the fluid was moved back and forth between the two cylinders

until a uniform mixture was formed as indicated by constant pump pressure readings at constant flow rate. During this process, the fluid was also continuously monitored using the HPM cell for indications of the appearance of a second phase. If a second phase did not appear, propane was again injected from the PVT cell and whole process was repeated until a heavy pitch phase was observed.

The propane content at onset of the heavy pitch phase (LL boundary) was taken to be the intermediate content between the highest content at which no phase was observed and the lowest content at which the second phase was detected, Figure 3.5. Note that a small number of particles are visible below the onset, Figure 3.5a. These are toluene insoluble particles inherent in the bitumen. The onset of the heavy pitch phase is detected by a drastic increase in number of visible particles, Figure 3.5b. In most cases, the injection steps were set at intervals of 2 wt% propane and the uncertainty of the propane content was ±0.3 wt%; therefore, the uncertainty of the reported onset was ±1.4 wt%. The uncertainty in the propane content is discussed in Appendix A.

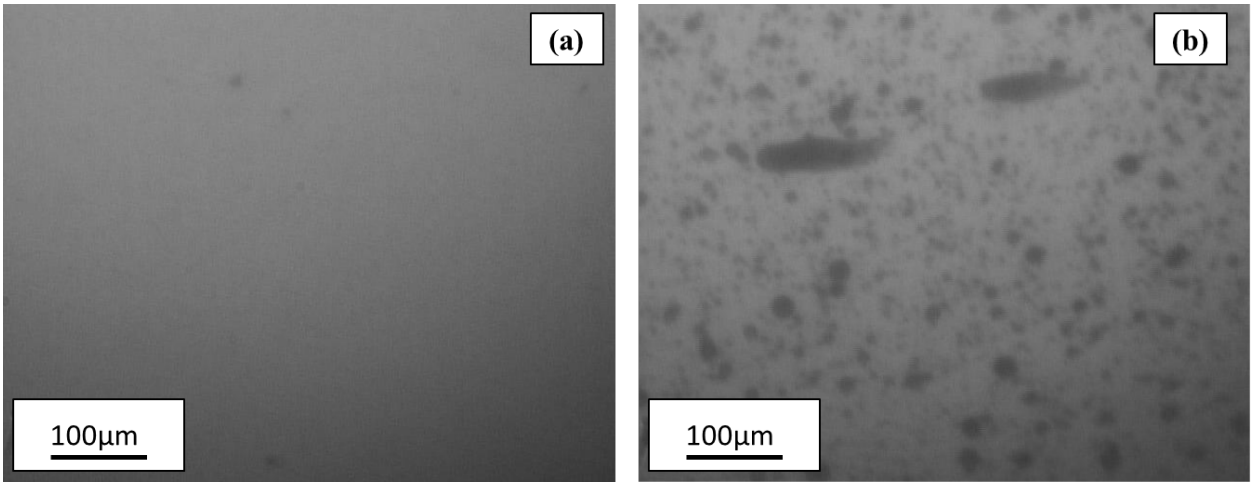

Figure 3.5 HPM micrographs of propane diluted WC-B-B3 bitumen at 90°C and 10 MPa at: a) 32 wt% propane; b) 34 wt% propane. The pitch onset was reported as 33 ±1.3 wt%.

3.4 Blind Cell Yield Measurements

The yield of the *n*-pentane insoluble asphaltenes (C5-asphaltenes) and solvent-free pitch (maltenes plus asphaltenes, which will be referred to as pitch*) for propane diluted WC-B-B3 and WC-B-

B4 bitumens were determined using the blind cell apparatus described below. C5-asphaltene and pitch* yields were determined at temperatures ranging from 20 to 130°C and pressures up to 10 MPa, and at propane feed content above 40 wt% in most cases. The composition of the light phase was measured directly and the yields were determined from a material balance as described below. All of the yield data were collected as part of this thesis.

3.4.1 Apparatus

The blind cell apparatus described in Section 3.2.1 was modified with the addition of a sample cylinders to each blind cell as shown in Figure 3.6. The sample cylinders are identical in design to the blind cells are each equipped with a piston.

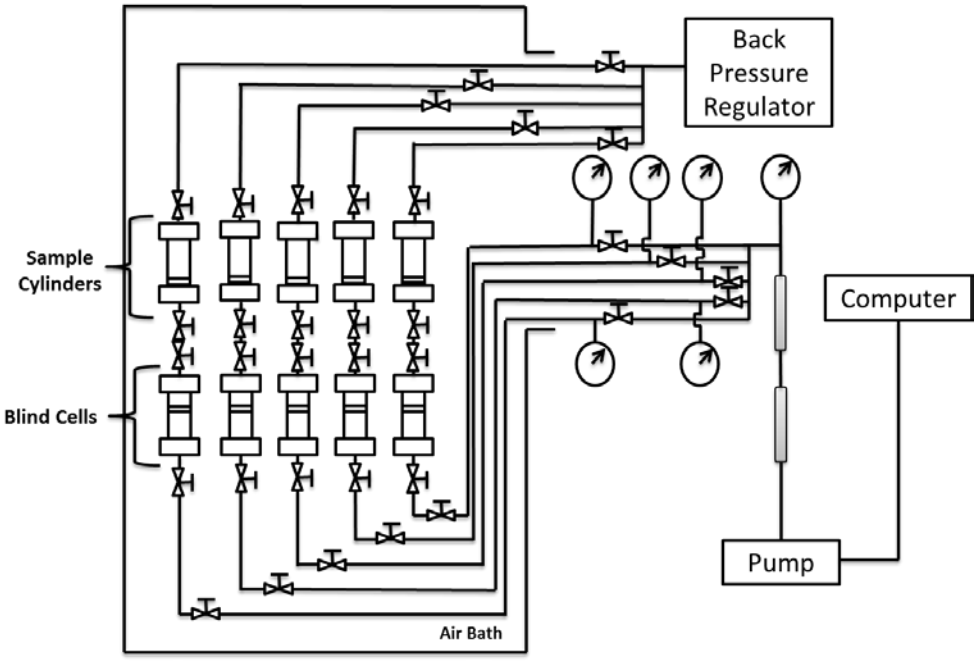

Figure 3.6 Schematic of the blind cell apparatus for yield measurements.

3.4.2 Procedure

Known masses of bitumen and propane were injected into the blind cells at ambient conditions. For ambient temperature yield measurements, the samples were mixed at 21°C on a roller for 3 days to ensure complete mixing. For higher temperature yields, the sample was mixed by inverting

the blind cell once daily for five days. The blind cells were then installed in the oven and oriented so that the heavy pitch phase settled on the floating piston. Once the sample reached the target temperature, the pressure and temperature were maintained for a minimum of three days to ensure equilibrium was reached. A sample of the light propane-rich phase was displaced at experimental pressure and temperature into a sample cylinder.

The sample cylinders used for collecting the light solvent-rich phase were identical to the blind cells used for the feed mixtures. The sample cylinders were assembled with a piston at the topmost position to minimize the dead volume and vacuumed out at ambient conditions. Dead volume from the blind cell to the sample cylinder were approximately 0.5 to 1.0 cm^3. The pump was used to displace approximately 30 cm^3 from the feed blind cell to the sample cylinder and compressed air (N_2 will be used for future applications) was used to maintain pressure in the sample cylinder at experimental conditions. Note, the heavy pitch phase could not be sampled with the blind cell procedure since the position of the interface between the light and heavy phase is not known.

The light solvent-rich phase was allowed to dry at 21°C and atmospheric pressure for approximately 5 days and the mass of the evaporated propane was determined gravimetrically. The remaining propane-free residue (pitch*) was diluted with *n*-pentane at 40 cm^3 per gram of residue to separate the asphaltenes from the maltenes. The mixture was sonicated and agitated for 1 hour until the pitch* was completely dispersed, then it was left to settle for 24 hours. The sample was then centrifuged for 5 minutes at 4000 rpm and the supernatant was decanted. The remaining residue, C5-asphaltenes with some residual maltenes, was washed with 20 cm^3 *n*-pentane, sonicated for 60 minutes, and centrifuged for 5 minutes. The supernatant was decanted and the C5-asphaltenes left to dry in a vacuum oven until the mass was constant. The C5-asphaltene content is the mass of the dried final residue divided by the initial mass of the light solvent-rich phase sample. The pitch* mass is the mass of the light solvent-rich phase sample less the mass of the evaporated propane. The pitch* content is the pitch* mass divided by the mass of the light phase. The uncertainty in the mass measurements is discussed in Appendix A.

3.4.3 Mass Balance Calculation

A material balance was required to determine the mass and composition of the heavy pitch phase. However, there was one degree of freedom unspecified. Therefore, the propane content in the heavy pitch phase was assumed and the C5-asphaltene and pitch* contents and yields were determined from the mass balance. As will be discuss later in Section 5.3, the directly measured propane contents of the pitch phase ranged between 2 and 27 wt%. Furthermore, it is expected that the solvent content would decrease towards the onset because the heavy pitch phase contains the heaviest bitumen components at this condition. Therefore, sensitivities were performed at zero and 30 wt% propane. A base case solvent content was assumed that either matched a measured propane content, if available, or maintained an approximately constant ratio of pitch* to C5-asphaltene yield in the calculation. For the sake of simplicity, this solvent content was assumed to be the same at all dilutions at the given temperature and pressure. The yields calculated with the sensitivities are shown in Figure 3.7a. Henceforth, the yield data will be presented as the base case with error bars representing the combined uncertainty between the yield measurements and the difference of the yields between zero and 30% sensitivity cases at each solvent content, as shown in Figure 3.7b. Note, the uncertainty in the calculated yields is large near the onset but relatively small at high dilutions. The uncertainty in the C5-asphaltene yields is approximately ±1.0 wt% at propane contents above 40 wt%. The uncertainty in the pitch* is less than ±8.5 wt% at propane content above 50 wt%.

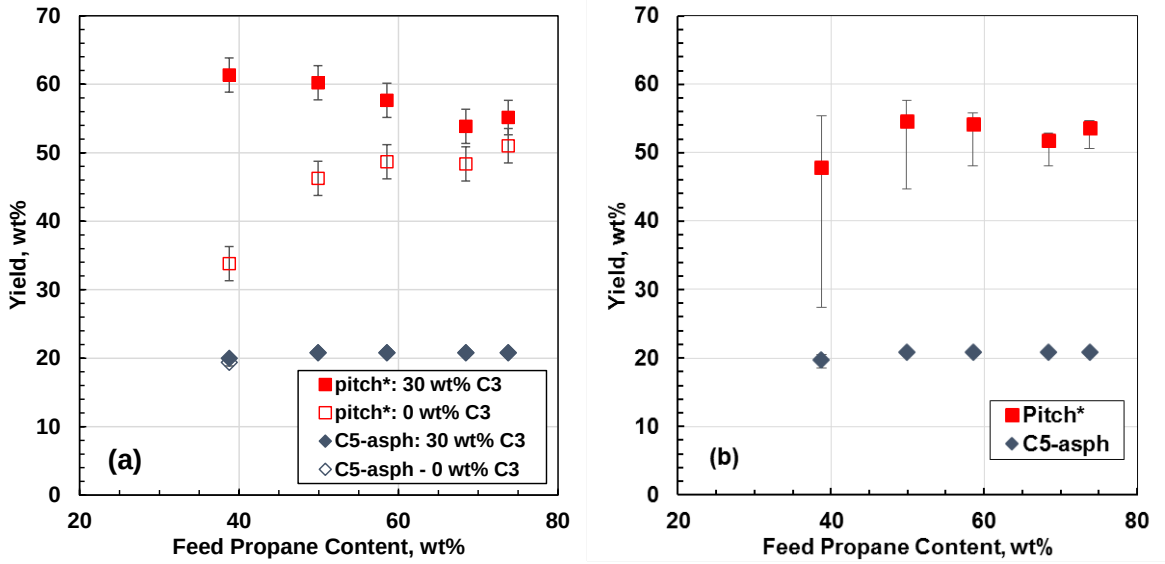

Figure 3.7 Calculate pitch* and C5 asphaltene yields from WC-B-B3 bitumen at 20°C and 10 MPa: a) assuming 0 and 30 wt% propane content in the heavy phase with error bars indicating the measurement error; b) assuming 22 wt% in the pitch* phase with error bars representing the uncertainty of the measurements.

3.5 PVT Cell Phase Composition and Yield Measurement

Pitch-rich and propane-rich phase compositions were measured for propane diluted WC-B-B3 bitumen mixtures from temperatures ranging from 50 to 130°C and pressures up to 10 MPa, all at 50 wt% propane content in the feed except for one case at 75 wt% propane. A new procedure was developed as part of this thesis to measure the phase compositions in a PVT cell as described below.

3.5.1 Apparatus

The phase composition measurements were performed using a DB Robinson Jefri PVT cell placed in a temperature controlled air bath, Figure 3.8. The temperature is controlled within ±0.1°C. The maximum pressure rating for the PVT cell is 69 MPa and it can operate at temperatures from -15 to 200°C. The maximum capacity of the PVT cell is 100 cm^3. The PVT cell is equipped with a floating piston but the magnetic mixer was removed to minimize the dead volume and ensure a clean separation of the light phase from the heavy phase. The floating piston separates the hydraulic fluid from the bitumen/solvent mixture. The volume of the sample fluid inside the cell

is determined from fluid level measurements using a calibrated cathetometer. The cathetometer is precise to $\pm 10^{-6}$ m^3. The volume of the fluid sample is controlled by a computer-controlled positive displacement pump, which allows the injection and removal of hydraulic oil. The dead volume of the PVT cell was measured similarly to the one described for the HPM in section 3.3.1. The dead floating piston of the PVT cell were displaced to the bottom. Toluene was injected using a computer-controlled pump at a pressure lower than that recorded by the BPR. The volume of injection was determined from the pump displacement once the pressure stabilized and was determined to be 0.8 ±0.2 cm^3.

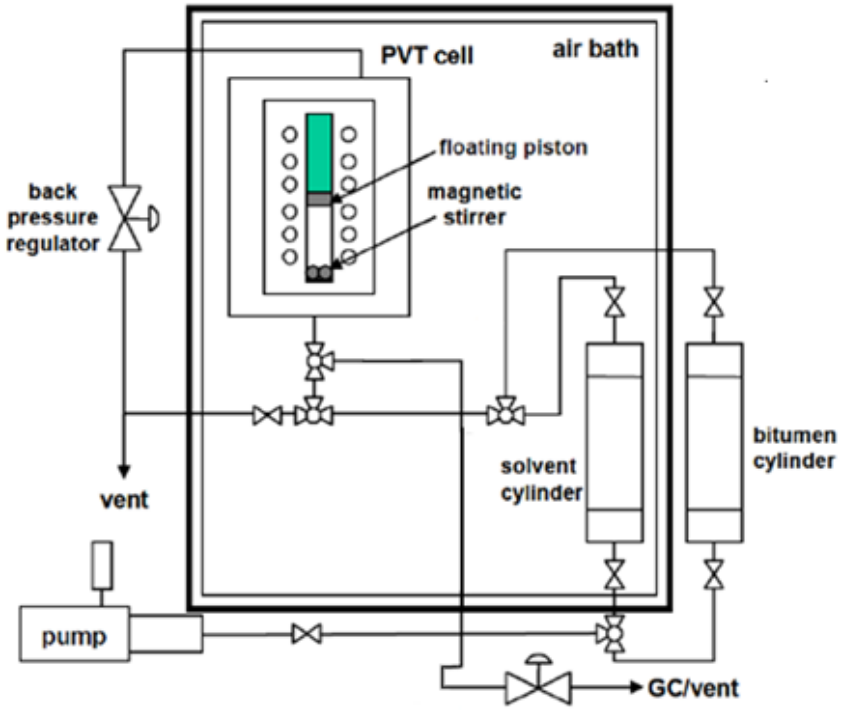

Figure 3.8 Schematic of PVT cell apparatus.

3.5.2 Procedure

Prior to any measurements, the PVT cell was cleaned with toluene and vacuumed ensuring the presence of no air in the system. A feed composition (propane wt% and bitumen wt%) was selected so that the overall mixture split into two phases (the light solvent-rich phase and the heavy pitch phase) and sufficient heavy pitch phase was formed. Bitumen was transferred from a cylinder to

the PVT cell at 50°C and 1.4 MPa. A temperature of 50°C was selected to reduce the bitumen viscosity sufficiently to inject the bitumen. The transfer procedures are similar to those described for the HPM in Section 3.3.2.

The PVT cell apparatus was then heated to experimental temperature and the pressure was maintained at experimental condition using the hydraulic pump. The required amount of propane was injected at the same conditions. The bitumen and propane injection volumes were measured in two ways, one from the PVT cell using the cathetometer and the other from volume of the fluid displaced using the pump. The mass of the fluid was calculated based on the averaged injected volume (cathetometer and pump measurements) and the injected fluid density. The feed composition was determined from the mass of the bitumen and diluent injected.

The bitumen and the diluent were mixed by inverting the PVT cell several times daily for 3 days until equilibrium was reached. Once equilibrium was reached, the PVT cell was rotated to allow the heavy pitch phase to settle on the piston. The volume of the heavy pitch phase was clearly visualized and measured using the cathetometer. The light solvent-rich phase was collected at pressure by displacing the light solvent-rich phase into a sample cylinder with a known mass. Sufficient pressure to maintain a single phase liquid state was set in the sample cylinder using compressed air as the hydraulic fluid. Finally, toluene was injected from a transfer vessel into the PVT cell to assure the heavy pitch phase remained in liquid state when it was cooled. The mixture (toluene + heavy pitch phase) was displaced into another sample cylinder using the same collection procedure as for the propane-rich phase, Figure 3.9.

After releasing the air pressure, the mass of each phase collected in the sample cylinders and the mass of injected toluene were measured directly using the scale within a precision of ±0.01 g. The sample cylinders were re-pressurized above their saturation pressure and re-mixed on the roller mixer. Two samples of the light solvent-rich phase and heavy pitch phase were transferred to test tubes at ambient temperature and pressure to perform the compositional analysis. The mass fraction of propane, maltenes, and C_5 asphaltenes in each sample was determined as described in section 3.4.3. Note that, the toluene added in the heavy pitch phase must be subtracted. The C5-

asphaltene and pitch* yields were determined directly from heavy pitch phase measurements and indirectly from a material balance based on the feed and light solvent-rich phase data. The uncertainty of the C_5 asphaltene and pitch* yields were ±1.7 and ±2.6 wt%, respectively. Details of the uncertainty estimation are provided in Appendix A.

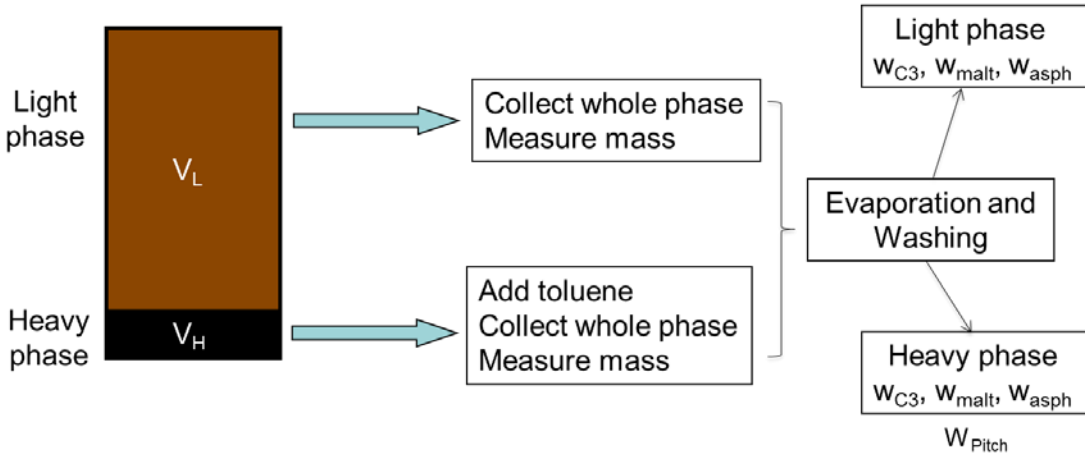

Figure 3.9 Sketch of the sample collection methodology to measure phase composition and yields.

Chapter 4: Phase Behavior Modeling

In this chapter, a description is provided of the cubic equation of state (CEoS) and oil characterization used to fit the phase behavior data for mixtures of propane and bitumen. The Advanced Peng-Robinson (APR) Equation-of-State (VMG 2017) with the oil characterization recommended by Agrawal *et al*. (2012) and Johnston *et al*. (2017) was employed to model the phase behavior of propane diluted bitumen systems. Both symmetric and compositionally dependent mixing rules for the equation of state attractive parameter are presented. The characterization of the bitumen into a series of pseudo-components required to implement the equation-of-state model is also described.

4.1 Cubic Equation of State Model

The model chosen for this study was the Advanced Peng Robinson cubic equation of state (APR EoS) (VMG 2017). This EoS is well suited for petroleum fluids and is implemented in the VMGSim^{TM} software used for this study. The Peng-Robinson cubic EoS (Peng and Robinson, 1979) is given by:

$$P = \frac{RT}{v-b} - \frac{a\alpha(T_r,\omega)}{v(v+b)+b(v-b)} \quad \textbf{4.1}$$

where P is pressure, v is the molar volume, a and b are constants related to the attractive and repulsive forces, $\alpha(T_R,\omega)$ is a function specific to the equation of state, T_R is the reduced temperature, and ω is the acentric factor. The constants a and b for a pure component are related to its critical properties as follows:

$$a_i = 0.457235R^2T_{ci}^2/P_{ci} \quad \textbf{4.2}$$

$$b_i = 0.0777969RT_{ci}/P_{ci} \quad \textbf{4.3}$$

where T_c is the critical temperature, P_c is the critical pressure, and the subscript i denotes the component.

CEoS such as the Peng-Robinson EoS do not accurately predict liquid phase densities since they predict a fixed compressibility factor at the critical point (Whitson and Brule, 2000). The molar volume calculated using the CEoS is underestimated and must be corrected to match experimental

volumes (Jhaveri and Youngren, 1988). Volume translation is a correction factor that is applied to the volume calculated from the CEoS in order to improve the accuracy of the calculated molar volume without altering the phase behavior calculation. The Peneloux volume translation (1982) was applied to the PR EoS by Jhaveri and Youngren (1988) as follows:

$$P = \frac{RT}{v-b} - \frac{a\alpha(T_r,\omega)}{(v+c)(v+b+2c)+(b+c)(v-b)} \quad \textbf{4.4}$$

where *c* is the volume translation. The APR EoS (VMG 2017) is the Peng Robinson EoS with volume translation implemented.

4.1.1 Mixing Rules

For multicomponent mixtures, mixing rules are employed to determine the EoS parameters a_m and b_m. The classical van der Waals mixing rules are the most commonly used mixing rule and are given by:

$$a_m = \sum_i \sum_j x_i x_j \sqrt{a_i a_j}(1-k_{ij}) \quad \textbf{4.5}$$

$$b_m = \sum_i x_i b_i \quad \textbf{4.6}$$

where, x_i and x_j are the mole fraction of components *i* and *j*, respectively, and k_{ij} is the binary interaction parameter between the two components. Binary interaction parameters are commonly fitted by minimizing the difference between the modeled and the experimental data. Therefore, in practice, they are not treated as physical term but as a fitting parameter.

Several authors have attempted to develop correlations to estimate k_{ij} values (Chueh and Prausnitz, 1968; Anai *et al*., 1988). For instance, Gao *et al*. (1992) developed the following correlation in terms of the critical temperatures of the components:

$$k_{ij} = 1 - \left[\frac{2\sqrt{T_{ci}T_{cj}}}{T_{ci}+T_{cj}}\right]^n \quad \textbf{4.7}$$

where T_{ci} is the critical temperature of component *i* and the exponent *n* has a default value of 0.27. The binary interaction parameter can be made temperature dependent when fitting data over a broad range of temperatures.

Van der Waals mixing rules are considered to be symmetric because there is only one interaction parameter for each binary pair ($k_{ij} = k_{ji}$). Symmetric mixing rules are unable to adequately represent the phase behavior of mixtures involving species with significantly different polarities (Castellanos-Diaz *et al*., 2011; Agrawal *et al*., 2012). For these mixtures, asymmetric van der Waals mixing rules, can be employed to better match their highly non-ideal phase behavior of mixtures (Johnston *et al*., 2017b). The simplest asymmetric mixing rules have two distinct interaction parameter values for each binary pair ($k_{ij} \neq k_{ji}$).

It has been shown that binary interaction parameters can vary with composition, specifically for highly polar and asymmetric systems (Adachi and Sugie, 1986; Panagiotopoulos and Reid, 1986). When k_{ij} is defined as a function of composition, the mixing rules is defined to be assymetric compositionally dependent. Panagiotopoulos and Reid (1986) developed a two-parameter mixing rule with k_{ij} as a linear function of composition. They obtained a significant improvement in the representation of binary and ternary phase equilibrium data for highly polar and asymmetric mixtures. Recently, Johnston *et al*. (2017b) developed a compositionally dependent binary interaction parameter correlation to match the asphaltene precipitation data for heavy oil and *n*-pentane mixtures.

4.2 Modeling Workflow

The modeling methodology is provided in Figure 4.1. The bitumen was first characterized into pseudo-components based on a distillation assay. The maltenes and asphaltenes were characterized separately, as will be detailed in Section 4.3. The characterization was input into the equation of state model along with an initial guess for the binary interaction parameters. Flash calculations were performed using VMGsim^{TM} (Version 8-9), which combines the material balance equations of the Rachford-Rice algorithm (1952) with a stability analysis similar to the Michelsen algorithm (1982) in order to minimize the Gibbs free energy. The binary interaction parameters were then iteratively optimized until the best match to experimental data was obtained. Both symmetric

(SvdW) and compositionally dependent (CDvdW) van der Waal mixing rules were evaluated. A more detailed description is provided in Section 4.3.3.

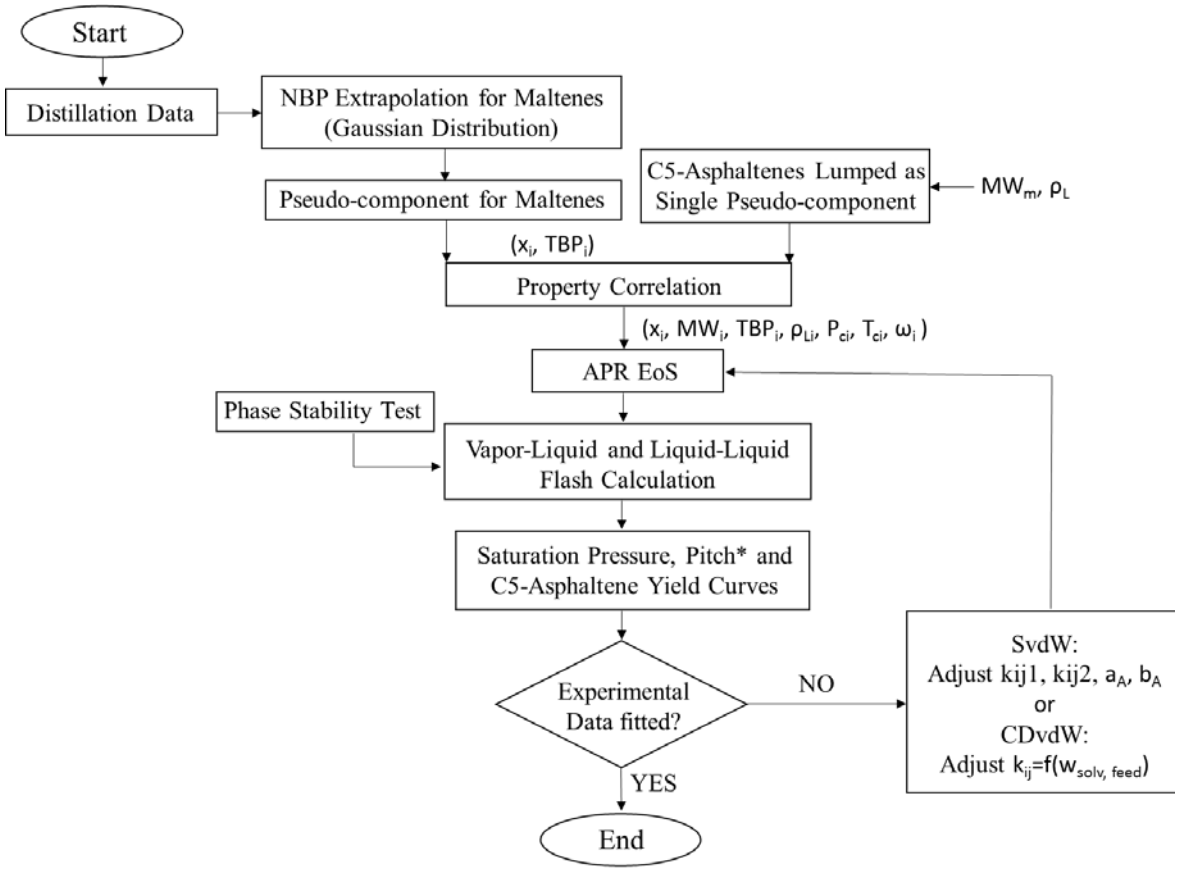

Figure 4.1 Modeling methodology algorithm.

4.3 Bitumen Characterization

Propane was treated as an individual component. The bitumen was characterized into pseudo-components and components, each with a respective mass fraction, density, critical properties and acentric factor. The non-associating species (approximated as maltenes) and the associating species (approximated as C5-asphaltenes) were characterized separately. The maltenes fraction was characterized following the methodology recommended by Agrawal *et al*. (2012), and the C5-asphaltene fraction characterization was lumped into a single pseudo-component as recommended by Johnston *et al*. (2017b). The bitumen characterization was performed on the WC-B-B3 bitumen.

The C5-asphaltene content was 19.2 wt%, Table 3.1, and therefore, the maltene content is 80.8 wt%.

4.3.1 Maltene Characterization

The maltenes fraction was divided into pseudo-components based on a normal boiling point (NBP) curve generated from the spinning band vacuum distillation data presented in Table 3.2. The raw vacuum distillation data was first interconverted from the experimental vapor temperature at vacuum conditions to an atmospheric equivalent temperature (AET) using the Maxwell and Bonnell (1957) correlations. The AET is equivalent to the normal boiling point. The vacuum distillation data was measured on a volume basis and was converted to mass basis using measured liquid densities of "cuts" from a refinery distillation assay of a bitumen from the same field. Note that the distilled fraction was equivalent to approximately 30 wt% of the bitumen. The remaining section of the NBP curve was extrapolated using a Gaussian distribution function as shown in Figure 4.2.

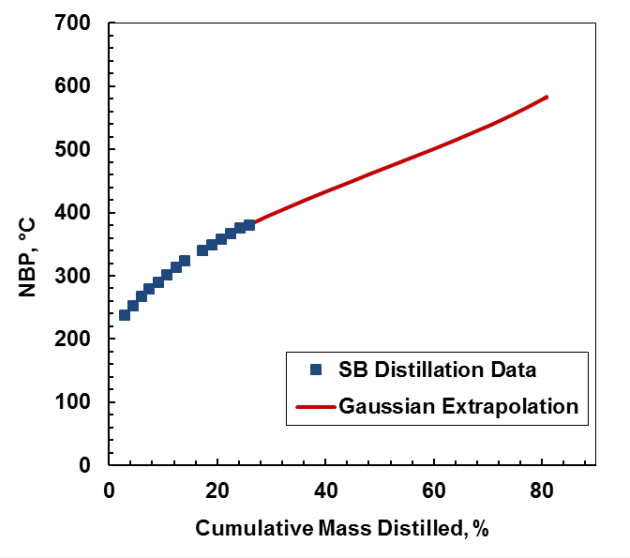

Figure 4.2 Extrapolation of NBP curve for the maltene fraction of the WC-B-B3 bitumen using a Gaussian distribution function.

The NBP curve was then divided into pseudo-components. Agrawal *et al*. (2012) found that ten pseudo-components were enough to recreate the distillation curve for the maltenes: three in the

light oil section (200-375°C), five in the medium oil section (375-515°C), and two in the heavy maltene section (515-586°C). The molecular weight and specific gravity of each pseudo-component were determined using the Lee-Kesler (1975) and Katz-Firoozabadi (1978) correlations, but constrained to match the average molecular weight (450 g/mol) and liquid density (1005 kg/m^3) of the maltenes. The critical properties and acentric factor were estimated with the Lee-Kesler correlations (1975). The maltene pseudo-component properties are presented in Table 4.1.

Table 4.1 Bitumen pseudo-component properties.

Species	Mole Fraction	Mass Fraction	MW	NBP °C	Density @ 15.5°C kg/m^3	Pc kPa	Tc °C	Acentric Factor
Malt1	0.126	0.058	244	236	920	2746	449	0.47
Malt2	0.138	0.081	307	295	949	2321	506	0.58
Malt3	0.162	0.118	383	355	977	1973	562	0.70
Malt4	0.081	0.068	440	397	997	1764	601	0.79
Malt5	0.084	0.077	480	425	1010	1643	626	0.84
Malt6	0.082	0.082	521	452	1022	1528	651	0.90
Malt7	0.077	0.083	564	480	1033	1416	675	0.96
Malt8	0.070	0.081	610	508	1041	1303	698	1.03
Malt9	0.076	0.095	663	540	1050	1182	723	1.11
Malt10	0.048	0.065	717	571	1057	1070	748	1.19
C5Asph	0.056	0.192	1800	721	1120	1057	906	1.27

4.3.2 C5-Asphaltene Characterization

The C5-asphaltenes fraction was characterized as a single lumped pseudo-component. The average molecular weight and density of the asphaltenes were set to typical values for asphaltenes from bitumen sources: 1800 g/mol and 1120 kg/m³, respectively (Barrera *et al.*, 2013). The true boiling point (TBP) was the estimated using the Søreide correlation (1989) and the critical properties and acentric factor were calculated using the Twu correlations (1984). The asphaltene pseudo-component properties are included in Table 4.1.

4.3.3 Tuning of Binary Interaction Parameters

Symmetric Mixing Rules

The symmetric mixing rules were tested with the following binary interaction parameters correlations recommended by Agrawal *et al.* (2012):

Maltenes/Maltenes and Maltenes/Solvent: $$\boldsymbol{k_{ij} = k_{ij}^{0}\left(1 + \frac{k_{ij}^{1}}{T} + k_{ij}^{2}\, ln(T)\right)} \qquad \textbf{4.8}$$

Asphaltenes/Maltenes and Asphaltenes/Solvent: $$\boldsymbol{k_{ij} = k_{ij}^{0}(1 + a_A T + b_A T^2)} \qquad \textbf{4.9}$$

where, k_{ij}^{1}, k_{ij}^{2}, a_A, and b_A are fitting constants and k_{ij}^{0} is given by Equation 4.7. The exponent n was set to the default value of 0.27. Equation 4.8 was used primarily to match the vapor-liquid data and Equation 4.9 to match the liquid-liquid data. The parameters used to fit the propane/bitumen saturation pressure and pitch phase onset data from this study are provided in Table 4.2.

Table 4.2 Tuned parameters for the symmetric binary interaction parameter correlations.

Component Pair	k_{ij}^{1}	k_{ij}^{2}	a_A	b_A
$Malt_i$ – $Malt_j$	-350	0.014	-	-
$Malt_i$ – Propane	-350	0.014	-	-
C5Asph – $Malt_i$	-	-	0	$6.44\ 10^{-6}$
C5Asph – Propane	-	-	0	$6.44\ 10^{-6}$

Compositionally Dependent Mixing Rules

A compositionally dependent set of binary interaction parameters was developed to capture the pitch* and C5-asphaltene yields. Note that although the compositionally dependent interaction parameters are symmetric ($k_{ij} = k_{ji}$), compositionally dependent mixing rules are defined as asymmetric because the interaction parameters can be different in each phase. At each composition and temperature, the binary interaction parameters for the maltene/solvent and C5-asphaltene/solvent pairs were manually modified until the pitch* and C5-asphaltenes yields were both matched. It was necessary to tune the k_{ij} between the solvent with Maltenes 6 to 10 and the

C5-asphaltenes to match the experimental yield data. The rest of the binary interaction parameters were determined from Equations 4.8 and 4.9.

The fitted k_{ij} correlation is shown in Figure 4.3 as a function of propane feed composition. The following correlation was developed to appropriately represent the $k_{ij}s$ as a function of NBP of the pseudo-component and propane feed composition:

$$k_{ij}^{*} = a + b(1 - e^{-0.065(w_{solv}-35)}) \quad \textbf{4.10}$$

With the following constraint

$$\text{If } k_{ij}^{*} > 0, k_{ij} = k_{ij}^{*}$$

$$\text{If } k_{ij}^{*} \leq 0, k_{ij} = 0$$

and where,

$$a = 0.00014736 * NBP - 0.05536225 \quad \textbf{4.11}$$

$$b = 0.0002374 * NBP - 0.05660673 \quad \textbf{4.12}$$

and w_{solv} is the weight percent of solvent in the feed and NBP is the normal boiling point of the pseudo-component. The fitted k_{ij} correlation were found to be temperature independent.

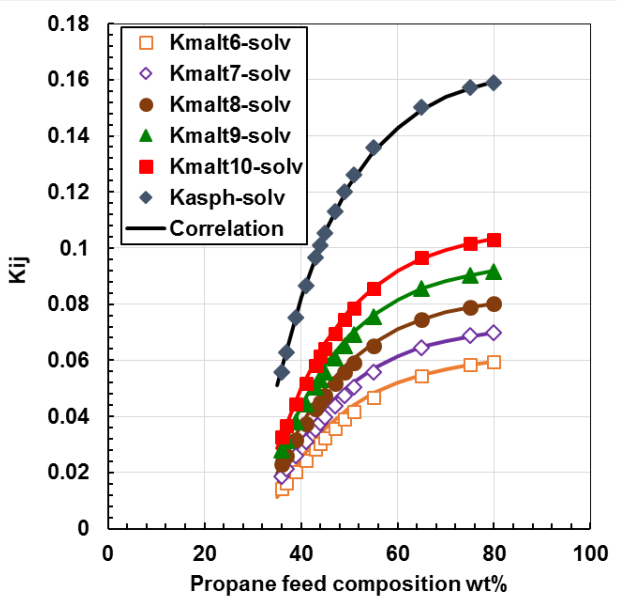

Figure 4.3 Values of the compositionally dependent binary interaction parameters, k_{ij}, used to match yield data. Symbols are fitted k_{ij} and lines are the correlation.

Chapter 5: Results and Discussion

This chapter summarizes the experimental phase behavior data and modeling results from this thesis for mixtures of propane and bitumen. The saturation pressures (vapor-liquid boundary) and heavy (pitch) phase onsets (liquid-liquid boundary) are presented. The morphology of the pitch phase is examined. The yields of solvent free heavy phase (pitch*) and C5-asphaltenes are presented and the compositions of the light phase and the pitch phase measured are reported. Finally, the model results are discussed.

5.1 Phase Boundaries and Morphology

Both liquid-vapor and liquid-liquid phase boundaries were observed for the mixtures of propane and bitumen. The vapor-liquid boundaries were determined from saturation pressure measurements and the liquid-liquid boundaries were determined from titrations performed in the high pressure microscope.

5.1.1 Vapor-Liquid Boundary: Saturation Pressures

Note that the saturation pressures of propane and WC-B-B3 bitumen mixtures were measured by another student in the same lab (Richardson, 2017). The data are provided in Table 5.1 and shown in Figure 5.1. As expected, the saturation pressures increased monotonically with increasing solvent content and temperature.

Table 5.1 Saturation pressure of propane diluted WC-B-B3 bitumen. The uncertainty of the propane content is ±0.1 wt%. The uncertainty in the saturation pressure measurements is ±0.30 MPa based on 90% confidence interval.

Temperature °C	Propane Content wt%	Saturation Pressure MPaa
50	1.1	0.33
50	2.8	0.43
50	5.6	0.62
50	11.4	0.92
75	1.1	0.46
75	2.8	0.56
75	5.6	1.07
75	11.4	1.77
89	1.1	0.66
89	2.8	0.83
89	5.6	1.49
89	11.4	2.35
135	1.1	0.78
135	2.8	1.55
135	5.6	2.72
135	11.4	4.51
180	1.1	1.69
180	2.8	2.88
180	5.6	4.59
180	11.4	7.59

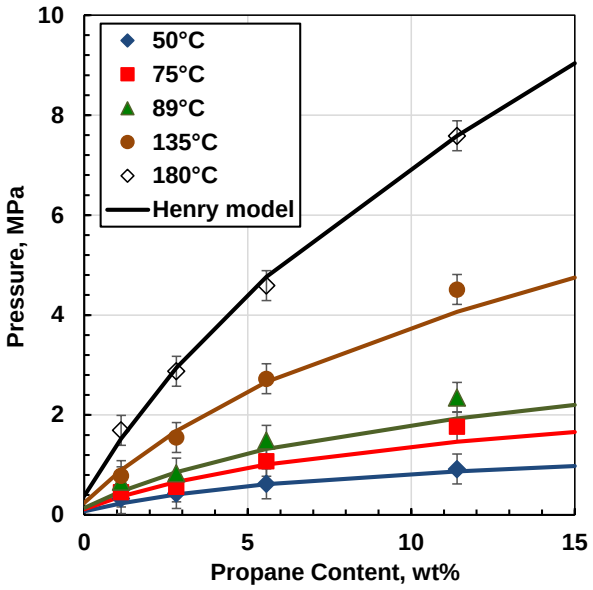

Figure 5.1 Saturation pressures for propane diluted WC-B-B3 bitumen at 50, 75, 89, 135, and 180°C. Symbols are data and lines are the modified Henry's law model.

As noted in Section 3.2, the uncertainties in the saturation pressure measurements could not be determined *a priori*. Instead, the uncertainties in the measurements were determined from the deviations of each data point from a modified Henry's law model (Badamchi *et al.*, 2009b) fitted to all of the data. The modified Henry's law model was defined as follows:

$$P_{sat} = x_{c3}H_{c3} + x_{bit}\gamma_{bit}P_{v,bit} \quad \textbf{5.1}$$

where,

$$H_{C3} = \exp\left(A_{C3} + \frac{B_{C3}}{T} + \frac{C_{C3}P_{sat}}{RT}\right) \quad \textbf{5.2}$$

$$P_{v,bit} = \exp\left(A_{bit} - \frac{B_{bit}}{T}\right) \quad \textbf{5.3}$$

and where P_{sat} is the predicted saturation pressure, x is the mole fraction, H is the Henry's law constant, γ is the activity coefficient, P_v is the vapour pressure, A, B, and C are fitted constants, and subscripts *C3* and *bit* represent propane and bitumen, respectively.

The mole fractions of propane and bitumen were determined from their mass fractions measured from experiments and their respective molecular weight. The vapor pressure of bitumen was

estimated based on a measurement of 380 kPa at 180°C and an assumption of 90 kPa at 60°C (the barometric pressure at the temperature of the dewatering procedure). The activity coefficient of the bitumen was assumed to be unity for lack of data and because the contribution of the bitumen to the saturation pressure was small. The Henry's law constants were fitted to the experimental saturation pressure dataset by minimizing the sum of the absolute deviation between the measured and the predicted values. The fitted constants are provided in Table 5.2 and the fitted curves are shown in Figure 5.1. The uncertainty in the saturation pressures was ±0.3 MPa based on 90% interval confidence. Note, the modified Henry model is not intended to be a rigorous phase behavior model and is only used to fit the data to assess the uncertainty of the measurements.

Table 5.2 Fitted Henry's law model constants for Equation 5.3 and Equation 5.2 for WC-B-B3 bitumen. Pressure is in MPa and temperature is in K.

Constants	Value
A_{bit}	9.99
B_{bit}, *K*	1836.85
A_{C3}	13.87
B_{C3}, *K*	-2160.95
C_{C3}, *L/mol*	0.15

5.1.2 Liquid-Liquid Phase Morphology

The liquid phases formed in the propane and WC-B-B3 bitumen mixtures were observed in the high pressure microscope (HPM) apparatus. The light phase was a solvent-rich liquid and was transparent in the HPM as shown in Figure 5.2. The heavy phase was opaque and, as will be shown later, was a pitch at most conditions, consisting of all of the C5-asphaltenes, a significant fraction of maltenes, and some solvent. At a propane content near the onset, the pitch phase appeared as particles at 20°C (Figure 5.2a), as irregular particles that merged on the HPM glass surface at 50°C (Figure 5.2b), and as droplets that coalesced into a continuous liquid phase at 90°C and above (Figure 5.2c). At propane contents above the onset, the pitch was a liquid at all the temperatures considered in this thesis, as shown at 50°C in Figure 5.3.

As will be shown later, above the onset, the pitch contained a significant fraction of maltenes and therefore was a liquid at all of the temperatures considered. The near onset behavior is interpreted

as a glass transition process between 50 and 90°C. Sirota (2005) and Johnston *et al*., (2017a) reported similar morphologies for asphaltenes and such behavior was also attributed to glass transition. Similar glass transitions were also observed in asphalts and verified with differential scanning calorimetry (Kriz *et al*., 2011). The formation of a glass suggests that the maltenes content in the pitch phase is low near the onset, as is expected with the low yields at this condition.

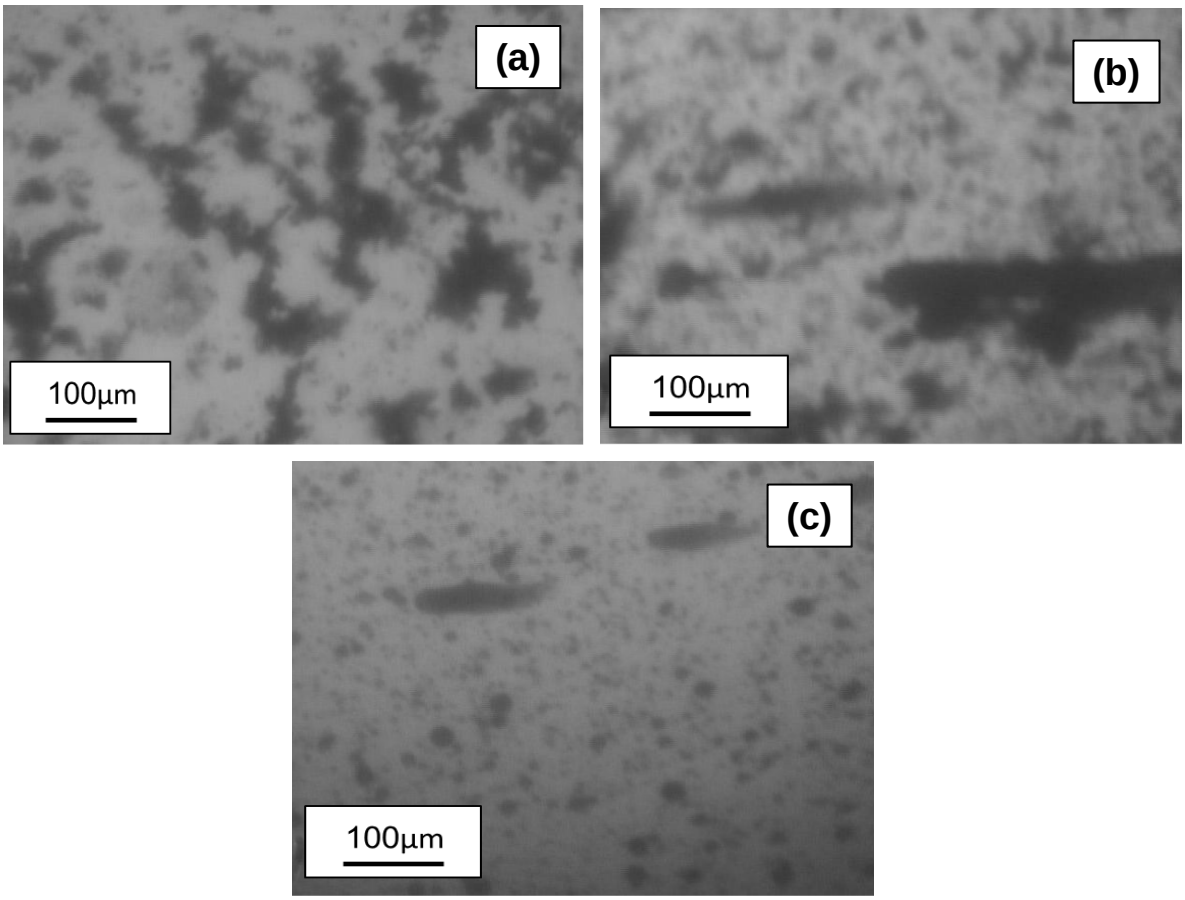

Figure 5.2 HPM micrograph images of heavy pitch phase (dark) from WC-B-B3 bitumen at propane contents immediately above the onset: a) 35 wt% propane, 20°C, and 10 MPa; b) 31 wt% propane, 50°C, and 7 MPa; c) 33wt% propane, 90°C, and 10 MPa.

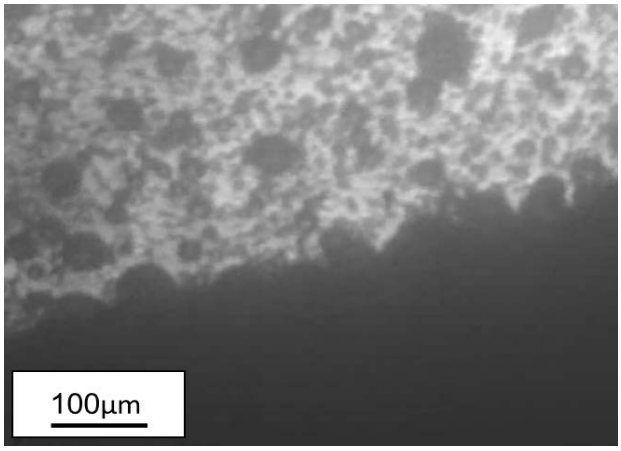

Figure 5.3 HPM micrograph image of heavy pitch phase from WC-B-B3 bitumen at 50°C, and 2 MPa and a propane content above the onset: 30 wt% propane versus onset of 21 wt% propane.

5.1.3 Liquid-Liquid Boundary: Heavy (Pitch) Phase Onset

The pitch phase onsets (propane content at liquid-liquid boundary) from propane diluted WCB-B3 bitumen are provided in Table 5.3 and shown in Figure 5.4. The onsets ranged from 20 to 40 wt% propane in the feed and increased with pressure. In other words, the bitumen became more soluble in propane with increasing pressure (more propane was required to initiate the second phase). According to regular solution theory, solubility depends on the molar volumes and relative solubility parameters of the components (Hirschberg *et al.*, 1984). The change in solubility with pressure is primarily due to the change in the solvent-bitumen mixture density, as observed in asphaltene precipitation from depressurized live oils (Tharanavasan et al., 2011). The trend between solvent content of onset and pressure is also consistent with the literature data for *n*-alkanes diluted heavy oil (Akbarzadeh *et al.*, 2005; Johnston *et al.*, 2017a). Interestingly, temperature had very little effect on the onset condition. It appears that the decrease in solubility expected with decreased density (Saryazdi *et al.*, 2013) is offset by a relative change in the solubility parameters of the bitumen and propane.

Table 5.3 Measured solvent content at the onset of heavy pitch phase in propane diluted WC-B-B3 bitumen. The uncertainty in the propane content measurement is ± 1.3 wt%.

Temperature °C	Pressure MPa	Propane Content wt%
20	2.1	21
20	5.0	27
20	10.3	35
50	2.0	21
50	6.9	31
50	10.3	35
90	6.9	31
90	10.3	33
130	10.0	33

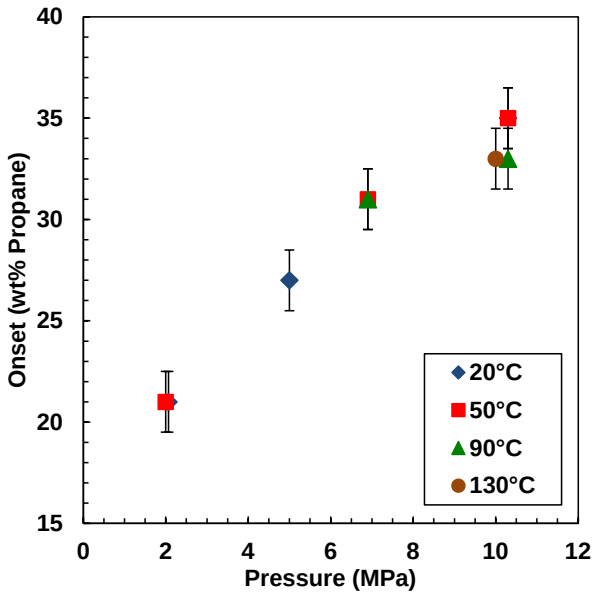

Figure 5.4 Onsets of the pitch phase from propane diluted WC-B-B3 bitumen at pressures up to 10 MPa and temperatures from 20 to 130°C.

5.1.4 Pressure-Composition (P-X) Phase Diagrams

The saturation pressure and heavy pitch phase onset data were combined to generate the pressure-composition (P-X) phase diagrams shown in Figure 5.5. Dini *et al*. 2016 also presented P-X phase diagrams for mixtures of propane and Peace River bitumen. The VL equilibria collected at 50, 75,

and 90°C up to a propane feed composition of 11 wt% are in agreement within the uncertainty of the measurements. However, there are discrepancies in the representation of the LL boundary. For example, the formation of the propane/maltene-rich and bitumen-rich phases (L_1L_2) was observed that ranges from 21 to 40 wt% propane, increasing with pressure as stated in section 5.1.3. Whereas, Dini *et al*. 2016 predicted the LL boundary at approximately 29 wt% propane as a straight vertical line (no pressure dependence). Nourozieh *et al*. 2015 presented propane solubility data (VL boundary) for mixtures with an Athabasca bitumen that are also in agreement with the VL data presented in this thesis.

The P-X diagrams are qualitatively similar to those obtained for *n*-pentane diluted bitumen (Johnston *et al.*, 2017b). The saturation pressures are higher for the relatively more volatile propane. The onsets are shifted to lower solvent contents with the lower solubility parameter for propane. The onsets show more pressure dependence possibly because propane is more compressible than pentane. Also, the temperatures are close to the propane critical temperature of 97°C. Zou and Shaw (2007) has noted that pseudo-ternary phase diagrams near the solvent critical point have more curvature in the liquid-liquid phase boundary.

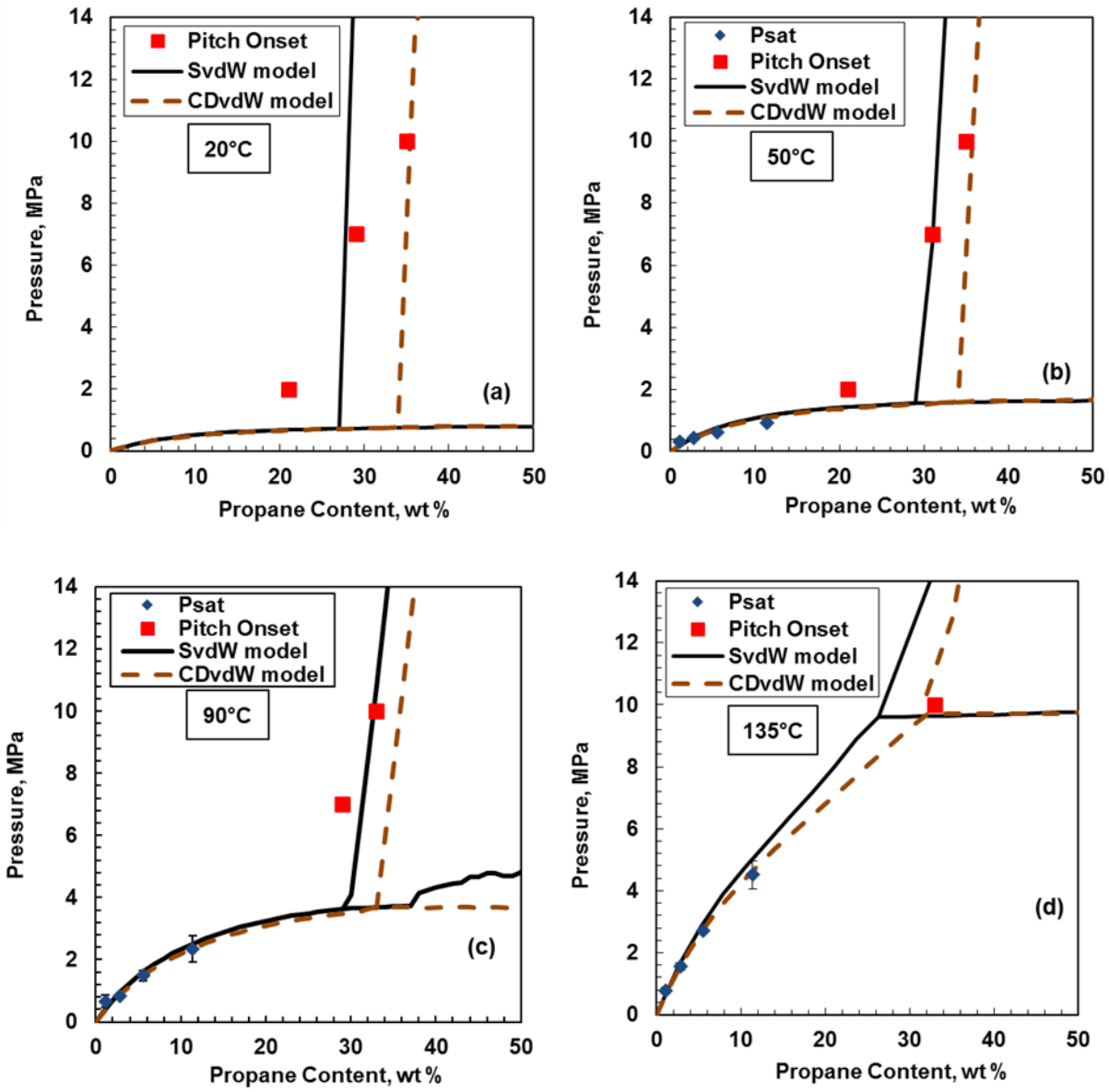

Figure 5.5 Pressure-composition phase boundary diagrams for mixtures of propane and WC-B-B3 bitumen at (a) 20°C, (b) 50°C, (c) 90°C, and (d) 130°C. Symbols are the experimental data. Solid lines are the APR EoS with symmetric van der Waals mixing rules (SvdW). Dashed lines are the APR EoS with the compositionally dependent van der Waals mixing rules (CDvdW).

5.1.5 CEoS Model Phase Boundaries

The phase diagrams were modeled with the APR CEoS described in Chapter 4, first with temperature dependent binary interaction parameters (Eqs. 4.8 and 4.9) and then with composition dependent parameters. For convenience the former model is referred to as the SvdW (Symmetric van der Waals) model and the latter as the CDvdW (Compositionally Dependent van der Waals) model. The composition dependent parameters were required to match yield data as will be discussed later. Note, the composition dependent parameters were independent of temperature. The tuned model results are shown in Figure 5.5.

Results with Temperature Dependent Binary Interaction Parameters (SvdW)

After tuning the binary interaction parameters, the model matched the measured VL boundary data to within the uncertainty of the measurements with the exception noted below. The model could be tuned to match the onset at any one pressure but did not match the effect of pressure on the LL boundary. The reason for this problem is not known but may be related to the poor compressed liquid density predictions from a cubic equation-of-state.

The model predicted an unexpected increase in the saturation pressure above 37 wt% propane at 90°C as shown in Figure 5.5c. The VL behavior is expected to be nearly constant pressure above the onset (liquid-liquid region) as predicted from 30 to 37 wt% propane. The heavy phase has become saturated with the solvent and additional solvent mainly changes the amount of the light phase but not the VLE (Konynenburg and Scott, 1980; Dini *et* al., 2016). This constant saturation pressure was predicted at the other temperatures. The error occurs because the flash calculation did not converge correctly at these conditions. The error at 90°C was not observed when the model was run with constant binary interaction parameters and must be caused by the use of temperature dependent binary interaction parameters.

Results with Composition Dependent Binary Interaction Parameters (CDvdW)

The tuned model with composition dependent binary interaction parameters fits the VL boundary with similar accuracy as the first model. However, it also predicts constant saturation pressures at the base of the liquid-liquid region at all temperatures. The LL boundaries moved to higher propane

contents (higher solubility) after the temperature dependence was removed from the compositionally dependent interaction parameters.

5.2 Pitch Phase Yields

5.2.1 Measured Yields

The yields of the propane diluted WC-B-B3 and WC-B-B4 bitumens were measured in the blind cell apparatus. Yield is defined as the mass of the component divided by the mass of bitumen in the feed. Recall that, in this apparatus, the solvent content of the pitch phase could not be measured. Therefore, the C5-asphaltene and pitch* yields are reported, where pitch* includes the asphaltenes and maltenes but no solvent.

The yields are provided in Table 5.4 and shown in Figure 5.6. As discussed in Section 3.4, the yields were calculated based on assumed propane contents in the pitch phase of 0, 30 wt%, and the expected propane content based on the independent measurements reported later. The error bars in Figure 5.6 represent the combined uncertainties between the yields measurements and the yield difference based on the minimum and maximum assumed propane contents. The symbols are the yields based on the expected propane content. The expected propane contents and the corresponding yields are provided in Table 5.4. The C5-asphaltene yields and pitch* yields at high dilution were insensitive to the assumed propane content. However, the uncertainty in the pitch* yields increased significantly near the onset.

The yields increased steeply at propane contents above the onset reaching plateaus at approximately 40 wt% propane. The plateau pitch* yields ranged from approximately 50 to 70 wt%; in other words more than half of the bitumen reported to the pitch phase. These yields are considerably higher than observed with higher carbon number *n*-alkanes. For example, only a few wt% maltenes report to the heavy phase in *n*-pentane diluted bitumen (Johnston *et al*., 2017a). The higher yields in propane confirm that propane is a poorer solvent for bitumen, as expected from its solubility parameter: 13.5 $MPa^{0.5}$ for propane versus 14.9 $MPa^{0.5}$ for *n*-pentane. Note, solvents with lower solubility parameters are less compatible with bitumen (Alboudwarej *et al.*, 2003).

The C5-asphaltene yields were insensitive to pressure and temperature because all of the asphaltenes precipitated at almost all conditions. Curiously, although the onsets depended on pressure, the pitch* yields were relatively insensitive to pressure. Nonetheless, the yield decreases slightly with pressure as expected with the higher density fluid. The pitch* yields were insensitive to temperature except at 130°C where higher yields were observed. The critical point of propane is 97°C and the shape of the phase diagram is known to change when the mixture approaches the solvent critical point (Dini *et al*., 2016).

Table 5.4 Pitch* and C5-asphaltene yield data from propane diluted bitumen. The uncertainty in the C5-asphaltene yields is less than ±0.5 wt% at propane contents above 40 wt%. The uncertainty in the pitch* yields is less that ±5 wt% at propane contents above 50 wt%. The uncertainty increases significantly towards the onset (see Figure 5.6). C3 indicates propane. Bold values indicate where propane content in the heavy pitch phase was measured; other values are assumed as noted in the experimental methods.

Oil	Temperature °C	Pressure MPa	Feed C3 Content wt%	Pitch Phase C3 Content wt%	C_5-Asph Yield wt%	Pitch* Yield wt%
WC-B-B3	20	2	26.5	22	3.7	-
	20	2	32.1	22	11.1	-
	20	2	40.0	22	20.0	-
	20	2	48.9	22	20.3	-
WC-B-B4	20	2	25.9	22	2.1	18
	20	2	30.7	22	15.7	56
	20	2	39.7	22	21.9	61
	20	2	50.3	22	22.3	59
WC-B-B3	20	5	32.9	22	15.0	41
	20	5	39.2	22	20.4	55
	20	5	49.1	22	20.8	57
	20	5	60.0	22	20.8	56
	20	5	69.4	22	20.8	56
WC-B-B3	20	10	38.8	22	19.7	48
	20	10	49.9	22	20.8	55
	20	10	58.5	22	20.8	54
	20	10	68.4	22	20.8	52
	20	10	73.8	22	20.8	54
WC-B-B3	50	10	39.8	26	18.6	35
	50	10	49.8	**26**	20.8	51

Oil	Temperature °C	Pressure MPa	Feed C3 Content wt%	Pitch Phase C3 Content wt%	C_5-Asph Yield wt%	Pitch* Yield wt%
WC-B-B3	50	10	60.4	26	20.8	58
	50	10	71.2	26	20.8	55
	50	10	75.5	26	20.8	53
	90	10	40.0	15	20.7	53
WC-B-B3	90	10	49.8	15	20.8	57
	90	10	59.4	15	20.8	57
	90	10	70.5	15	20.8	55
	90	10	75.0	15	20.8	56
WC-B-B4	90	10	40.1	15	21.7	51
	90	10	50.7	15	22.2	57
	90	10	60.0	15	22.3	56
	90	10	70.0	15	22.3	54
	90	10	75.3	15	22.3	51
WC-B-B4	130	10	40.3	2	22.3	56
	130	10	51.4	**2**	22.3	68
	130	10	60.3	2	22.3	67
	130	10	70.0	2	22.3	63
	130	10	74.9	2	22.3	64

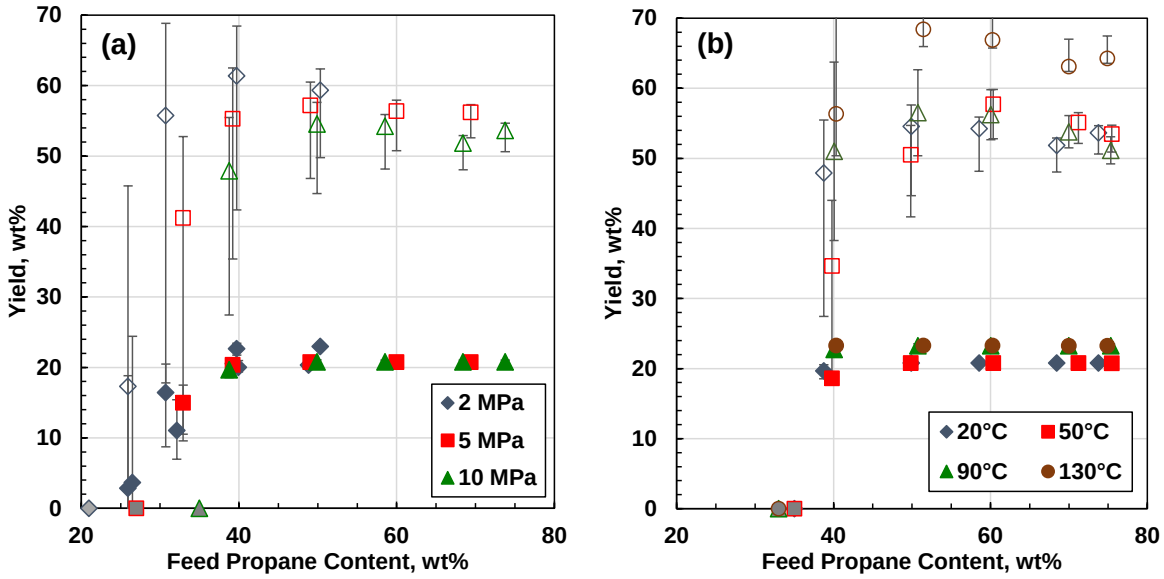

Figure 5.6 C5-asphaltene and pitch* yields from mixtures of propane and bitumen: a) effect of pressure at 20°C; b) effect of temperature at 10 MPa. Data at 2 MPa and at 90 and 130°C from WC-B-B4 bitumen; all other data from WC-B-B3 bitumen.

5.2.2 CEoS Model Yields

Results with Temperature Dependent Binary Interaction Parameters (SvdW)

Figure 5.7 shows a typical model prediction for the C5-asphaltene and pitch* yields. While the model almost matches the C5-asphaltene yield, it significantly underpredicts the pitch* yield. The same issue was observed at all other temperatures and pressures. The symmetric structure of the CEoS model did not allow the tuning to match both the onset and the yield. Recall that the model shown here was tuned to match the onset. If the model was tuned to match the yield, the predicted propane content at the onset would be much lower than the measured value. The same problem occurred when using a symmetric CEoS to model asphaltene precipitation for *n*-pentane diluted bitumen (Agrawal *et al.*, 2012; Johnston *et al.*, 2017b). Johnston *et al.*, (2017b) developed composition dependent binary interaction parameters to address this issue.

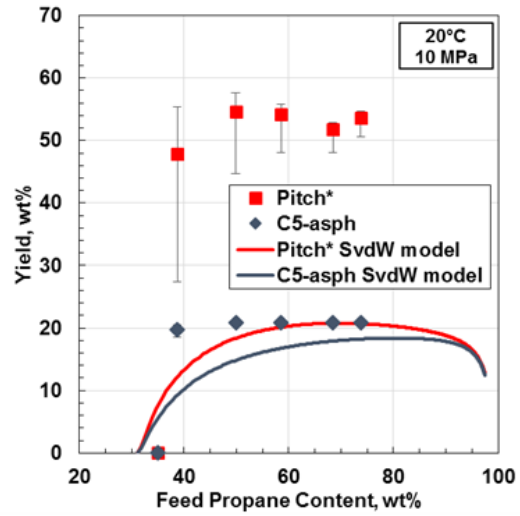

Figure 5.7 Pitch* and C5-asphaltene yield curves from propane diluted WC-B-B3 bitumen systems at 10 MPa and 20°C. Symbols are the experimental data and lines are the APR EoS model with temperature dependent binary interaction parameters.

Results with Composition Dependent Binary Interaction Parameters (CDvdW)

As discussed in Chapter 4, a set of composition dependent binary interaction parameters was tuned to match the yield data for propane diluted bitumen (Eq. 4.10). The use of composition dependent binary interaction parameters significantly improved the predictions of the C5-asphaltene and pitch* yields as shown in Figure 5.8. The model matched the pitch* and C5 asphaltene yields at

different temperatures up to 90°C at 10 MPa. However at 130°C, the model predicted an incorrect sudden jump in the pitch* yield at onset, then over-predicted the pitch* yield until 80 wt% of propane in feed, and finally predicted a single liquid phase when propane content in feed was over 80 wt%. This incorrect trend occurs when the temperature exceeds the critical temperature of propane. The flash calculations became unstable at this point and so far the only solution found for this issue was to use composition dependent binary interaction parameters.

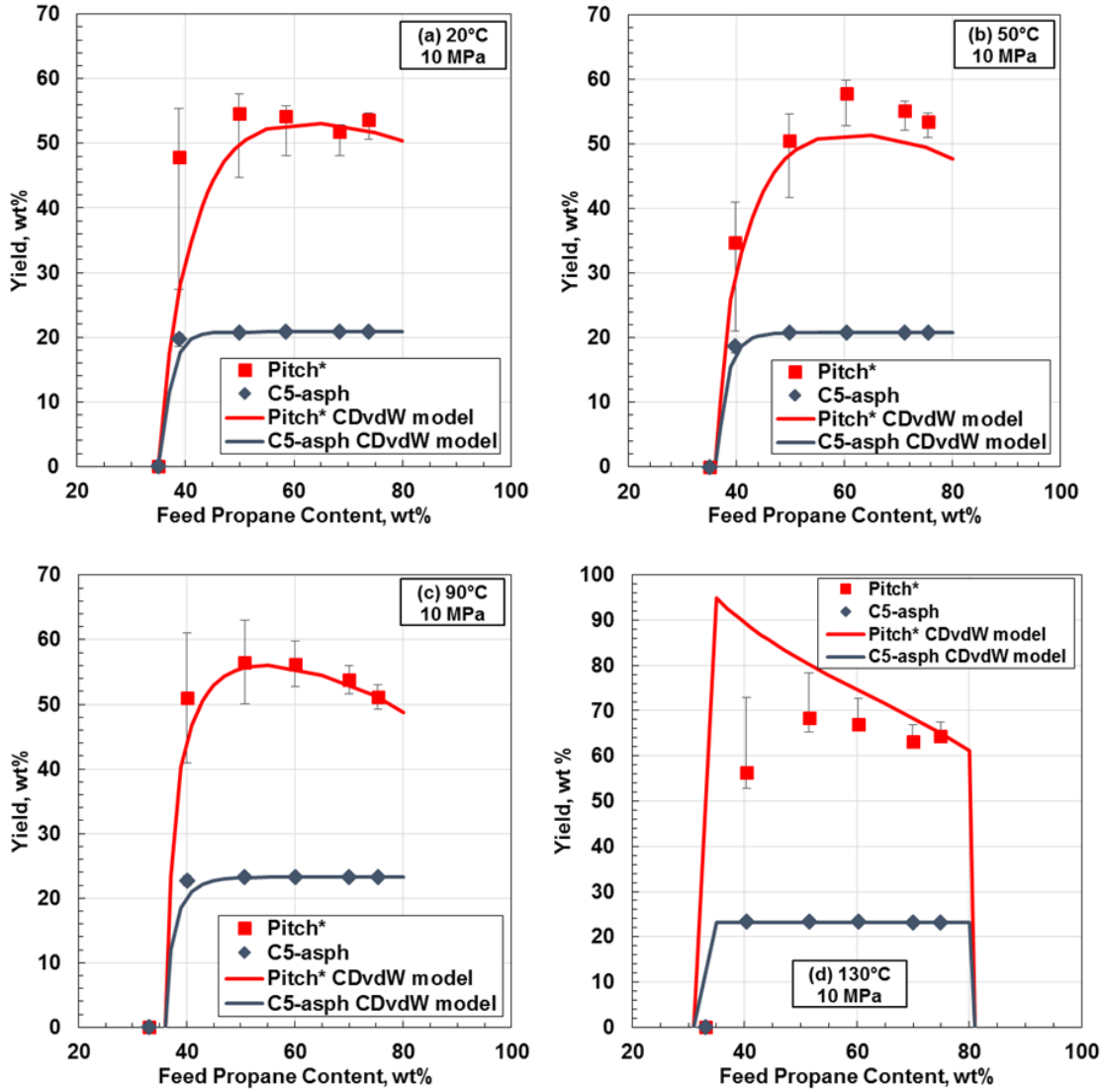

Figure 5.8 Pitch* and C5-asphaltene yield curves from propane diluted WC-B-B3 bitumen systems at: (a) 20°C, 10 MPa; (b) 50°C, 10 MPa. Pitch* and C5-asphaltene yield curves from propane diluted WC-B-B4 bitumen systems at: (c) 90°C, 10 MPa; and (d) 130°C, 10 MPa.

Symbols are the experimental data and lines are the APR EoS model with composition dependent binary interaction parameters.

5.3 Liquid-Liquid Phase Compositions

5.3.1 Measured Yields

The phase composition can only be measured in the PVT cell when the pitch phase is a liquid; that is, at temperatures above approximately 90°C or propane contents in feed of at least 50 wt%. The composition experiments are also time intensive limiting the amount of data that could be collected. A total of 5 compositions were measured at conditions listed in Table 5.5. The C5-asphaltene and pitch* yields are also provided. The C5-asphaltene yields are within the experimental error of the previously reported blind cell yields at the same conditions. The pitch* yields are consistently higher between 10 and 20 wt%. The smallest deviation is at 130°C, where the pitch* yields from each method are almost within the experimental error (68 ±6 wt% from blind cell; 75 ±3 wt% from PVT cell). The error comes from the light phase compositions; the light phase samples taken from the blind cell has a lower propane content. As yet, no explanation has been found for this discrepancy. The procedures in both experiments are almost identical and the same mass evaporation method was performed to collect and analyze the light phase samples. It is possible that the system did not reach equilibrium in one or both methods.

The compositions for the conditions listed in Table 5.5 are shown in Table 5.6 to Table 5.10 in the same order. The material balance errors were determined for each component in each case as follows:

$$MB\ error = \frac{\left(m^{L}_{component} + m^{H}_{component}\right) - m^{F}_{component}}{m^{F}_{component}} * 100 \qquad \textbf{5.4}$$

where m is mass, L is the light phase, H is the heavy pitch phase, and F is the feed. The material balance error was less than 5% except for C5 asphaltene at 130°C and 10 MPa. Note, entrained fluid in the heavy phase will not cause a material balance error but rather an incorrect composition and yield.

Table 5.5 Pitch* and C_5 asphaltene yields from propane diluted WC-B-B3 bitumen at 2 MPa and 50°C (1. 50 wt% C3 in feed; 2. 75 wt% C3 in feed), 5 MPa and 50°C, and 10 MPa and 130°C. The uncertainty of the C5-asphaltene and pitch* yields are ±1.7 and ±2.6 wt%, respectively.

Conditions	Feed Propane Content wt%	C5-Asphaltene Yield wt%	Pitch* Yield wt%	Heavy/Feed w/w
2 MPa, 50°C (1)	49.5	19.4	70.9	0.46
2 MPa, 50°C (2)	74.2	21	64.5	0.21
5 MPa, 50°C	49.7	19.3	66.6	0.46
6.9 MPa, 90°C	49.5	19.0	77.5	0.48
10 MPa, 130°C	50.0	20.1	74.7	0.39

Table 5.6 Feed, light solvent-rich phase, heavy pitch phase compositions from propane diluted WC-B-B3 bitumen at 2 MPa and 50°C and propane concentration in feed of 50 wt%. The uncertainty of the phase compositions is ±1.5 wt%.

Component	Measured				CDvdW model	
	Feed wt%	Light Phase wt%	Heavy Phase wt%	MB error %	Light Phase wt%	Heavy Phase wt%
Propane	49.5	72.6	22.1	-0.4	75.9	6.5
Maltenes	40.8	27.3	56.4	-0.3	24.0	57.3
C5-Asph	9.7	0.0	21.5	2.1	0.0	36.2

Table 5.7 Feed, light solvent-rich phase, heavy pitch phase compositions from propane diluted WC-B-B3 bitumen at 2 MPa and 50°C and propane concentration in feed of 75 wt%. The uncertainty of the phase compositions is ±1.0 wt%.

Component	Measured				CDvdW model	
	Feed wt%	Light Phase wt%	Heavy Phase wt%	MB error %	Light Phase wt%	Heavy Phase wt%
Propane	74.2	88.0	20.7	0.0	86.8	4.2
Maltenes	20.8	12.0	53.5	-0.6	13.2	59.4
C5-Asph	5.0	0.0	25.8	9.4	0.0	36.3

Table 5.8 Feed, light solvent-rich phase, heavy pitch phase compositions from propane diluted WC-B-B3 bitumen at 5 MPa and 50°C and propane concentration in feed of 50 wt%. The uncertainty of the phase compositions is ±1.1 wt%.

Component	Measured				CDvdW model	
	Feed wt%	Light Phase wt%	Heavy Phase wt%	MB error %	Light Phase wt%	Heavy Phase wt%
Propane	49.7	69.6	26.8	+0.7	67.0	6.7
Maltenes	40.6	30.3	51.7	-1.7	33.0	56.4
C5-Asph	9.7	0.0	21.5	+1.2	0.0	36.8

Table 5.9 Feed, light solvent-rich phase, heavy pitch phase compositions from propane diluted WC-B-B3 bitumen at 6.9 MPa and 90°C and propane concentration in feed of 50 wt%. The uncertainty of the phase compositions is ±1.0 wt%.

Component	Measured				CDvdW model	
	Feed wt%	Light Phase wt%	Heavy Phase wt%	MB error %	Light Phase wt%	Heavy Phase wt%
Propane	49.5	76.9	18.4	-0.5	72.2	9.9
Maltenes	40.8	23.1	61.6	+2.0	27.8	61.0
C5-Asph	9.7	0.0	20.0	-1.0	0.0	29.1

Table 5.10 Feed, light solvent-pitch phase, heavy pitch phase compositions from propane diluted WC-B-B3 bitumen at 10 MPa and 130°C and propane concentration of 50 wt%. The uncertainty of the phase compositions is ±1.4 wt%.

Component	Measured				CDvdW model	
	Feed wt%	Light Phase wt%	Heavy Phase wt%	MB error %	Light Phase wt%	Heavy Phase wt%
Propane	50.0	79.8	1.8	-1.6	82.3	13.0
Maltenes	40.4	20.2	70.2	-4.3	17.7	64.7
C5-Asph	9.6	0.0	28.0	+9.7	0.0	22.3

5.3.2 Ternary Phase Diagrams

As noted previously, all of the C5-asphaltenes report to the heavy pitch phase at these conditions. Therefore, the phase composition is determined by the partitioning of the propane and the maltenes between the light and heavy phases. The partitioning is best observed on a ternary phase diagram. The phase composition data at 2 MPa and 50°C (50 and 75 wt% propane in feed), 5 MPa and 50°C, 6.9 MPa and 90°C, and at 130°C and 10 MPa all of these at 50 wt% propane in feed are plotted on ternary phase diagrams in Figure 5.9. In each ternary plot, Point B is the bitumen and the dashed line between Point B and the propane apex represents all the possible feed mixtures of propane and bitumen. Point F is the feed composition and Point O is the onset condition. The end-points of the tie-lines are the measured light solvent/maltene-rich phase compositions (L_1) and heavy pitch phase compositions (L_2) of the reported phase composition experiments. The LL phase boundary (dotted line) is a visual guide based on the measured light solvent-rich phase and heavy pitch phase compositions.

The liquid-liquid region at 10 MPa and 130°C is larger than the regions at 50°C and 90°C, corresponding to a lower propane content in the heavy phase; that is, lower propane solubility. For example, the propane content in the pitch phase decreased from 27 wt% at 50°C and 5 MPa to 2 wt% at 130°C and 10 MPa. Propane solubility increased with pressure; for example, the propane content in the heavy pitch phase increases from 22 to 27 wt% as the pressure increases from 2 to 5 MPa at 50°C. The propane solubility was also affected by the propane content in the feed. For instance, the propane content in the heavy pitch phase decreases from 22 to 20 wt% as the propane feed composition was incremented from 50 to 75 wt% at 50°C and 5 MPa.

Note, if any of the light phase was entrained in the heavy pitch phase and was not visually detected, it would be reported as part of that phase. Hence, the reported heavy pitch phase propane and maltene contents and the pitch* yields could err on the high side. This potential error is more likely at the lower temperatures. The relatively high propane contents at 50°C should be treated with caution.

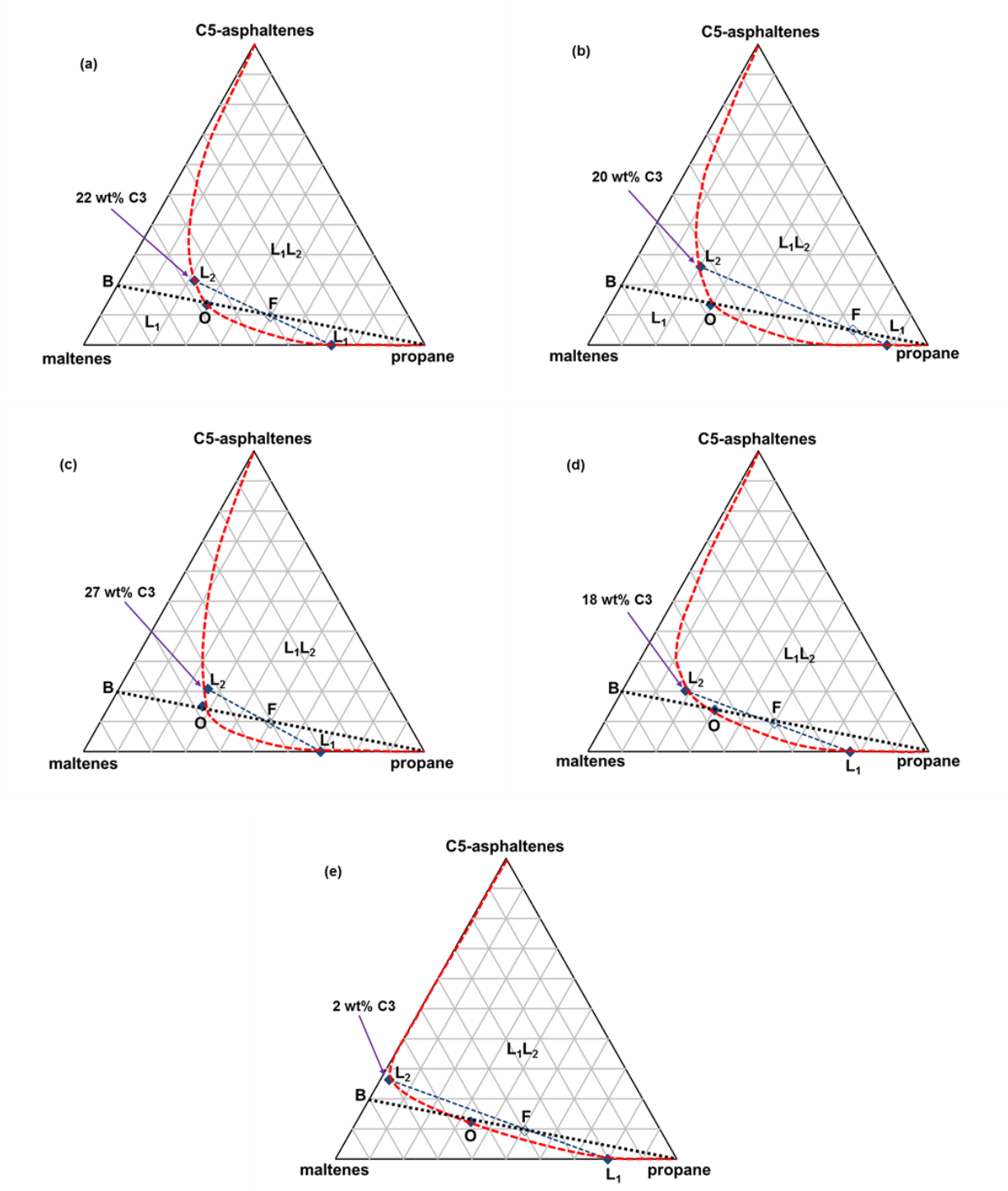

Figure 5.9 Pseudo-ternary diagram for propane diluted WC-B-B3 bitumen at: (a) 50°C and 2 MPa, 50 wt% C3; (b) 50°C and 2 MPa, 75 wt% C3; (c) 50°C and 5 MPa; (d) 90°C and 6.9 MPa; (e) 130°C and 10 MPa. Intervals on diagrams are 10 wt%.

Finally, it is interesting to compare the data for mixtures of bitumen and higher carbon number n-alkanes, such as *n*-pentane. For example, when *n*-pentane is added to bitumen in sufficient quantity, a solvent-rich and an asphaltene-rich phase form. In effect, asphaltenes are rejected from the mixture. When propane is added, a propane/maltene-rich and a bitumen-rich phase form. In effect, the light components are stripped from the bitumen-rich pitch phase which is left with 55 to 70 wt% of the original bitumen. At temperatures above 90°C, the mutual solubility of the bitumen components and the propane decreases resulting in higher yield (less stripping) and lower propane content in the pitch phase.

5.3.3 CEoS Model Compositions

Since the model with temperature dependent binary interaction parameters failed to match the yield data, the phase compositions were only modeled with the composition dependent parameters (CDvdW model). The model matched the light phase compositions to within 5 wt% but only matched the heavy phase compositions to within 20%. The main source of error was the predicted propane content in the heavy phase which was significantly under-predicted in all cases except at 130°C. Given the uncertainty in the measured compositions below 130°C, it is not clear if the discrepancies are due to the data or the model. At 130°C, the propane content was over-predicted by 12 wt% and here the data are believed to be sound and the error is attributed to the model. Johnston *et al*. (2017b) also found that the CEoS with composition dependent binary interaction parameters could not accurately predict the phase compositions. It appears that the limit of the CEoS approach for bitumen/solvent pseudo-binaries is the prediction of phase compositions and yields.

Chapter 6: Conclusions and Recommendations

The main contribution of this thesis is to provide data for the phase behavior of heavy oil and propane mixtures at different pressures, temperatures and feed compositions. These data are required for the design and operation of solvent based *in situ* heavy oil recovery processes. A second contribution is an evaluation of the ability of a cubic equation of state (Advanced Peng-Robinson EoS) to model the data. The major conclusions and recommendations for future research are listed below.

6.1 Conclusions

6.1.1 Experimental Methodology

Two new methodologies were developed to: 1) collect yield data from blind cells for pitches containing asphaltenes and maltenes; 2) measure phase compositions and yields in a PVT cell. The issue with yields from blind cells is that only the light phase composition can be measured but not the heavy phase composition nor the mass of each phase. It was demonstrated that yields could be determined from a material balance with an assumed solvent content in the heavy phase. The uncertainty caused by the assumption was ±0.5 wt% for the C5-asphaltene yields, ±8.3 wt% for the pitch* (solvent-free pitch) yields at propane contents above 50 wt%, but high for pitch* yields near the onset of the pitch phase formation.

The previous methodology for determining compositions in a PVT cell required the calculation of the mass of each phase from phase volume and composition measurements. A new procedure was developed to collect the entire volume of each phase and measure the phase masses gravimetrically. The compositions were measured as before. The new procedure resulted in more accurate mass determinations and could be checked with a material balance. The material balance for each component closed to within 5% except for C5-asphaltene at 130°C and 10 MPa. The uncertainties of pitch*(solvent-free heavy phase) yield, C5-asphaltene yield, propane-rich light phase and heavy pitch phase compositions were estimated to be 2.6, 1.7, 1.6, and ±0.8 wt%, respectively.

6.1.2 Experimental Data

The phase behavior of bitumen and propane mixtures were examined at temperatures from 20 to 180°C and pressures from 2 to 10 MPa. Both vapor-liquid (VL) and liquid-liquid (LL) phase equilibria were observed. Saturation pressures (VL boundary) for these mixtures were measured at a propane content in feed from 1 to 11 wt% and at temperatures from 50 to 180°C. The estimated uncertainty was ±0.3 MPa. The saturation pressures increased monotonically with increasing solvent content and temperature, as observed in other bitumen/*n*-alkane systems. The saturation pressures at a given propane content (or equivalently propane solubilities at a given pressure) were consistent with data published in the literature.

The heavy pitch onsets (propane content at the LL boundary) were measured at temperature from 20 to 130°C and pressures from 2 to 10 MPa. The uncertainty of the measurement was ±1.4 wt% propane. The propane content at the onset ranged from 21 to 35 wt% and was observed to be insensitive to temperature but increased as pressure increased.

The heavy pitch phase appeared as glass-like particles at 20°C near the onset, and as droplets that coalesced into a continuous liquid phase at 90°C and above. A gradual glass transition process was inferred between 50 and 90°C. At propane content above the onset (where a significant amount of maltenes reported to the pitch phase), the pitch was observed to be a liquid regardless of temperature.

The pitch* and C5-asphaltene yield data were collected from mixtures of propane and bitumen at temperatures ranging from 20 to 130°C and pressures from 2 to 10 MPa. At above 40 wt% propane content in feed, all C5-asphaltenes report to the heavy pitch phase. The pitch* yields increased steeply at propane content above the onset reaching a plateau at approximately 40 wt% propane. The plateau pitch* yields ranged from approximately 50 to 70 wt%, indicating that more than half of the bitumen partitioned to the pitch phase. This high maltene content in the heavy phase is in contrast with mixtures of bitumen and higher carbon number *n*-alkane solvents (mainly *n*-pentane), where the heavy phase consists mainly of asphaltenes and the majority of the bitumen remains in

the solvent-rich phase. Pitch* and C5-asphaltene yields were relatively insensitive to pressure and temperature except at 130ºC where higher pitch* yields were observed.

Ternary diagrams for mixtures of propane and WC-B-B3 bitumen were constructed to best observe the partitioning of each component in a liquid-liquid equilibrium. Phase composition data were collected at temperatures from 50 to 130°C and pressures from 2 to 10 MPa. The largest liquid-liquid region and therefore the lowest propane content in the heavy phase were observed at 10 MPa and 130°C. The propane content decreased from 27 wt% at 50°C and 5 MPa to 2 wt% at 130°C and 10 MPa. At temperature above 90ºC, the mutual solubility of the bitumen component and the propane decreases in higher yields and lower propane contents in the heavy phase. The propane solubility was also affected slightly by pressure and the propane feed composition. The propane content in the heavy phase increased from 22 to 27 wt% as the pressure increased from 2 to 5 MPa at 50ºC, and decreased from 22 to 20 wt% as the propane feed composition was incremented from 50 to 75 wt% at 50°C and 5 MPa. Note that at 50ºC, the pitch phase is very viscous and there could be undetected light phase entrainment in the pitch phase. Entrainment would lead to falsely high reported propane and maltene contents in the heavy phase. Hence, the phase compositions at 50 and possibly 90°C should be treated with caution.

6.1.3 Modeling

The cubic APR EoS was applied to model phase boundaries, pitch* and C5-asphaltene yields, and liquid-liquid phase composition for bitumen and propane mixtures. Symmetric mixing rules (SvdW) and composition dependent mixing rules (CDvdW) were tested.

The APR EoS with the symmetric temperature dependent binary interaction parameters (SvdW) could fit the vapor-liquid boundary to within the uncertainty of the measurements. However, the model incorrectly predicted an increasing saturation pressure at 90ºC. The error was created by the tuning of the temperature dependent binary interaction parameters. The model could also be tuned to fit the liquid-liquid boundary at any given pressure but could not predict the pressure dependent boundary. The model could approximately match the C5-asphaltene yield curve but significantly under-predicted the pitch* yields. The symmetric structure of the CEoS did not allow the tuning

to match both onset and the yield. As a result, SvdW could not accurately predict the phase compositions in a liquid-liquid equilibrium.

The use of a compositional dependence binary interaction parameters (CDvdW) successfully fitted both pitch* and C5-asphaltene yields at 10 MPa and all temperatures except for 130°C, while retaining the accurate prediction of the VL boundary. A correlation was established for the pseudo-component (maltenes 6+)/propane binary interaction parameter to the solvent mass fraction and NBP (Normal Boiling Point) of the pseudo-component. However, the model still incorrectly predicted the yield curves (C5-asphaltenes and pitch* yields) when the temperature exceeded the critical temperature of propane, where the flash calculations became unstable. The model was able to match the light phase composition to within 5 wt% but could not accurately match the heavy phase composition. The propane content in the heavy phase was significantly under-predicted in all cases except at 130ºC where the propane content was over-predicted.

In general, although CEoS can be tuned to match saturation pressure, onset, yield and phase composition data for bitumen and propane mixtures, composition dependent binary interaction parameters were required and this type of interaction parameter is more complicated to tune and limits the generality of the model when considering other solvents.

6.2 Recommendations

In this thesis phase behavior data were collected for propane diluted bitumen, including phase composition data. It is recommended to measure the phase behavior of bitumen with other solvents of commercial interest such as butane and condensates.

It is recommended to examine other equations of state that have already shown promising results in modeling the phase behavior of heavy oil and *n*-alkanes mixtures, such as the CPA EoS and PC-SAFT EoS models. It is also recommended to develop and evaluate a hybrid model that combines regular solution model and equation of state.

Appendix A: Error Analysis

A.1 HPM Onset Data

The main source of uncertainty in measuring the propane content at which second phase appears is the mass of solvent (propane) injected at each injection step (typically at increments of 2 wt%). The mass of solvent injected at each step was estimated using the cathetometer readings and the solvent density at experimental conditions. The pump readings were used as verification, as described in Section 3.3.2. The uncertainty of propane content was estimated based on the uncertainties in the volume of propane injected at each step (± 0.01 cm^3 based on cathetometer readings) multiplied by the number of steps. The uncertainty of the solvent density (±0.001 g/cm^3) was also accounted for. Based on all of the HPM data collected to date, the uncertainty in the composition was determined to be ±0.35 wt%. This uncertainty is added to the precision of the measurement (half of the solvent increment and typically ±1 wt%) to obtain a total uncertainty of ±1.4 wt%.

A.2 PVT Cell Phase Composition and Yield Data

The major sources of error in the phase composition and yield calculations are as follows:

1. Mass of bitumen and diluent in Feed: The mass of bitumen and diluent injected at the experimental conditions was calculated in two ways, using the injected volume recorded from either the PVT cell (cathetometer) or the pump, as described in Section 3.5.2. The reported mass of diluent was taken as the average of these two values. The uncertainty of the mass measurement was determined as the 90% confidence interval from the deviations between the two measurements for all of the data collected to date. The uncertainty of the mass of bitumen and diluent injected were 0.6 and ±0.4 g, respectively. Note that, diluent refers to the solvent in use (in this case propane).
2. Phase Sample Composition: Two samples of each phase were collected and analyzed using the mass evaporation technique to determine the phase compositions, as described in Section 3.4.2. The reported phase compositions are the average of the two measured values. The uncertainty was calculated from the deviations of the two values for all of the data

collected to date using a 90% confidence interval. The uncertainty in the light phase and heavy phase compositions were ±1.6 and ±0.8 wt%, respectively.

3. Mass of light Phase: After equilibrium, the volume of both the light phase were measured using the cathetometer with a precision of ±0.01 cm^3. Both phases were collected through blind cells and the masses were measured with a precision of ±0.01 g. The mass of fluid in the transfer line was also measured with a precision of ±0.02 g. The propagated uncertainty of the light phase mass was ±0.05 g.

   Mass of heavy phase: The mass of the heavy phase was determined as described for the light phase. The dead volume of the PVT cell is also required and is an additional source of error. The mass of the fluid in the dead volume of the PVT cell was determined from the dead volume and solvent density with an uncertainty of ±0.23 g. The propagated uncertainty of the light phase mass was ±0.26 g.

The uncertainty in the yield calculations includes all three contributions and was determined from the propagation of error. The final uncertainty of the C5-asphaltene and pitch* yields were 1.7 and ±2.6 wt%.

A.3 Blind Cell Yield Data

The uncertainty of the yields were determined as the sum of the uncertainty of a yield measurement plus the uncertainty in the yield calculation based on the assumed solvent content in the heavy phase. The uncertainty of the yield measurement was determined as the 90% confidence interval of the deviations of the yield around a best fit yield curve. The repeatability of the pitch* and C5-asphaltene yield measurements were 2.5 and ±0.5 wt%. The uncertainty of the yield from the assumed solvent content was determined as the difference in yield at solvent contents of 0 and 30 wt%. The combined uncertainties were plotted versus the solvent content in the feed to obtain the following relationship:

$$Uncertainty = \left(1 - A * \left(1 - e^{\left(-B*(w_{solv}-0.2)\right)}\right)\right)*100 \qquad \textbf{A.1}$$

where *A* and *B* are the tuned constants, and w_{solv} is the solvent mass fraction. The fitted constants are shown in Table A1 for both the pitch* and C5-asphaltene yields. On average, the uncertainty of C5-asphaltene and pitch* yields are 1.0, ±12.5 wt%, respectively. Note that the uncertainty in the pitch* yield increases significantly near the onset (approximately ±30 wt% at <50 wt% propane in the feed).

Table A1. Tuned exponential correlation parameters to fit pitch* and C5-asph error curves.

Constants	Pitch* error	C5-asph error
A	0.975	0.995
B	8	25

References

Adachi, Y., and Sugie, H. (1986). A New Mixing Rule- Modified Conventional Mixing Rule. *Fluid Phase Equilibria* 28(2), 103-118. https://doi.org/10.1016/0378-3812(86)85072-5.

Agrawal, P., Schoeggl, F. F., Satyro, M. A., Taylor, S. D., and Yarranton, H. W. (2012). Measurements and Modeling of the Phase Behavior of Solvent Diluted Bitumens. *Fluid Phase Equilibria* 334, 51-64. http://dx.doi.org/10.1016/j.fluid.2012.07.025.

Agrawala, M., and Yarranton, H. W. 2011. An Asphaltene Association Model Analogous to Lineal Polymerization. *Ind. Eng. Chem. Res.* 40(21), 4664-4672. https://doi.org/10.1021/ie0103963.

Akbarzadeh, K., Alboudwarej, H., Svrcek, W. Y., and Yarranton, H. W. (2005). A Generalized Regular Solution Model for Asphaltene Precipitation from *n*-Alkane Diluted Heavy Oils and Bitumens. *Fluid Phase Equilibria* 232(1-2), 159-170. http://dx.doi.org/10.1016/j.fluid.2005.03.029.

Alboudwarej, H., Akbarzadeh, K., Beck, J., Svrcek, W. Y., and Yarranton, H. W. (2003). Regular Solution Model for Asphaltene Precipitation from Bitumens and Solvents. *AIChE J.* 49(11), 2948-2956. https://doi.org/10.1002/aic.690491124.

AlHammadi, A. A., Vargas, F. M., and Chapman, W. G. (2015). Comparison of Cubic-Plus-Association and Perturbed-Chain Statistical Associating Fluid Theory Methods for Modeling Asphaltene Phase Behavior and Pressure-Volume-Temperature Properties. . *Energy & Fuels* 29(5), 2864-2875. https://doi.org/10.1021/ef502129p.

Ali, L. H., and Al-Ghannam, K. A. (1981). Investigations into Asphaltenes in Heavy Crude Oils. I. Effect of Temperature on Precipitation by Alkane Solvents. *Fuel* 60(11), 1043-1043. http://dx.doi.org/10.1016/0016-2361(81)90047-8.

Altgelt, K. H., and Boduszynski, M. M. (1994). Composition and Analysis of Heavy Petroleum Fractions. New York: Marcel Deckker, Inc.

Andersen, S. I., and Birdi, K. S. (1991). Aggregation of Asphaltenes as Determined by Calorimetry. *J. Colloid Interface Sci.* 142(2), 497-502. http://dx.doi.org/10.1016/0021-9797(91)90079-N.

Andersen. S. I. (1994). Influence of Temperature and Solvent on the Composition of *n*-Heptane Asphaltenes. *Fuel Science and Technology International* 12(1), 51-74. http://dx.doi.org/10.1080/08843759408916165.

Andersen, S. I., Lindeloff, N., and Stenby, E. H. (1998). Investigation of Asphaltene Precipitation at Elevated Temperature. *J. Petr. Sci. Technol.* 16(3-4), 323-334. http://dx.doi.org/10.1080/10916469808949786.

Andersen, S. I. and Birdi, K. S. (2007). Influence of Temperature and Solvent on the Precipitation of Asphaltenes. *Fuel Science and Technology International* 8(6), 593-615. http://dx.doi.org/10.1080/08843759008915946.

Arya, A., von Solms, N., and Kontogeorgis, G. M. (2015). Determination of Asphaltene Onset Conditions Using the Cubic Plus Association Equation of State. *Fluid Phase Equilibria* 400, 8-19. https://doi.org/10.1016/j.fluid.2015.04.032.

Arya, A., von Solms, N., and Kontogeorgis, G. M. (2016a). Investigation of the Gas Injection Effect on Asphaltene Onset Precipitation Using the Cubic-Plus-Association Equation of State. *Energy & Fuels* 30(5), 3560-3574. https://doi.org/10.1021/acs.energyfuels.5b01874.

Arya, A., Liang, X., von Solms, N., and Kontogeorgis, G. M. (2016b). Modeling of Asphaltene Onset Precipitation Conditions with Cubic Plus Association (CPA) and Perturbed Chain

Statistical Associating Fluid Theory (PC-SAFT) Equation of State. *Energy & Fuels* 30(8), 6835-6852. https://doi.org/10.1021/acs.energyfuels.6b00674.

Badamchi-Zadeh, A., Yarranton, H. W., Svrcek, W. Y., and Maini, B. B. (2009a). Phase Behavior and Physical Property Measurements for VAPEX Solvents: Part I. Propane and Athabasca Bitumen. *JCPT* 48(01): 54-61. PETSOC-09-01-54. http://dx.doi.org/10.2118/09-01-54.

Badamchi-Zadeh, A., Yarranton, H. W., Svrcek, W. Y., and Maini, B. B. (2009b). Phase Behavior and Physical Property Measurements for VAPEX Solvents: Part II. Propane, Carbon Dioxide, and Athabasca Bitumen. *JCPT* 48(03), 57-65. PETSOC-09-03-57. http://dx.doi.org/10.2118/09-03-57.

Bianchi, U. (1965). Pressure Effects on Glass Transition in Polymers. *J. Phys. Chem.* 69 (5), 1497-1504. http://dx.doi.org/10.1021/j100889a010.

Barker, J. A., and Henderson, D. (1967). Perturbation Theory and Equation of State for Fluids II. A Successful Theory of Liquids. *The Journal of Chemical Physics* 47(11), 4714-4721. http://dx.doi.org/10.1063/1.1701689.

Castellanos-Diaz, O., Modaresghazani, J., Satyro, M. A., and Yarranton, H. W. (2011). Modeling the Phase Behavior of Heavy Oil and Solvent Mixtures. *Fluid Phase Equilibria* 304(1-2), 74-85. https://doi.org/10.1016/j.fluid.2011.02.011.

Castellanos Diaz, O., Sanchez-Lemus, M. C., Schoeggl, F. F., Satyro, M. A., Taylor, S. D., and Yarranton, H. W. (2014). Deep-Vacuum Fractionation of Heavy Oil and Bitumen, Part I: Apparatus and Standardized Procedure. *Energy & Fuels* 28(15), 2857-2865. https://doi.org/10.1021/ef500489y.

Chapman, W. G., Gubbins, K. E., Jackson, G., and Rodosz, M. (1989). SAFT: Equation-of-State Solution Model for Associating Fluids. *Fluid Phase Equilibria* 52, 31-38. https://doi.org/10.1016/0378-3812(89)80308-5.

Chueh, P. L., and Prausnitz, J. M. (1968). Calculations of High-Pressure Vapor-Liquid Equilibria. *Ind. Eng. Chem.* 60(3), 34-52. https://doi.org/10.1021/ie50699a007.

Dickie, J. P., and Yen, T. F. (1967). Macrostructures of the Asphaltic Fractions by Various Instrumental Methods. *Anal. Chem.* 39(14), 1847-1852. https://doi.org/10.1021/ac50157a057.

Dini, Y., Becerra, M., and Shaw, J. (2016). Phase Behavior and Thermophysical Properties of Peace River Bitumen + Propane Mixtures from 303 K to 393 K. *J. Chem. Eng. Data* 61(8): 2659-2688. http://dx.doi.org/10.1021/acs.jced.6b00034.

Farouq Ali, S. M. (2013). All You Need is Darcy's Equation to Determine EOR Success or Failure. Presented at the SPE Western Regional & AAPG Pacific Section Meeting 2013 Joint Technical Conference, Monterey, 19-25 April. SPE-165318-MS. http://dx.doi.org/10.2118/165318-MS.

Farouq Ali, S. M. (2015). Practical Heavy Oil Recovery. Book Draft, 1-1.

Fox, T. G., and Loshaek, S. (1955). Influence of Molecular Weight and Degree of Crosslinking on the Specific Volume and Glass Temperature of Polymers. *Journal of Polymer Science* 15(80), 371-390. https://doi.org/10.1002/pol.1955.120158006.

Gao, G., Daridon, J., Saint-Guirons, H., Xans, P., and Montel, F. (1992). A Simple Correlation to Evaluate Binary Interaction Parameters of the Peng-Robinson Equation of State: Binary Light Hydrocarbon System. *Fluid Phase Equilibria* 74, 85-93. http://dx.doi.org/10.1016/0378-3812(92)85054-C.

Gonzalez, D. L., Ting, P. D., Hirasaki, G. J., and Chapman, W. G. (2005). Prediction of Asphaltene Instability under Gas Injection with the PC-SAFT Equation of State. *Energy & Fuels* 19(4), 1230-1234. http://dx.doi.org/10.1021/ef049782y.

Gonzalez, D. L., Hirasaki, G. J., Creek, J., and Chapman, W. G. (2007). Modeling of Asphaltene Precipitation Due to Changes in Composition Using the Perturbed Chain Statistical Associating Fluid Theory Equation of State. *Energy & Fuels* 21(3), 1231-1242. http://dx.doi.org/10.1021/ef060453a.

Gray, M. R. (1994). Upgrading Petroleum Residues and Heavy Oils. New York: Marcel Dekker, Inc.

Gray M. R., Assenheimer, G., Boddez, L., and McCaffrey, W. C. (2004). Melting and Fluid Behavior of Asphaltene Films at 200-500°C. *Energy & Fuels* 18(5), 1419-1423. https://doi.org/10.1021/ef049923w.

Gross, J., and Sadowski, G. (2001). Perturbed-Chain SAFT: An Equation of State Based on a Perturbation Theory for Chain Molecules. *Ind. Eng. Chem.* 40(4), 1244-1260. https://doi.org/10.1021/ie0003887.

Hirschberg, A., deJong, L. N. J., Schipper, B. A., and Meijer, J. G. (1984). Influence of Temperature and Pressure on Asphaltene Flocculation. *SPE J.* 24(3), 284-293. SPE-11202-PA. http://dx.doi.org/10.2118/11202-PA.

Hu, Y., and Guo, T. (2001). Effect of Temperature and Molecular Weight of *n*-Alkane Precipitants on Asphaltene Precipitation. *Fluid Phase Equilibria* 192(1-2), 13-25. http://dx.doi.org/10.1016/S0378-3812(01)00619-7.

Huang, S. H., and Radosz, M. (1991). Phase Behavior of Reservoir Fluids IV: Molecular Weight Distributions for Thermodynamic Modeling. *Fluid Phase Equilibria* 66(1-2), 23-40. https://doi.org/10.1016/0378-3812(91)85045-V.

Jamaluddin, A. K. M., Kalogerakis, N. E., and Chakma, A. (1991). Predictions of CO_2 Solubility and CO_2 Saturated Liquid Density of Heavy Oils and Bitumens Using a Cubic Equation of State. *Fluid Phase Equilibria* 64, 33-48. https://doi.org/https://doi.org/10.1016/0378-3812(91)90004-Q.

Jhaveri, B. S., and Youngren, G. K. (1988). Three Parameter Modification of the Peng Robinson Equation of State to Improve Volume Predictions. *SPE J. Res. Eng.* 3(03), 1033-1040. https://doi.org/10.2118/13118-PA.

Johnston, K. A. (2017). Measurement and Modeling of Pentane-Diluted Bitumen Phase Behavior. Ph.D Thesis, University of Calgary. Calgary, Canada.

Johnston, K. A., Schoeggl, F. F., Satyro, M. A., Taylor, S. D., and Yarranton, H. W. (2017a). Phase Behavior of Bitumen and *n*-Pentane. *Fluid Phase Equilibria* 442, 1-19. http://dx.doi.org/10.1016/j.fluid.2017.03.001

Johnston, K. A., Satyro, M. A., Taylor, S. D., and Yarranton, H. W. (2017b). Can a Cubic Equation of State Model Bitumen-Solvent Phase Behavior. *Energy & Fuels*. http://dx.doi.org/10.1021/acs.energyfuels.7b01104

Joshi, N. B., Mullins, O. C., Jamaluddin, A., Creek, J., and McFadden, J. (2001). Asphaltene Precipitation from Live Crude Oil. *Energy & Fuels* 15(4), 979-986. http://dx.doi.org/10.1021/ef010047l.

Katz, D. L., and Firoozabadi, A. (1978). Predicting Phase Behavior of Condensate/Crude-Oil System Using Methane Interaction Coefficients. *J. Petr. Technol.* 30(11), 1649-1655. SPE-6721-PA. http://dx.doi.org/10.2118/6721-PA.

Kontogeorgis, G. M., Michelsen, M. L., Folas, G. K., Dewawi, S., von Solms, N., and Stenby, E. H. (2006). Ten Years with the CPA (Cubic-Plus-Association) Equation of State. Part 1. Pure Compounds and Self-Associating Systems. *Ind. Eng. Chem. Res.* 45(14), 4855-4868. https://doi.org/10.1021/ie051305v.

Kontogeorgis, G. M., and Folas, G. K. (2009). Thermodynamic Models for Industrial Applications: from Classical and Advanced Mixing Rules to Association Theories. John Wiley & Sons, Inc.

van Konynenburg, P. H., and Scott, R. L. (1980). Critical Lines and Phase Equilibria in Binary van der Waals Mixtures. *The Royal Society* 298(1442), 495-540. http://dx.doi.org/10.1098/rsta.1980.0266.

Kriz, P., Stastna, J., and Zanzotto, L. (2011). Glass Transition and Phase Stability in Asphalt Binders. *J. Road Material Pavement Design* 9(1), 37-65. http://dx.doi.org/10.1080/14680629.2008.9690158.

Lee, B. I., and Kesler, M. G. (1975). A Generalized Thermodynamic Correlation Based on Three-Parameter Corresponding States. *AIChE J.* 21(3), 510-527. http://dx.doi.org/10.1002/aic.690210313.

Li, Z., and Firoozabadi, A. (2010a). Cubic-Plus-Association Equation of State for Asphaltene Precipitation in Live Oils. *Energy & Fuels* 24(5), 2956-2963. https://doi.org/10.1021/ef9014263.

Li, Z., and Firoozabadi, A. (2010b). Modeling Asphaltene Precipitation by *n*-Alkanes from Heavy Oils and Bitumens Using Cubic-Plus-Association Equation of State. *Energy & Fuels* 24(2), 1106-1113. http://dx.doi.org/10.1021/ef9009857.

Linstrom, P. J., and Mallard, W. G. (2015). NIST Chemistry WebBook, NIST Standard Reference Database Number 69, National Institute of Standards and Technology, Gaithersburg, MD 20899.

Mannistu, K. D., Yarranton, H. W., and Masliyah, J. H. (1997). Solubility Modeling of Asphaltenes in Organic Solvents. *Energy & Fuels* 11(3), 615-622. http://dx.doi.org/10.1021/ef9601879.

Mansoori, G. A., Carnahan, N. F., Starling, K. E., and Leland, T. W. (1971). Equilibrium Thermodynamics Properties of the Mixtures of Hard Spheres. *The Journal of Chemical Physics* 54(4), 1523-1525. http://dx.doi.org/10.1063/1.1675048.

Maxwell, J. B., and Bonell, L. S. (1957). Derivation and Precision of a New Vapor Pressure Correlation for Petroleum Hydrocarbons. *Ind. Eng. Chem. Res.* 49(7), 1187-1196. https://doi.org/10.1021/ie50571a044.

Mehrotra, A. K., and Svrcek, W. Y. (1985). Viscosity, Density and Gas Solubility Data for Oil Sand Bitumens. Part II: Peace River Bitumen Saturated with N2, CO, CH4, CO2 and C2H6. *AOSTRA J. Res.* 1 (4), 269-279.

Mehrotra, A. K., and Svrcek, W. Y. (1988). Properties of Cold Lake Bitumen Saturated with Pure Gases and Gas Mixtures. *Can. J. Chem. Eng.* 66(4), 656-665. https://doi.org/10.1002/cjce.5450660419.

Mehrotra, A. K., Eastick, R. R., and Svrcek, W. Y. (1989). Viscosity of Cold Lake Bitumen and Its Fractions. *Can. J. Chem. Eng.* 67(6), 1004-1009. https://doi.org/10.1002/cjce.5450670620.

Memarzadeh, A., and Rahnema, H. (2015). Thermodynamic Analysis of Solvent Assisted Steam Injection. Presented at the SPE Annual Technical Conference and Exhibition, Houston, 28-30 September. SPE-178725-STU. http://dx.doi.org/10.2118/178725-STU.

Michelsen, M. L. (1982). The Isothermal Flash Problem. Part I. Stability. *Fluid Phase Equilibria* 9 (1), 1-19. http://dx.doi.org/10.1016/0378-3812(82)85001-2.

Mullins, O. C. (2007) Petroleomics and Structure-Function Relations of Crude Oil and Asphaltenes. In Asphaltenes, Heavy Oils and Petroleomics (pp. 1-16). New York: Springer.

Mullins, O. C. (2008). Review of the Molecular Structure and Aggregation of Asphaltenes and Petroleomics. *SPE J.* 13(01), 284-293. SPE-95801-PA. https://doi.org/10.2118/95801-PA

Nasr, T. N., Beaulieu, G., Golbeck, H., and Heck, G. (2003). Novel Expanding Solvent-SAGD Process "ES-SAGD". *JCPT* 42(01): 13-16. PETSOC-03-01-TN. http://dx.doi.org/10.2118/03-01-TN.

Nielsen, B. B., Svrcek, W. Y., and Mehrotra, A. K. (1994). Effect of Temperature and Pressure on Asphaltene Particle Size Distribution in Crude Oils Diluted with *n*-Pentane. *Ind. Eng. Chem. Res.* 33(5), 1324-1330. https://doi.org/10.1021/ie00029a031.

Nourozieh, H., Kariznovi, M., and Abedi, J. (2015). Experimental and Modeling Studies of Phase Behavior for Propane/Athabasca Bitumen Mixtures. *Fluid Phase Equilibria* 397, 37-43. http://dx.doi.org/10.1016/j.fluid.2015.03.047

Panagiotopoulos, A. Z., and Reid, M. C. (1986). A New Mixing Rule for Cubic Equation of State for Highly Polar, Asymmetric Mixtures. *ACS Symposium Series* 300(28), 571-582. https://doi.org/10.1021/bk-1986-0300.ch028.

Panuganti, S. R., Vargas, F. M., Gonzalez, D. L., Kurup, A. S., and Chapman, W. G. (2012). PC-SAFT Characterization of Crude Oils and Modeling of Asphaltene Phase Behavior. *Fuel 93*, 658-669. https://doi.org/10.1016/j.fuel.2011.09.028.

Pedersen, K. S., and Christensen, P. L. (2007). Phase Behavior of Petroleum Reservoir Fluids. Taylor & Francis Group.

Peneloux, A., Rauzy, E., and Freze, R. (1982). A Consistent Correction for Redlich-Kwong-Soave Volumes. *Fluid Phase Equilibria* 8(1), 7-23. https://doi.org/10.1016/0378-3812(82)80002-2.

Peng, D., and Robinson, D. B. (1976). A New Two-Constant Equation of State. *Ind. Eng. Chem. Fundam.* 15(1), 59-64. https://doi.org/10.1021/i160057a011.

Peramanu, S., Singh, C., Agrawala, M., and Yarranton, H. W. (2001). Investigation on the Reversibility of Asphaltene Precipitation. *Energy & Fuels* 14(4), 910-917. https://doi.org/10.1021/ef010002k.

Pfeiffer, J. P., and Saal, R. N. J. (1940). Asphaltic Bitumen as Colloid System. *J. Phys. Chem.* 44(2), 139-149. https://doi.org/10.1021/j150398a001.

Powers, D. P. (2014). Characterization and Asphaltene Precipitation Modeling of Native and Reacted Crude Oils. Ph.D Thesis. University of Calgary. Calgary, Canada.

Powers, D. P., Sadeghi, H., Yarranton, H. W., and van den Berg, F. G. A. (2016). Regular Solution Based Approach to Modeling Asphaltene Precipitation from Native and Reacted Oils: Part 1, Molecular Weight, Density, and Solubility Parameter Distributions of Asphaltenes. *Fuel* 178, 218-233. https://doi.org/10.1016/j.fuel.2016.03.027.

Prausnitz, J. M. (1969). Molecular Thermodynamics of Fluid Phase Equilibria. Englewood Cliffs, New Jersey: Prentice-Hall Inc.

Rachford Jr, H. H., and Rice, J. D. (1952). Procedure for Use of Electronic Digital Computers in Calculation Flash Vaporization Hydrocarbon Equilibrium. *J. Petr. Technol.* 4(10), 327-328. SPE-952327-G. http://dx.doi.org/10.2118/952327-G.

Rastegari, K., Svrcek, W. Y., and Yarranton, H. W. (2004). Kinetics of Asphaltene Flocculation. *Ind. Eng. Chem. Res.* 43(21), 6861-6870. http://dx.doi.org/10.1021/ie049594v.

Riazi, M. R. (2005). Characterization and Properties of Petroleum Fractions. West Conshohocken, PA: ASTM International.

Riazi, M. R., and Daubert, T. E. (1987). Characterization Parameters for Petroleum Fractions. *Ind. Eng. Chem. Res.* 26, 755-759. https://doi.org/10.1021/ie00064a023.

Richardson, W. (2016). Diffusivity of Light Hydrocarbon Gases in Bitumen. Ph.D Thesis. University of Calgary. Calgary, Canada.

Sanchez-Lemus, M. C., Schoeggl, F. F., Taylor, S. D., Ruzicka, K., Fulem, M., and Yarranton, H. W. (2014). Deep-Vacuum Fractionation of Heavy Oil and Bitumen, Part II: Interconversion Method. *Energy & Fuels* 28(5), 2866-2873. https://doi.org/10.1021/ef500490h.

Sanchez-Lemus, M. C. (2015). Extended Distillation and Property Correlation for Heavy Oil. Ph.D Thesis. University of Calgary. Calgary, Canada.

Saryazdi, F., Motahhari, H., Taylor, S. D., and Yarranton, H. W. (2013). Density of Hydrocarbon Mixtures and Bitumen Diluted with Solvents and Dissolved Gases. *Energy & Fuels* 27(7), 3666-3678. http://dx.doi.org/10.1021/ef400330j.

Sedghi, M., and Goual, L. (2010). Role of Resins on Asphaltene Stability. *Energy & Fuels* 24(4), 2275-2280. https://doi.org/10.1021/ef9009235.

Sheu, E. Y. (2002). Petroleum Asphaltene-Properties, Characterization, and Issues. *Energy & Fuels* 16(1), 14-82. https://doi.org/10.1021/ef010160b.

Sirota, E. B. (2005). Physical Structure of Asphaltenes. *Energy & Fuels* 19(4), 1290-1296. http://dx.doi.org/10.1021/ef049795b.

Søreide, I. (1989). Improved Phase Behavior of Petroleum Reservoir Fluids from a Cubic Equation of State. Ph.D Thesis, the Norwegian Institute of Technology and Applied Geophysics. Oslo, Norway.

Speight, J. G. (2007). *The Chemistry and Technology of Petroleum*, Forth edition. Boca Raton, Florida, USA: CRC Press.

Strausz, O. P., Mojelsky, T. W., and Lown, M. (1992). The Molecular Structure of Asphaltene: An Unfolding Story. *Fuel* 71(12), 1355-1363. https://doi.org/10.1016/0016-2361(92)90206-4.

Tharanivasan, A., Yarranton, H. W., and Taylor, S. D. (2011). Application of a Regular Solution-Based Model to Asphaltene Precipitation from Live Oils. *Energy & Fuels* 25(2), 528-538. http://dx.doi.org/10.1021/ef101076z.

Tharanivasan, A. (2012). Asphaltene Precipitation from Crude Oil Blends, Conventional Oils, and Oils with Emulsified Water. Ph.D Thesis, University of Calgary. Calgary, Canada.

Ting, P. D., Hirasaki, G. J., and Chapman, W. G. (2003). Modeling of Asphaltene Phase Behavior with the SAFT Equation of State. *J. Petr. Sci. Technol.* 21(3-4), 647-661. http://dx.doi.org/10.1081/LFT-120018544.

Twu, C. H. (1984). An Internally Consistent Correlation for Predicting the Critical Properties and Molecular Weights of Petroleum and Coal-Tar Liquids. *Fluid Phase Equilibria* 16(2), 137-150. http://dx.doi.org/10.1016/0378-3812(84)85027-X.

Vargas, F. M., Gonzalez, D. L., Hirasaki, G. J., and Chapman, W. G. (2009). Modeling Asphaltene Phase Behavior in Crude Oil Systems Using the Perturbed Chain Form of the Statistical Associating Fluid Theory (PC-SAFT) Equation of State. *Energy & Fuels* 23(3), 1140-1146. http://dx.doi.org/10.1021/ef8006678.

Vickers, A. K. (2002). Higher-Temperature Simulated Distillation with DB-HT Sim Dis Columns. Application. *Agilent Technologies Inc*., Hydrocarbon Processing, USA.

Virtual Materials Group Inc. VMG 2017, VMGSim Version 10.0, VMG Sim User's Manual, Calgary, Canada.

Whitson, C., and Brule, M. (2000). Phase Behavior. Richardson, Texas, USA: Society of Petroleum Engineers (SPE).

Wiehe, I. A., Yarranton, H. W., Akbarzadeh, K., Rahimi, P. M., and Teclemariam, A. (2005). The Paradox of Asphaltene Precipitation with Normal Paraffins. *Energy & Fuels* 19(4), 1261-1267. http://dx.doi.org/10.1021/ef0496956.

Yarranton, H. W., and Masliyah, J. H. (1996). Molar Mass Distribution and Solubility Modeling of Asphaltenes. *AIChE J.* 42(12), 3533-3543. https://doi.org/10.1002/aic.690421222.

Yarranton, H. W., Alboudwarej, H., and Jakher, R. (2000). Investigation of Asphaltene Association with Vapor Pressure Osmometry and Interfacial Tension Measurements. *Ind. Eng. Chem. Res.* 39 (8), 2916-2924. https://doi.org/10.1021/ie000073r.

Yarranton, H. W., Fox, W. B., and Svrcek, W. Y. (2007). Effect of Resins on Asphaltene Self-Association and Solubility. *Can. J. Chem. Eng.* 85(5), 635-642. https://doi.org/10.1002/cjce.5450850510.

Yarranton, H. W., van Dorp, J. J., Verlaan, M. L., and Lastovka, V. (2013). Wanted Dead or Live: Crude Cocktail Viscosity: A Pseudo-Component Method to Predict the Viscosity of Dead Oils, Live Oils and Mixtures. *J. Can. Petr. Technol.* 52(3), 176-191. https://doi.org/10.2118/160314-PA.

Zhang, Y., Takanohashi, T., Sato, S., and Saito, I. (2004). Observation of Glass Transition in Asphaltenes. *Energy & Fuels* 18(1), 283-284. https://doi.org/10.1021/ef0301147.

Zou, X., Zhang, X., and Shaw, J. M. (2007). Phase Behavior of Athabasca Vacuum Bottoms + *n*-Alkane Mixtures. *SPE Prod. Operations* 22(2), 265-272. SPE-97661-PA. http://dx.doi.org/10.2118/97661-PA.